SANDIA REPORT

SAND90—2926 • UC—706
Unlimited Release
Printed March 1991

1990 Sandia Rocket-Triggered Lightning Field Tests at Kennedy Space Center, Florida

Richard J. Fisher, George H. Schnetzer

Prepared by
Sandia National Laboratories
Albuquerque, New Mexico 87185 and Livermore, California 94550
for the United States Department of Energy
under Contract DE-AC04-76DP00789

Issued by Sandia National Laboratories, operated for the United States Department of Energy by Sandia Corporation.

Available to DOE and DOE contractors from
Office of Scientific and Technical Information
PO Box 62
Oak Ridge, TN 37831

Prices available from (615) 576-8401, FTS 626-8401

Available to the public from
National Technical Information Service
US Department of Commerce
5285 Port Royal Rd
Springfield, VA 22161

NTIS price codes
Printed copy: A06
Microfiche copy: A01

SAND90-2926
Unlimited Release
Printed March 1991

SAND--90-2926

DE91 011263

1990 SANDIA ROCKET-TRIGGERED LIGHTNING FIELD TESTS AT KENNEDY SPACE CENTER, FLORIDA

Richard J. Fisher and George H. Schnetzer
Division 7554
Electromagnetic Testing
Sandia National Laboratories
Albuquerque, New Mexico 87185

ABSTRACT

During 1990, the Sandia Transportable Triggered Lightning Instrumentation Facility (SATTLIF) was designed, fabricated, and fielded at the Kennedy Space Center (KSC) rocket-triggered lightning test range in Florida. In preparation for lightning tests of a specially fitted munitions storage bunker during 1991, instrumentation for directly measuring lightning channel currents and response currents in structures was evaluated and demonstrated to function well. A set of 77-mil-thick 2024-T3 aluminum and 35-mil-thick 4130 steel metallic samples was exposed to measured triggered lightning flash currents. The resultant damage spots on these specimens represent the first such data points produced by known lightning currents. They are intended for use as benchmarks against which to improve and quantify the fidelity of laboratory simulations of lightning penetration. Two particularly significant results were obtained. In the first, a damage spot of approximately 0.3-inch diameter and >0.01-inch depth was produced by a continuing current of well less than median-level severity that transferred less than 13.6 coulombs of charge. In the second case, one of the steel samples was virtually burned through under a return-stroke/continuing current combination transferring an eightieth percentile charge of approximately 49 coulombs. Photographic evidence of upward-going streamers preceding return strokes initiated by dart leaders was also obtained and is presented.

ACKNOWLEDGEMENTS

The authors wish to express their appreciation to the Kennedy Space Center and specifically to Mr. William Jafferis, Rocket-Triggered Lightning Program Manager, for the opportunity to participate in their 1990 RTL campaign. We are particularly indebted to Mr. Jafferis for his enthusiastic personal support and efforts on behalf of the present experiments. Our thanks are also due to Messrs. Andre Eybert-Berard and Louis Barret of CENG for their cooperation and support in all phases of the rocket operations. The considerable overall technical input of Dr. Larry D. Scott, Division 7554 and his contribution in setting up the LeCroy digitizer system software are acknowledged. The design and fabrication supervision of the rocket-launch system was largely carried out by C. S. Chocas, at that time of Division 7554.

CONTENTS

ILLUSTRATIONS

TABLES

ACRONYMS

APS	area protection system
ARDEC	U.S. Army Armament Research, Development, and Engineering Center
CCD	charge-coupled device
CENG	Centre D'Etudes Nucleaires De Grenoble
CVR	current viewing resistor
EMA	Electromagnetic Applications, Inc.
FM	frequency modulated
FOL	fiber optic data link
ICC	initial continuing current
KSC	Kennedy Space Center
LEWG	Lightning Environment Working Group
PVC	polyvinyl chloride
RTL	rocket-triggered lightning
SAF	Safing, Arming, and Firing
SATTLIF	Sandia Transportable Triggered Lightning Instrumentation Facility
SLS	Sandia Lightning Simulator
VCR	video cassette recorder

1990 SANDIA ROCKET-TRIGGERED LIGHTNING FIELD TESTS AT KENNEDY SPACE CENTER, FLORIDA

1.0 INTRODUCTION AND SUMMARY

A transportable rocket-triggered lightning (RTL) test facility was designed, developed, and fielded by Division 7554 at the Kennedy Space Center's (KSC) Atmospheric Sciences Field Laboratory test site in Florida during the period of July 8 through August 17, 1990. The facility, called the Sandia Transportable Triggered Lightning Instrumentation Facility (SATTLIF), was jointly sponsored by the U.S. Army Armament Research, Development, and Engineering Center (ARDEC) and by Department 8160 of Sandia National Laboratories. The field test constituted both a shakedown trial of the SATTLIF systems and an opportunity to obtain damage data produced by fully characterized (recorded) flash currents on specimens of aluminum and steel. The SATTLIF will be fielded at Ft. McClellan, Alabama, during the summer of 1991 for use in conducting triggered lightning tests on a specially equipped munitions storage igloo.

The trial fielding of the SATTLIF at KSC satisfied all of its stated objectives.

- The instrumentation for directly measuring lightning channel currents was demonstrated to function properly, although two minor problems were encountered and resolved.

- Data were acquired that definitively establish that burnthrough of thicknesses of aluminum commonly employed in weapon designs can be fully penetrated by lightning currents of well less than median-level severity.

- Virtual burnthrough of 35-mil-thick ferrous steel was obtained during a flash that contained a moderately severe continuing current.

- Experiments were successfully performed to acquire damage data spots produced by fully recorded lightning currents on a total of six disks of 77-mil-thick 2024-T3 aluminum and three of 35-mil-thick 4130 ferrous steel. Through detailed examination of high-speed, 16-mm cinematic film records, the full complement of recorded current data, and the samples themselves, many of the individual damage spots have been successfully correlated with the specific return strokes and continuing currents that produced them. The data therefore represent a definitive basis against which the fidelity of laboratory simulations of the penetration of lightning in these materials can be improved and quantified.

- The instrumentation for measuring the responses of large test items was shown to perform adequately. An experimental amplifier, designed to increase the effective dynamic range of the recording channel, was found to have practical problems associated with baseline drift. Since the increased dynamic range it offered was found not to be required, use of the amplifier will be discontinued. All other aspects of the instrumentation performed well.

The results of these field tests of the SATTLIF demonstrate the practicality of the transportable rocket-triggered lightning test technique for appropriate applications. These applications include, but are not limited to, cases in which test objects are either too large or immobile to be transported to a conventional test facility or cannot be driven adequately by such a facility. A further case involves the situation in which test objectives require features in the test current that cannot be obtained from a conventional simulation source.

The present results specifically pave the way for the confident and successful fielding of the SATTLIF in support of triggered lightning tests of the munitions storage bunker at Ft. McClellan during the summer of 1991. The materials damage data obtained during 1990 represent the first of their kind and will be of significant value not only within the weapons development establishment, but also to the aerospace lightning technology community in general.

2.0 BACKGROUND

In 1988, establishment of the Lightning Environment Working Group (LEWG) was directed by the Department of the Army in part to assess the effects of lightning environments on weapons inside storage structures and maintenance and assembly buildings. In support of the LEWG, a finite-difference time-domain computer model for predicting the environments induced by lightning inside these types of facilities was developed by Electromagnetic Applications, Inc. (EMA). Validation of this model for general application to various structures of interest to the Army was set as a high priority by the LEWG.

A model validation methodology involving the use of a Marx bank or other conventional lightning test source was considered and judged to be inadequate for two major reasons. First, the relatively large physical size of the type of test object of interest would make it very difficult to realize an adequate rate of rise of the test current, a dominant controlling quantity in the coupling process. Second, the distribution of ground return current paths in and around a structure hit by lightning strongly influences the coupling of energy into the structure itself. Use of a conventional pulser would artificially distort and concentrate these currents and, on that basis, strongly bias the test results. For these reasons, the use of rocket-triggered lightning, which circumvents both technical objections, was therefore proposed by Sandia.

Coincident with the activities of the LEWG, an investigation of the fidelity of laboratory lightning burnthrough simulation techniques was in process by Division 7554. The results of various tests conducted both at Sandia and elsewhere indicate a strong dependence on the particulars of the electrode arrangement and other test configurational factors for a given applied current. An extensive literature review was conducted and led to the conclusion that there existed no adequate available data or reliable theory that would support a quantitative assessment of burnthrough simulation fidelity *vis-a-vis* natural lightning [1]. It was suggested that development of a data base of damage produced on materials of interest by natural lightning of known (i.e., measured) characteristics would provide a definitive reference basis against which to compare and improve laboratory results obtained with the same applied currents. Acquisition of such data using triggered lightning appeared to be straightforward in principle and could be done on a minimal-interference basis with other test operations using the same triggered flashes. Approval in January 1990 of the proposed development of the SATTLIF offered an early opportunity to conduct this type of damage experiment.

The immediate objective of the LEWG is the validation of the EMA model against measured responses of the test igloo at Ft. McClellan under known incident lightning currents (Figure 1). In order to reduce instrumentation and operational uncertainties going into such a large-scale test and to enhance confidence in the results, a two-phase program was designed. During the first phase, carried out during FY90, the facility was developed and fielded for a shakedown trial of a limited number of instrumentation channels of each required type. Since RTL operations have been conducted routinely each year at KSC since 1985, arrangements were made for the shakedown exercise to be conducted there. This offered the additional advantage that all environmental and safety responsibilities for the handling and employment of the rockets could be left to KSC. Furthermore, the existing KSC launch site facilities admirably suited the requirements of the materials damage experiments. The second phase of the program, scheduled for FY91, will include refinement of the SATTLIF instrumentation design based on the experience gained during the 1990 trials, expansion of the number of recording channels, and the actual execution of the igloo test at Ft. McClellan.

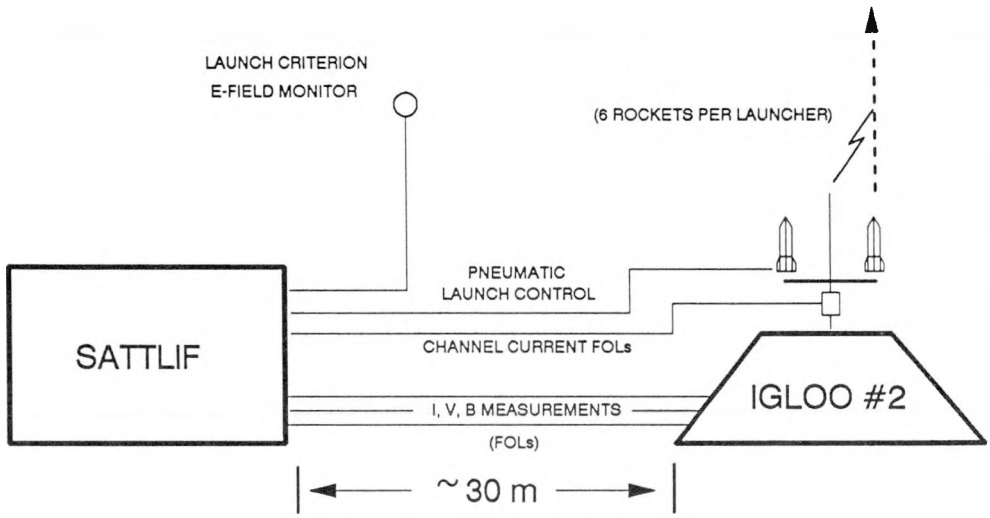

Figure 1. Configuration for Rocket-Triggered Lightning Test of Igloo 2 at Ft. McClellan, Alabama

The remainder of this report presents a summary discussion of the rocket-triggered lightning technique, documents the design and performance of the SATTLIF as it was fielded during 1990, and describes the the materials damage experiments that were conducted with the SATTLIF at KSC.

3.0 THE ROCKET-TRIGGERED LIGHTNING TECHNIQUE

The triggering of natural lightning using small rockets and the direct measurement of the resultant flash currents at the channel base are now considered to be technically routine. Proof of the triggering concept dates back to 1961 [2]. The first practical demonstration took place when lightning was triggered to a specially fitted ship in Tampa Bay [3]. Following that, French experimenters began developing and refining the technique and have been continuously using it in France, New Mexico, and Florida since 1973 [4-6]. Elsewhere, both in Japan [7] and in the U.S., several other organizations, including Sandia National Laboratories [8-10], have employed triggered lightning either as a vehicle for the study of the physics of lightning or as a source for engineering tests.

The triggering technique involves the launching of small rockets during appropriate thunderstorm conditions in which the ambient electric field is indicative of impending lightning. Attached to the rocket is one end of a very thin wire (typically 7.9 mils in diameter). In applications in which the lightning is to be used as a test source, the other end of the wire is tied to ground on or adjacent to the test item. As the rocket ascends to several hundred meters, electric field enhancement at the rocket end of the wire first causes corona and then the development of self-sustaining streamers that propagate toward the cloud and lead to the initiation of a lightning to ground. The ensuing flash generally follows the channel prepared by the vaporized trailing wire and consequently can be directed to a desired strike point.

In this type of triggered flash, the wire vaporizes very early in the sequence due to the preliminary streamer current. The initial return stroke is then preceded by a low-level (several hundred amperes) current flow very similar to the normal interstroke continuing current observed in naturally initiated lightning. This initial continuous current (ICC) lasts up to several hundred milliseconds. A short period of several tens of milliseconds, during which no appreciable current flows, then precedes the onset of a normal sequence of return strokes and interstroke continuing current. Given a properly-timed launch into an ambient electric field somewhat in excess of 3.5 kV/m during the appropriate phase of a storm, a nearly 100% triggering success is achievable.

There are certain differences between the early portions of naturally and artificially initiated lightning. In the context of engineering testing, however, they are either not significant or they can be circumvented. Figure 2 schematically indicates the deviations of this type of triggered lightning from its purely natural counterpart. A detailed discussion of these differences is beyond the scope of the present needs but can be found, for example, in References 11 and 12. From a testing viewpoint, there are two main differences. One is that in this type of triggered lightning the first of the return strokes is preceded by the initial continuous current described above, which is not the case in naturally initiated lightning. The second difference is that the first return stroke in the triggered lightning is not normally initiated by a stepped leader but rather by a dart leader. Thus, the first return stroke in the triggered flash has the same characteristics as a subsequent stroke in a naturally initiated flash. This latter difference is a subtle one that, for testing purposes in general and for the specific purposes of this program, is of no technical consequence. The key point is that the distributions of the various parameters of the return strokes and continuing currents in a triggered flash subsequent to the ICC fall within the corresponding statistical envelopes of naturally initiated lightning [13-15]. This is specifically true for important parameters such as return-stroke current rate of rise, interstroke intervals, and interstroke continuing current.

4.0 OBJECTIVES

The specific objectives of the 1990 field trial of the SATTLIF were

1. Validation of the lightning channel current instrumentation, including calibration against the simultaneous measurements performed by KSC;
2. Validation and optimization of the instrumentation for measuring test system response;
3. Validation and refinement of operational procedures under the guidance of experienced KSC and French experimenters; and
4. Acquisition of training in rocket handling and launching techniques.

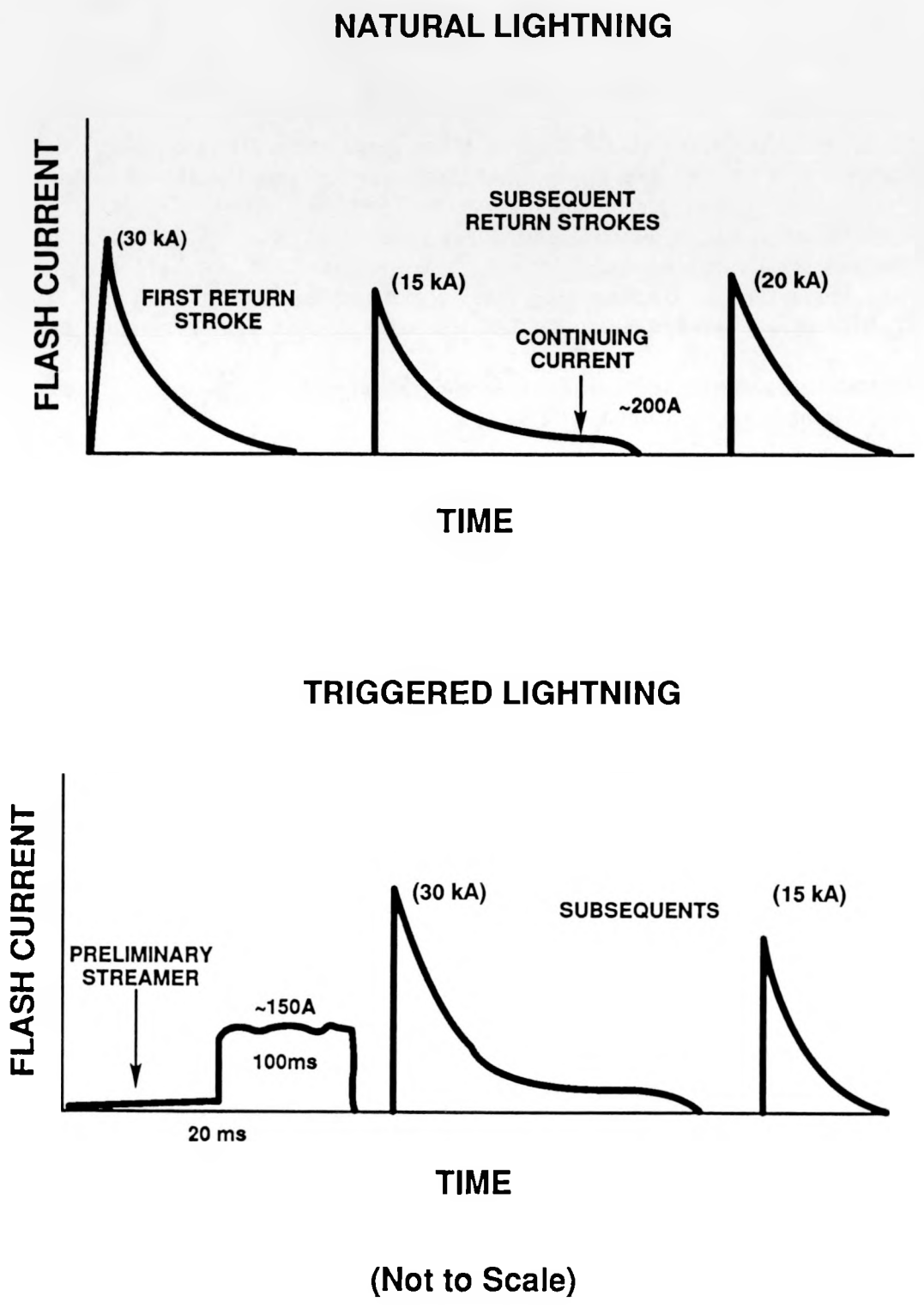

Figure 2. Comparison of Natural and Rocket-Triggered Lightning Flash Currents

The objective of the materials damage experiment was the acquisition of witness data spots created on a variety of metal samples by recorded lightning currents.

5.0 SATTLIF

The SATTLIF enclosure is an all-steel, ocean-going cargo transportainer, modified into an instrumentation shelter. All data and other signal lines running from the shelter to the launch site and test object are either fiber optic cables or nonconductive pneumatic tubing. Three-phase, 208-V electrical power is required and is provided from either commercial mains or a 25-kW diesel generator located immediately next to the shelter. During lightning triggering sessions, the shelter is always disconnected from commercial power and operated from the generator. Figure 3 shows an overview of the SATTLIF subsystems. The subsystems include

1. Ambient electric field monitoring, for launch decision purposes;
2. Electro-pneumatic rocket launch system;
3. Lightning current measurement instrumentation;
4. Test object response instrumentation;
5. National Lightning Location Network* satellite ground terminal;
6. Super VHS black and white video recording system;
7. 16-mm film fast framing camera;
8. Instrumentation control and data processing computer;
9. Range radio communications; and
10. 20-kW, 3-phase diesel generator.

Figure 4 shows the SATTLIF deployed at KSC approximately 80 feet from the triggered lightning strike point. Figure 5 shows the physical layout of the interior of the shelter.

5.1 SATTLIF INSTRUMENTATION

For discussion purposes, the electronic instrumentation is presented in two parts, which address the direct measurement of the incident lightning channel current and the measurements of the responses of a system under test, respectively.

5.1.1 Lightning Channel Current Measurement

The lightning channel current contains both very high amplitude (tens of kiloamps) current pulses with rise times as short as 0.1 μs and long-duration (hundreds of milliseconds), low-level (hundreds of amps) continuing currents. Both types of components are of significant interest. Two types of recording channels were therefore implemented to cover the various amplitude and frequency ranges of the different components. Figure 6 diagrams the arrangement that was employed.

---

* Developed and run by the State University of New York at Albany [16].

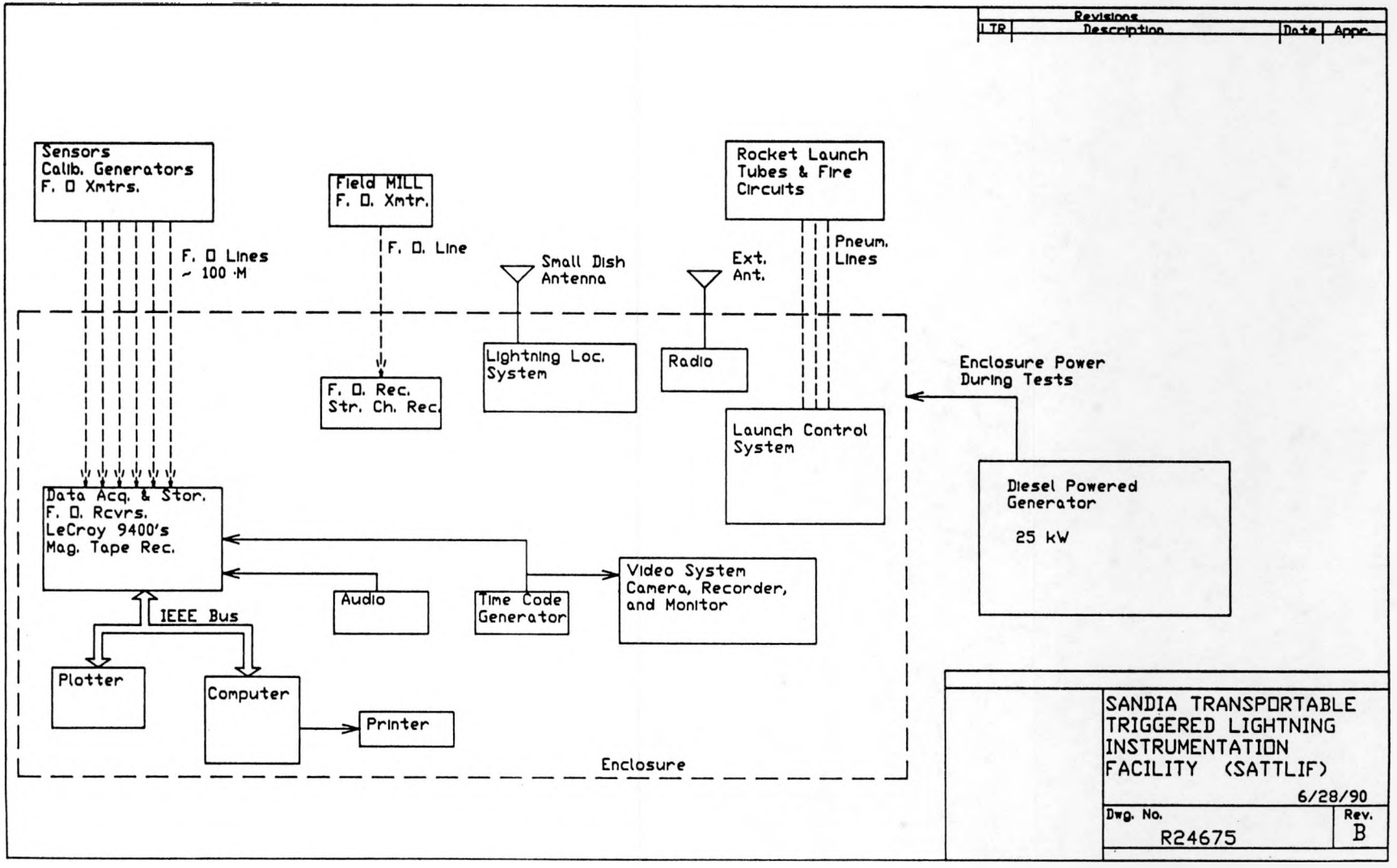

Figure 3. Block Diagram of SATTLIF Subsystems

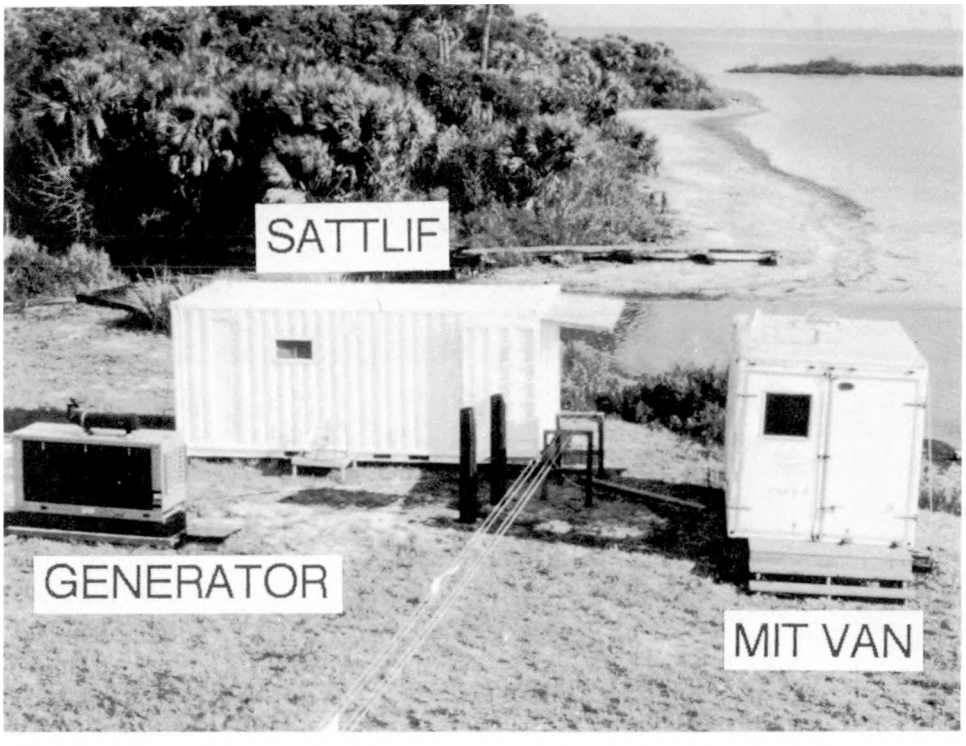

Figure 4. SATTLIF Deployed at KSC During the 1990 RTL Campaign

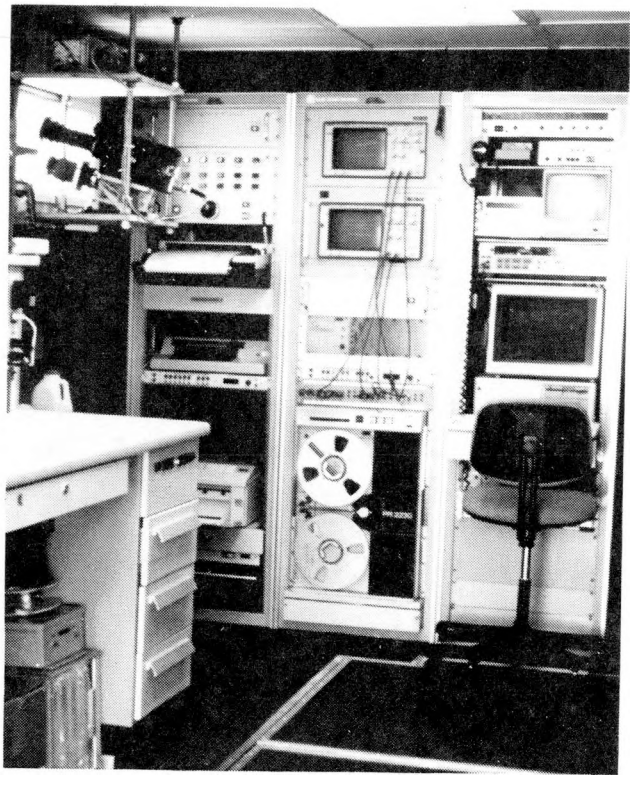

Figure 5. Physical Layout of the Interior of the SATTLIF

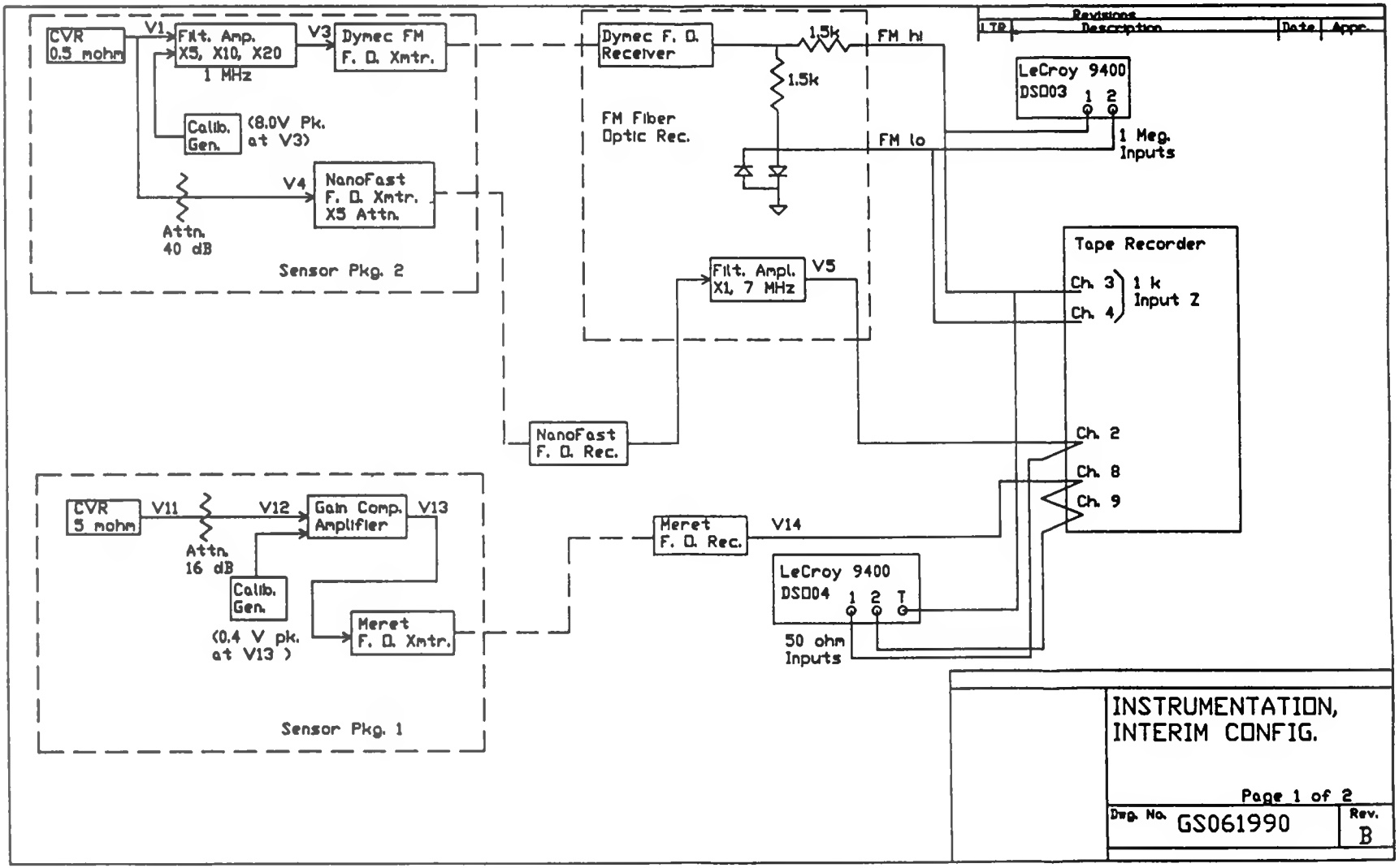

Figure 6. SATTLIF Instrumentation Channels for Direct Measurements of RTL Flash Currents

Current collected by the strike rod was sensed directly by means of a 0.5 milliohm T&M R-14000-20N coaxial current viewing resistor (CVR) inserted between the base of the strike rod and its grounding system (Figure 7). The signal from the CVR was transmitted via two different types of fiber optic data links (FOLs) to the SATTLIF.

Recording of return-stroke currents was done using a wideband NanoFast 300-2A analog FOL and LeCroy 9400A digitizing oscilloscope. The bandwidth of the NanoFast system is ~200 MHz, and that of the LeCroy is 50 MHz. Overall recording bandwidth was therefore set by the CVR, which has a rise time of 0.164 μs (~2.1 MHz bandwidth). The LeCroy digitizer is equipped with memory partitioning and multiple sequential triggering features. Sampling at a rate of once each 80 ns was used to capture the first 200 μs of up to 8 strokes per flash. The output of the NanoFast receiver was also recorded on a direct-record magnetic tape channel in order to provide a record of the entire flash sequence.

Because of the long durations of continuing currents that are possible, their accurate measurement requires a dc recording capability. This was achieved using a Dymec frequency modulated (FM) FOL and FM tracks on the Ampex PR2230 tape recorder. This combination provides an overall bandwidth of dc to 500 kHz. The FM FOL signals were also written to two digitizer channels (40-μs sampling rate), thereby providing additional recording flexibility and immediate viewing capability.

The return-stroke recording channel sensitivities were chosen to accommodate a peak stroke current of 100 kA. The digitizer trigger level was set at 1 kA. The continuing current digitizer trigger level was also 1 kA, and the sensitivities of that channel were set to allow recording resolution down to a noise floor of 2 A.

5.1.2 Test System Response Instrumentation

During the planned test of the storage igloo in 1991, measurements will be made of structural rebar current, ground bus current, open-circuit voltages and short-circuit currents between ceiling and floor, and magnetic fields interior to the structure. With the exception of the sensors for the various types of measurements, the basic instrumentation channel employed for each will be the same. In order to test this basic design, one such channel configuration was fielded during the 1990 tests.

The lightning studies being conducted by KSC include evaluation of a prototype area protection system (APS). Their experimental version consists of an array of steel wire cables assembled under the rocket launching platform that was used for the Sandia tests (Figure 8). In this arrangement, the bottom of the lightning strike rod on the platform is tied to the top center of the array of cables shown in the figure. This cage of cables is closely analogous to the rebar framework of the test igloo to be tested in Alabama and, therefore, served as a suitable checkout vehicle for the instrumentation.

Figure 6 includes the instrumentation configuration that was employed for this measurement. It incorporates a second T&M CVR (F-4000-8-N) inserted in series with one of the down conductor cables of the APS. Data transmission back to the SATTLIF was via a Meret 35-MHz analog FOL, which was the leading candidate for use during the 1991 igloo test. As an experiment, a technique was evaluated for increasing the available dynamic range of the channel by incorporating a gain compression amplifier in the channel. The response of the amplifier as

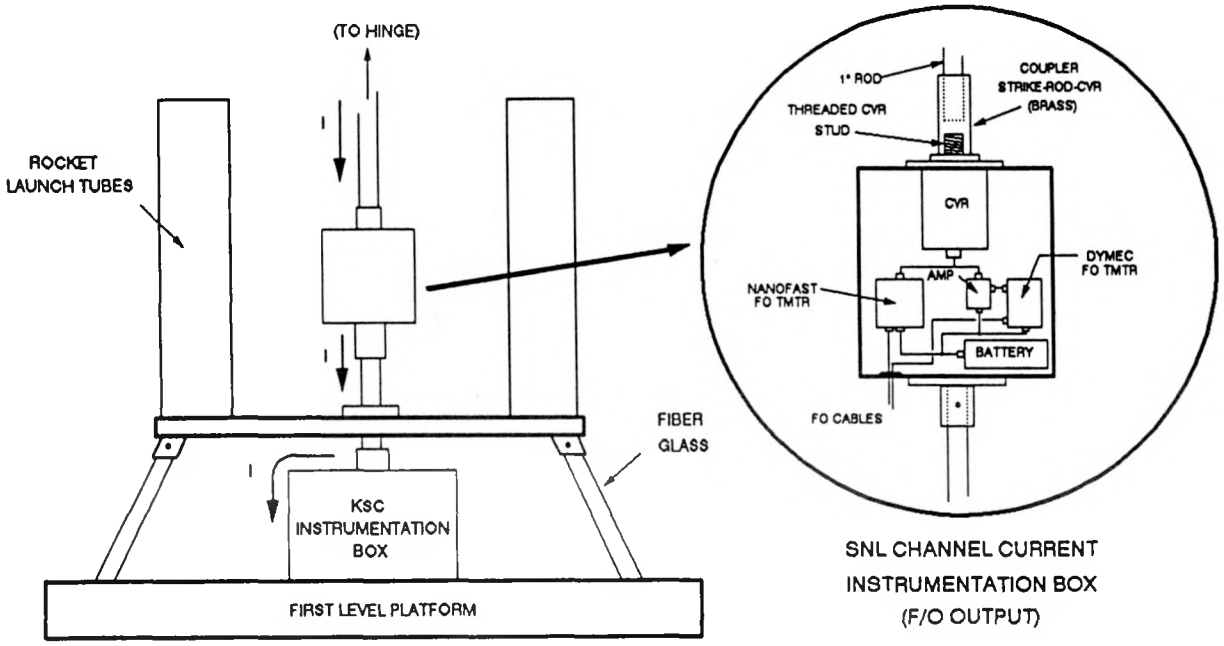

Figure 7. SATTLIF Lightning Current Sensor and Fiber Optic Transmission Instrumentation

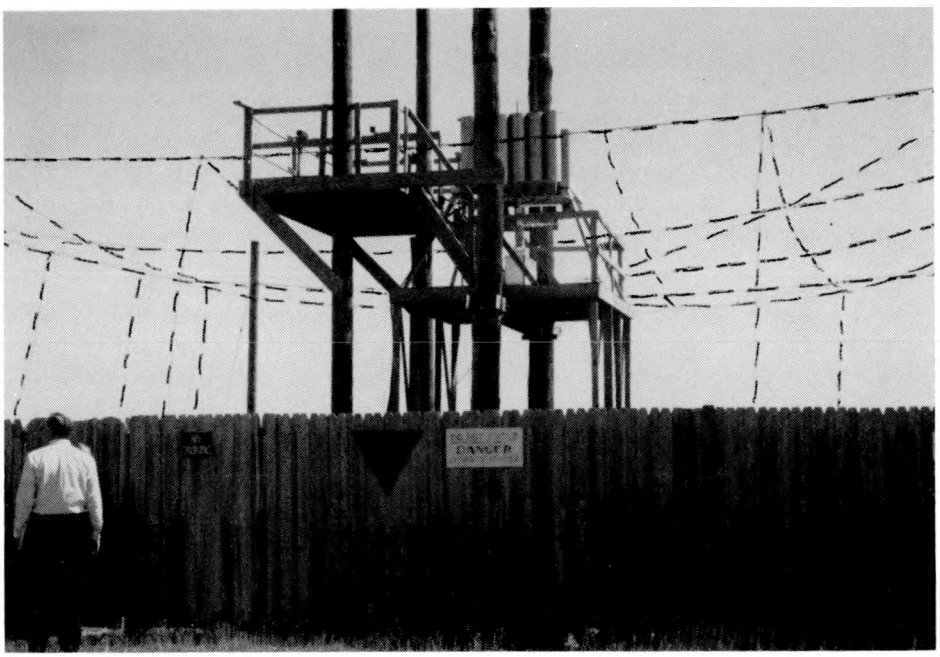

Figure 8. The KSC Land-Site RTL Test Platform with APS Cable Array (cables have been dotted-in for clarity)

a function of input voltage is linear with a fixed gain up to a set point. At that point the gain is abruptly reduced but remains constant. The two gain factors are selected to enhance low-level inputs and reduce large ones, as is indicated in Figure 9. In principle, the original signal is unfolded from the recorded data by multiplying by the inverse of the amplifier's response function. In practice, difficulties were encountered with this arrangement, due to the nonuniform effects of amplifier drift over the the different segments of the response curve. This issue will be discussed further in Section 5.4.1. Fortunately, the experience gained during the field trial indicates that the Meret analog FOL performs well, and that, for the measurement of responses to return strokes, the added sophistication of the gain compression function is not required.

5.1.3 Signal-to-Noise and Calibration

Filtering was added to each channel, as indicated in Figure 6, to preclude aliasing in the digitized records and to improve signal-to-noise quality. Considerable digitization noise reduction can be achieved by adjusting the full-scale signal level downwards from 100 kA. That, of course, is simply a matter of choice in trading off the desirability of capturing the infrequent large stroke versus improving the record quality of the bulk of the data, which is below 50 kA.

Provisions were made for the injection of calibration signals into the fiber optic transmitters of each channel. The Dymec and Meret FOLs were provided with external, pneumatically actuated calibration generators, while the NanoFast unit comes equipped with an internal calibration generator that is actuated via a fiber optic cable to the transmitter. The arrangement is indicated in Figure 6 and was used to obtain pre- and post-shot calibration records during data collection as part of the procedural check list.

5.2 SATTLIF ROCKET SYSTEM

Responsibility for rocket launching was not part of the 1990 program. Nevertheless, a complete system, capable of launching up to six rockets during any triggering session, was designed, built, and successfully dry-run in the field. The following sections describe the rockets and wire dispensing assemblies that are to be used during 1991 and the launch control system that was fielded during 1990.

5.2.1 Rocket and Wire Dispensing Assembly

Requirements on the rocket itself for successful triggering of lightning are not extreme. An ascent velocity of the order of 200 m/s while dispensing the trailing wire up to an altitude of several hundred meters is thought to be the key requirement [12]. Dispensing the wire without its breaking constitutes the most difficult aspect of the operation. Wire breakage during launching was the single most common cause of failure to trigger encountered during early development of the technique.

As mentioned earlier, French experimenters from the Centre D'Etudes Nucleaires De Grenoble (CENG) have been continuously refining the rocket-triggered lightning technique since 1973. Their design uses a commercially available plastic anti-hail chaff rocket manufactured by Ruggieri, a French firm. The black powder rocket motor has been customized

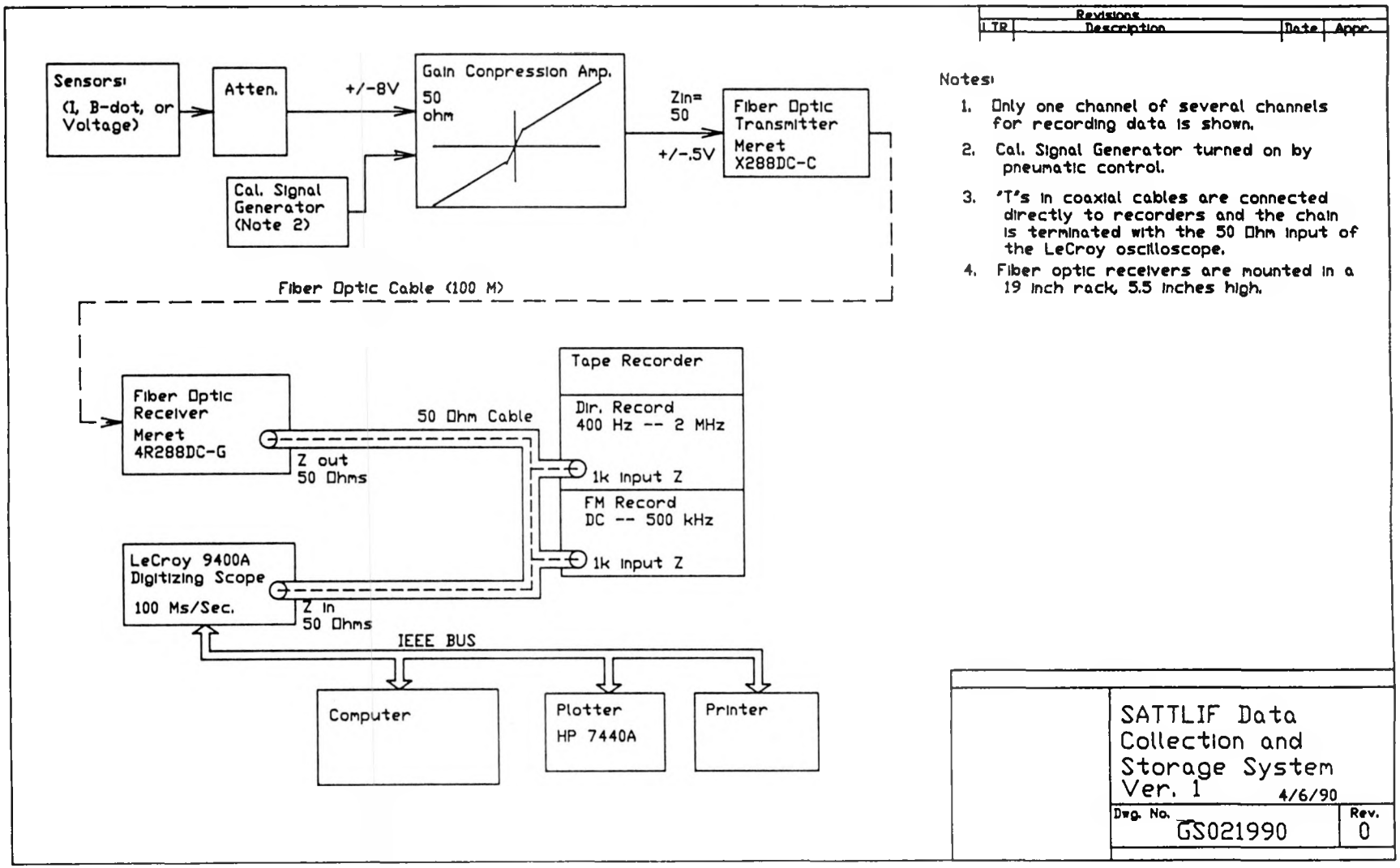

Figure 9. APS Current Measurement Instrumentation

according to CENG specifications for the lightning triggering application and comes separately, each encased in a plastic cartridge. The wire is dispensed from a specially designed spool (patented by CENG) that is attached to the tail end of the rocket. The wire is 7.9-mil-diameter copper and is jacketed by a kevlar fiber material to provide additional strength. Functional reliability of this assembly now approaches 100% percent. Figures 10 and 11 show the assembled rocket bodies with their wire spools attached, ready for the insertion of their motors and firing fuses.

Because of the demonstrated effectiveness and reliability of the system described above, arrangements have been made to procure complete rocket units from CENG for use during the 1991 tests in Alabama. During the 1990 KSC activities, Sandia personnel received training from CENG on the handling and assembly of the rockets and on their launching procedures. A summary of the rocket specifications is given in Appendix A.

Figure 10. CENG Rocket Assemblies Prior to Installation of Propellant Cartridges (Specifications are presented in Appendix A.)

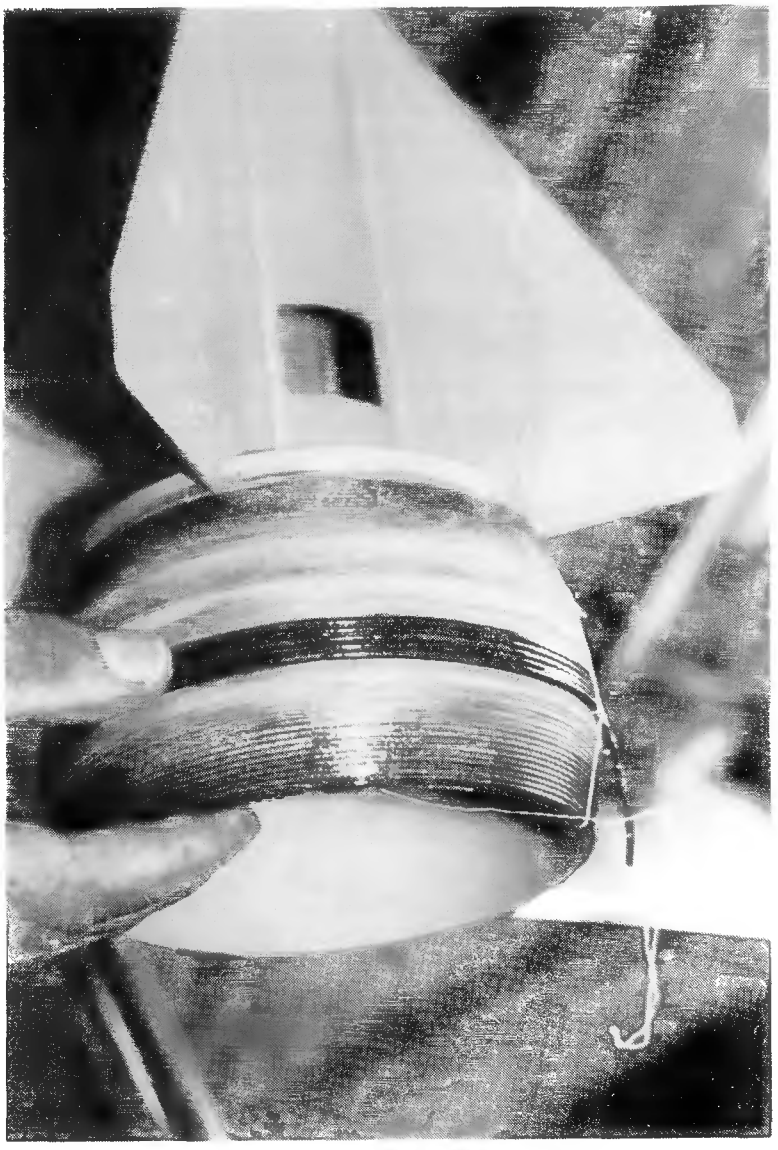

Figure 11. CENG RTL Wire-Dispensing Spools

5.2.2 Launch Control System

The control system is electro-pneumatic. Two pneumatic lines connect the SATTLIF to a Safing, Arming, and Firing (SAF) box at the base of each launch tube. Each SAF box contains a 9-V battery attached to its associated rocket fuse through two separate pneumatic pressure switches (arm and fire functions) and two prearm plugs, all in series (Figure 12). The pneumatic signals to these switches are controlled from the rocket launch panel, which is mounted on the instrumentation rack adjacent to the shielded observation window inside the SATTLIF shelter. Panel switches (Figure 13) control 24-Vdc solenoids that apply pressure individually to the relays in the SAF boxes to arm and subsequently fire each upon command. Arming pressure is applied by activating any one of the six key switches, all of which operate from a single, common key. The single key assures that only one rocket can be armed at a

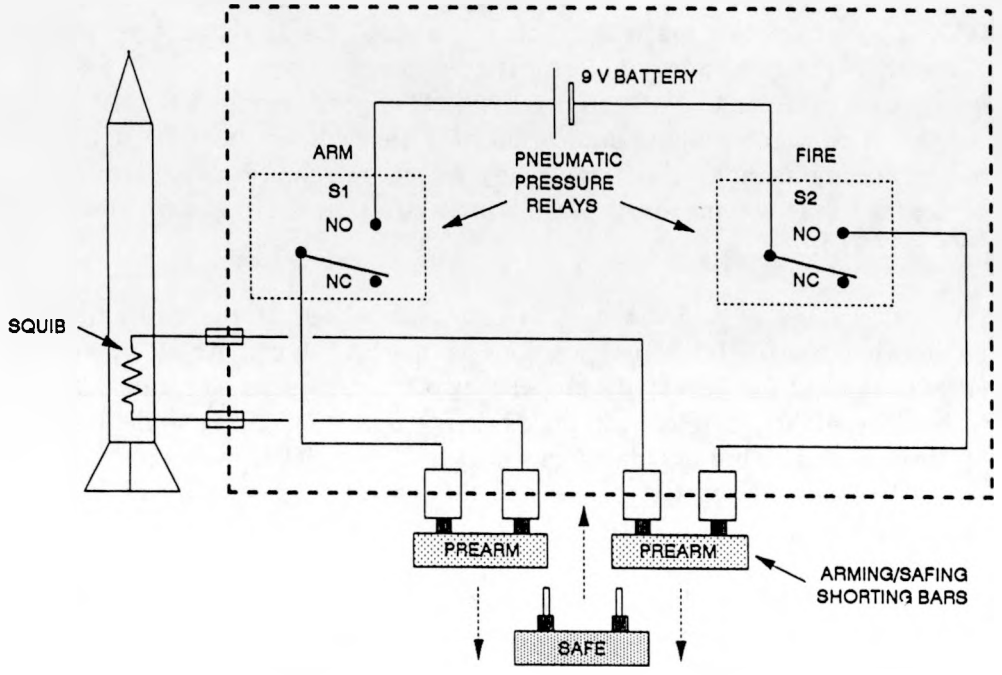

Figure 12. SATTLIF Rocket Launch Safing, Arming, and Firing Circuit

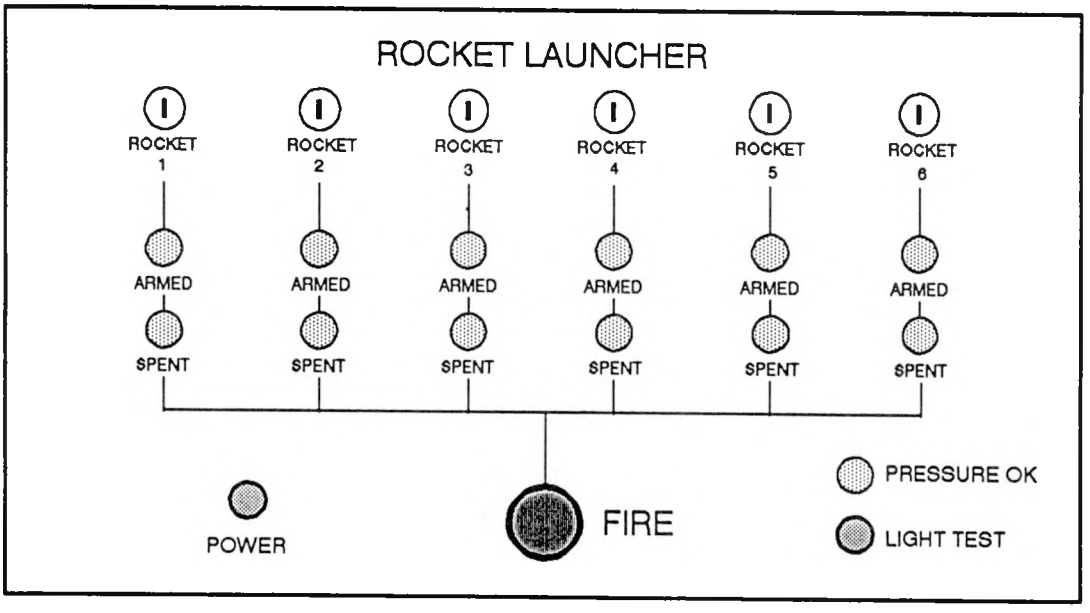

Figure 13. SATTLIF Rocket Launch Control Panel Layout

time. Panel lights indicate the status of each rocket: one light for armed condition and a second light to indicate that the proper launch signal pressure has been applied to the indicated rocket. The ARMED light goes out once the launch takes place and the key switch is turned off. (With the switch in the OFF position, the relay returns to a normally open position and automatically vents the arming line pressure.) All activated SPENT lights remain lit until panel power is interrupted, so that a continuous status indication of which rockets have been fired is provided throughout the triggering session. The single key to the switches is always to be pocketed by personnel working at the launching tubes as an added safety measure against inadvertent arming from within the SATTLIF.

In order for the arming of a given unit to take place, both of the two external prearming plugs must be inserted into their proper positions in the SAF box. At all other times a third, positive-safing plug will be inserted into the two center jacks (Figure 12) as an added precaution against the effects of electrostatic discharge onto the rocket squib line. The proper installation of these external jumper plugs can be visually verified at a glance to confirm that work can safely take place adjacent to the launch tubes with no possibility of inadvertent firing being initiated from within the SATTLIF.

Air pressure to operate the launch control system is provided by a Thomas T-30 air compressor with an integral 2-gallon reservoir tank. Nominal operation pressure is 80 psi. Monitoring of the system pressure is via a gauge on the tank and a pressure sensitive indicator light on the panel.

The entire system was checked out while fully deployed at KSC. One SAF box was mounted adjacent to the existing launch tubes. A series of dummy brigewires was successfully burned upon command from SATTLIF during dry runs and during the countdowns of actual rocket launches. Four live rocket fuses, without rockets, were also successfully fired on command. The checkout included attempts to fire the brigewires and squibs with the system in each of its safed modes. The safety tests included, of course, exposure of the SAF box to the intense electromagnetic environment due to the lightning current immediately next to the actual strike point. No failures occurred.

5.3 AUXILIARY INSTRUMENTATION

5.3.1 Ambient Electric Field Monitor

During storm conditions, the electric field is monitored to provide the basis for rocket launch decisions. Figure 14 is a block diagram of this system. Figure 15 shows the sensing instrument deployed at KSC approximately 50 feet from the SATTLIF shelter. This unit is manufactured by Mission Instrument Co. and is powered by a rechargeable battery pack that provides eight hours or more of continuous operation. The output of the field mill is an analog signal, 0 to ±10 V, which corresponds to an electric field range of ±20 kV/m. The bandwidth of the system is approximately 10 Hz.

Absolute calibration of the system is not a stringent requirement for the RTL application. Nevertheless, the output of the SATTLIF system was checked against two other instruments that were deployed nearby within ~100 feet of the SATTLIF sensor. This was done by comparing readings with those being announced over the radio net during the course of triggering

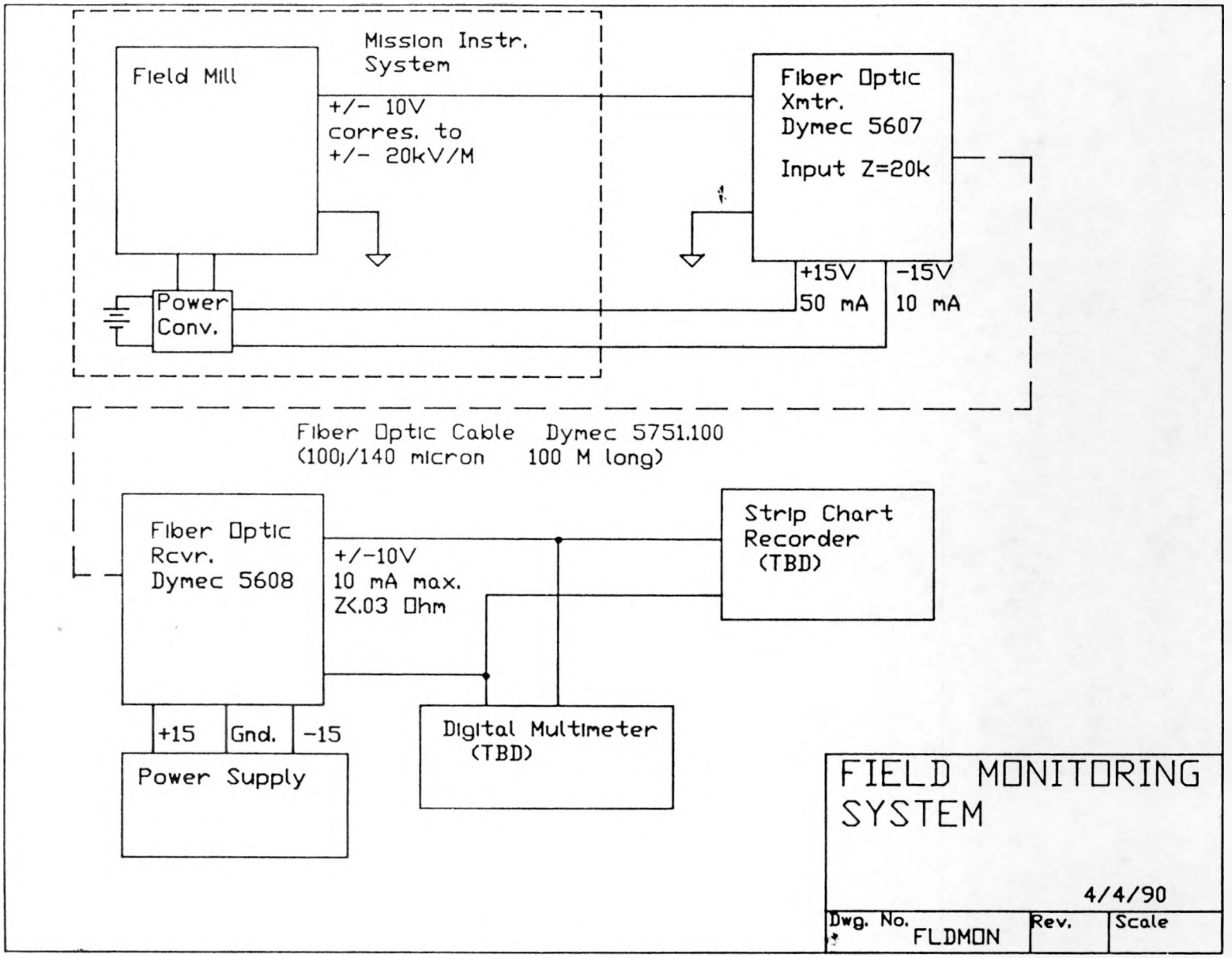

Figure 14. SATTLIF Electric Field Monitoring System

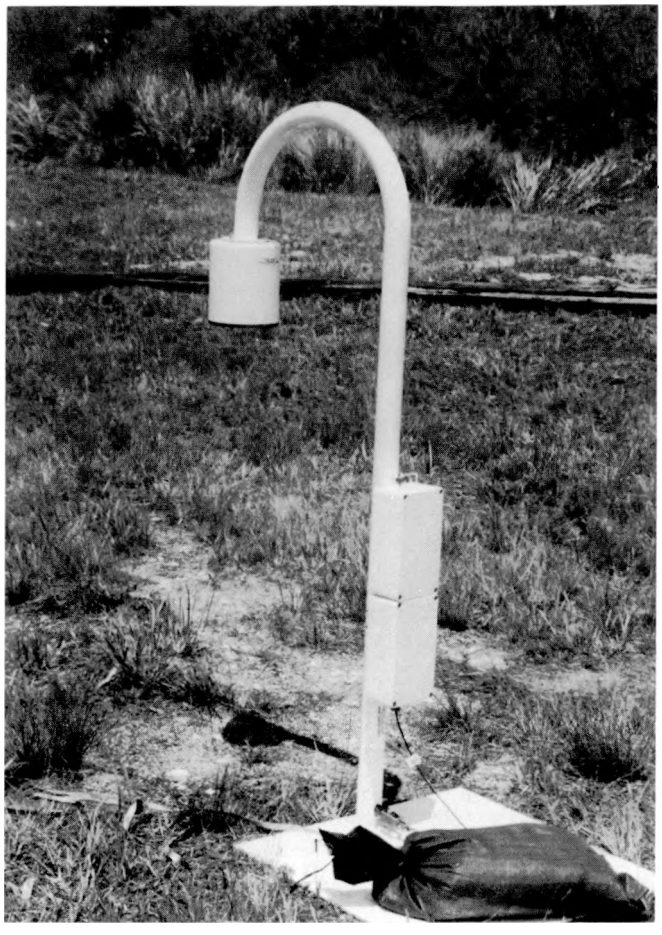

Figure 15. SATTLIF Electric Field Mill Deployed at KSC

sessions, by comparing fair weather readings, and by comparing strip chart recordings. In all cases, agreement was within a couple of hundred volts per meter, which is more than adequate for launch decision purposes and as close as can be anticipated between instruments not precisely co-located and under actual outdoor field conditions.

5.3.2 Video Recording System

A black and white video recording system was employed to monitor 1 meter above and below the intended strike point during the materials damage experiments. A Pulnix TM545 high-resolution, charge-coupled device (CCD) camera was purchased with γ=1 (linear response) and disabled automatic gain control options for this application. A Vivitar 70- to 210-mm macro zoom lens was used with neutral density filters added to provide up to eight stops equivalent of additional attenuation beyond the f/22 lens aperture limit. This added attenuation permitted better resolution of the core features of the channel. The time resolution of the system was limited to ~30 ms, which corresponds to the time between successive video frames. The recorder was a JVC BR-S600U Super VHS video cassette recorder (VCR), which provides several useful stop-frame and editing features. A FOR-A VTG-33 video timer was used to insert a Greenwich time display onto the video record.

The results obtained with this arrangement are thought to represent the closest photographs of actual lightning attachment points on record, and they reveal several features of lightning phenomena (Section 7.5) that are of interest to the lightning physics community.

5.3.3 16-mm Filming System

The 30-ms resolution obtainable with the video recorder is inadequate to guarantee separation of individual return strokes or to define the durations of some of the shorter continuing currents. In order to provide that capability, a 16-mm Action Master 500 movie camera was run during each triggered event. During most flashes, the field of view was adjusted to cover the full launch tower so as to establish where each stroke of the flash terminated. The shutter speed was 1/1000 of a second, and the framing rate was 200 fps, yielding a 5-ms resolution. The camera provides a 100-Hz timing mark at the edge of the frames. Correlation of the recorded channel currents with the optical features of the flashes on the films was both straightforward and very instructive.

Figure 16 shows the mounting of both the video and film cameras inside the SATTLIF. Figures 17 through 19 are individual frames of 16-mm records that show the lift-off of a rocket, a portion of the ICC following the channel of the vaporized wire, and the attachment of a return stroke to the strike rod. (Refer to Figure 2 for correlation.)

6.0 MATERIALS DAMAGE EXPERIMENT

6.1 DESCRIPTION

The materials damage experiment consisted of exposing 2.5-inch-diameter metal disk samples atop a 10-foot strike rod on the experiment platform while simultaneously measuring the current that struck them. The bottom of the pole was connected via low inductance braided strap to the input of the coaxial CVR discussed in Section 5.1.1. As indicated in Figure 7, this sensor was positioned so that only the lightning current injected directly onto the sample (or its supporting pole) was detected. In order to increase the data return during a given storm, a system was devised that allowed the sequential raising and lowering of up to four different samples during any given triggering session.

Each sample was held in a machined brass fixture cup that fit onto the top of one of the 1.5-inch hollow aluminum strike poles. Because of electric field enhancement, the preferred attachment path of the incident lightning would normally be to the edge of the fixture cup. In order to prevent this, a woven-phenolic dielectric sleeve was machined to slide down over the top of the sample and fixture. This sleeve simultaneously served to hold the sample in place in the fixture and suppress streamer formation from the corners of the cup, thereby encouraging attachment to the surface of the sample. No special treatment of the surface of the samples was given other than a wiping with a soft cloth. Once installed on the strike poles, the sample remained in place until an opportunity for triggering lightning occurred. In some cases, this was many days.

On occasion in the past, one or more strokes of a triggered flash had been observed to attach to the side of strike poles below their tops. To prevent this in the present experiment, each of the strike poles was fitted with a dielectric jacket from just below the brass fixture to the top of the hinging mechanism at the bottom of the pole. This jacket consisted of a 2-in polyvinyl chloride (PVC) pipe of ~3/16-in wall thickness.

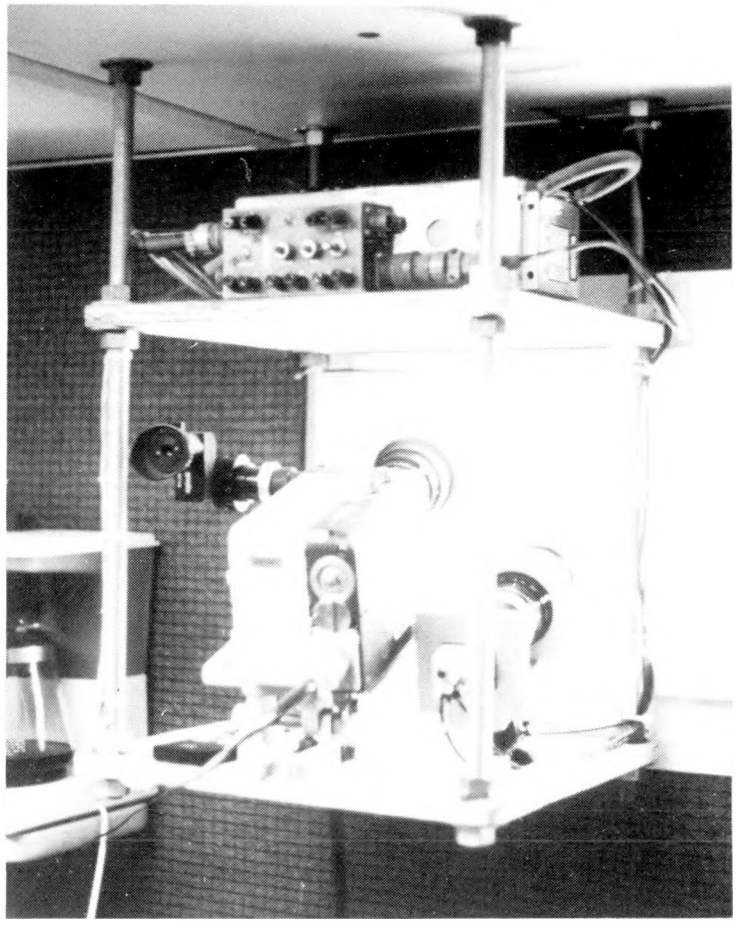

Figure 16. SATTLIF Fast Framing and Black and White TV Cameras

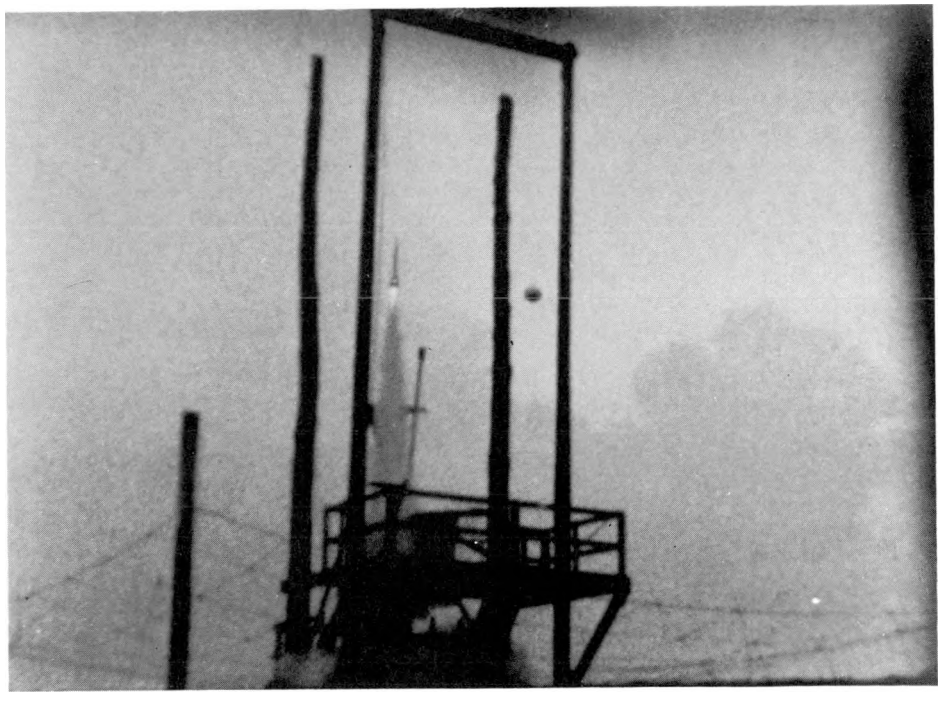

Figure 17. Triggered Lightning Rocket Lift-Off

Figure 18. RTL ICC Following the Vaporized Wire Channel to the Launch Tube

Figure 19. Triggered Lightning Stroke Jumps to the Top of an Upright Metal Sample

Figure 20 illustrates the design. One shortcoming of this arrangement was caused by the necessity to provide water drain holes at the top of the fixture as shown in the figure. On several occasions, streamers from the edge of the brass cup propagated out of these 1/2-inch holes and led to the attachment of the lightning through the hole to the edge of the cup, thereby interfering with opportunities for acquiring the intended data. A modified fixture design has been developed that should eliminate this problem in the future.

Figure 21 shows the design for the hinging mechanism at the bottom of the strike poles, and Figure 22 is a photograph showing the braided strap connections from each pole to the input terminal of the coaxial CVR. Figure 23 shows the four strike poles with the samples installed. A series of pulleys and dielectric ropes that led to a wooden "hitching rack" just outside the door of the SATTLIF was used to raise and lower the samples during a triggering session. The ropes ran over metal pulleys and through metal eyelet bolts at three points on the way to the hitching rack. At two of these points, the pulleys or eyebolts were tied together with heavy braid that was brought to ground to strip off any leakage current that might be tracking along the possibly wet rope. The braided strap tying the eyelets together at the hitching rack was grounded directly to the SATTLIF structure and to a 60-foot-deep earth grounding rod. Thus, the rope, the SATTLIF structure, and the operator were maintained at the same local ground potential. Figure 24 shows one of the samples positioned in readiness for a strike.

6.2 OPERATIONAL PROCEDURES

The SATTLIF was manned by the two authors during all tests. The standard operational procedures involved the use of a formal checklist that was divided into sections covering preliminary setup, launch imminent, final, and post-shot activities. The checklist was read by one operator and acted upon and responded to by the other. The checklists were printed out in a format that provided designated spaces for entering setup particulars and post-shot notes on each shot, so that they served as the master test log sheets as well. Setup included the recording of pre-shot calibration signals through each channel.

The launching of rockets was carried out by the French experimenters from CENG. This activity was conducted from a separate instrumentation shelter located approximately 150 feet from the SATTLIF. Communications with SATTLIF and all other participating stations was via radio link. As storm conditions matured, various alerts concerning the ambient electric field and the imminence of triggering conditions were broadcast from the control van. Once each of the participating stations reported readiness, control was turned over to the CENG launch operator, who continued to broadcast the ambient field periodically and initiated a 10-second countdown at the appropriate moment. It was at this point that the final SATTLIF countdown was also executed to arm the digitizers and spin up the 16-mm camera and magnetic tape recorder.

The post-shot checklist included downloading of the digitized data, recording of post-shot calibrations, review of the video recording to confirm an attachment to the sample, reloading of 16-mm film magazines, and positioning of a fresh sample. The latter operation was conducted by first obtaining permission from the launch operator to leave the SATTLIF, and then exiting the SATTLIF to the area just outside the door under the metal safety roof (Figure 4). Using the ropes anchored to the hitching rack, the exposed sample was lowered, and a fresh one was hauled up. Upon re-entering the SATTLIF, the launch operator was notified, and the watch for the next suitable launch opportunity was commenced. The process of exchanging samples was typically accomplished in less than a minute.

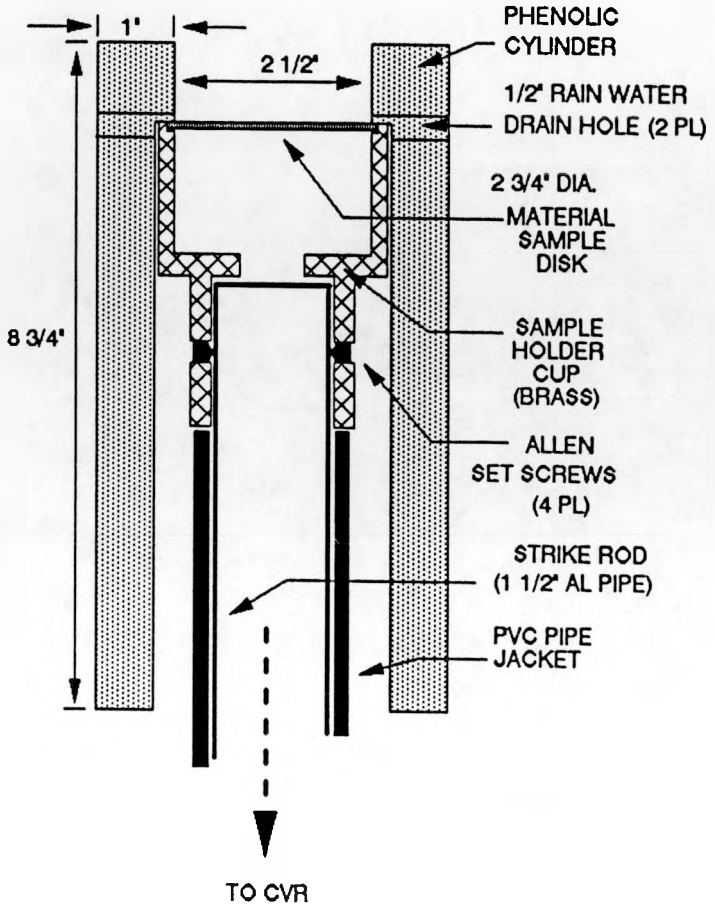

Figure 20. Test Sample Fixture Design

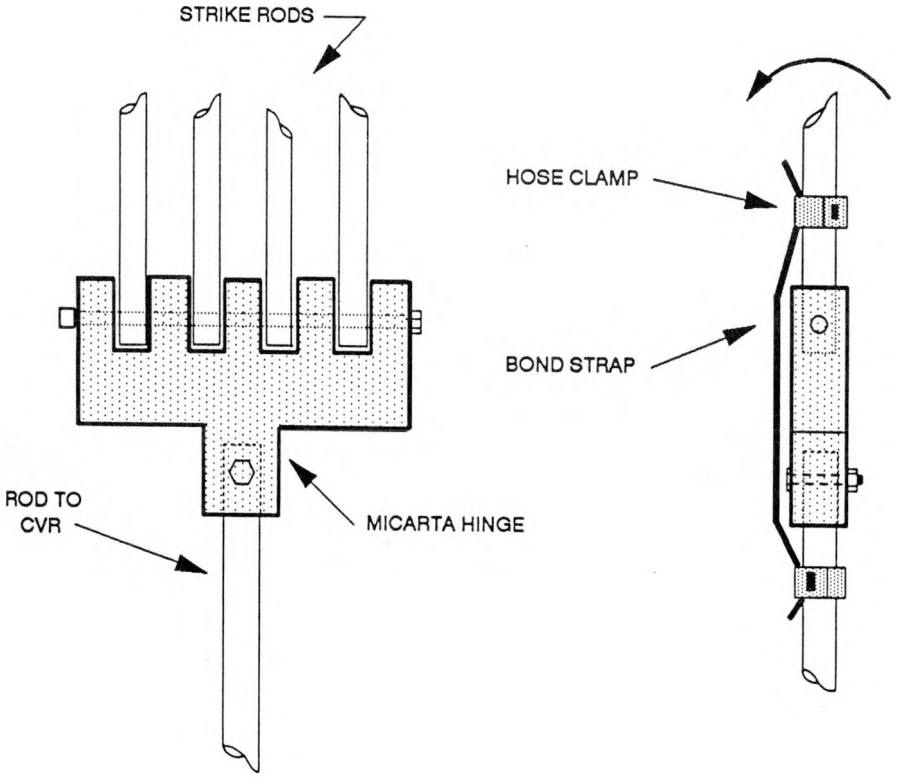

Figure 21. Dielectric Hinging Mechanism for Raising and Lowering Samples

Figure 22. Connection of the Sample Strike Poles to the Flash Current Instrumentation

Figure 23. The Four Strike Poles with Samples Installed

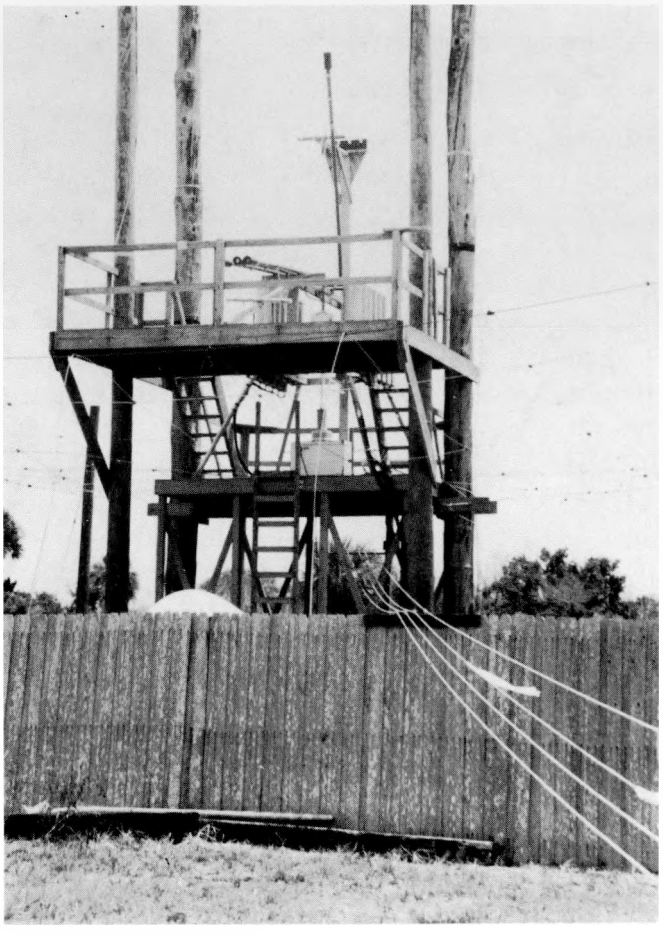

Figure 24. A Strike Pole with Sample Installed Raised in Readiness for a Triggered Lightning

Between-shot turnaround was controlled primarily by the time required to download the digitizers and change film in the 16-mm magazines. The latter bottleneck can be readily eliminated by increasing the number of magazines maintained on hand. The data downloading time is largely fixed by the LeCroy software constraints. Modification of some of the data labeling procedures and possible software automation options are being considered for the future. Since there were two active launch sites at KSC to support different kinds of experiments, triggering was alternated between each launch pad in turn as the opportunities permitted. This generally provided sufficient time for setup for the next Sandia launch opportunity without delaying the overall operation. During the three active storms in which the present data were obtained, approximately 30 launches were conducted, counting those from the alternate pad.

7.0 DATA

7.1 CHANNEL CURRENTS

Table 1 summarizes all the attempted triggerings in which Sandia participated. Of the 16 total rocket launches, 5 did not result in lightning. Since the experimental objectives of the other participants in the program involved evaluating triggering under non-optimum conditions (low fields, immediately after naturally initiated lightning, etc.), no significance relative to achievable triggering success should be attached to these numbers. That is, the success ratio could readily have been increased if that had been the sole objective of the effort.

One of the main objectives of the Sandia tests was verification of the proper performance of the SATTLIF instrumentation in directly recording the lightning channel currents. Table 2 summarizes the set of common data measured simultaneously by KSC and Sandia. These data include only return strokes since the present KSC instrumentation does not have the low-frequency bandwidth necessary to record continuing currents. The KSC peak currents I_p in the table were read from a set of hard copy plotted on a time base of 4 μs per division. Given

TABLE 1
1990 RTL SHOT SUMMARY

SHOT ID	DAY	TIME (GMT)	E-FIELD (kV/m)	COMMENT
90-01	7-24	2107:29	+1.5	NO LIGHTNING
90-02	8-08	1910:29	-3.2	DATA ON 0.077" Al
90-03	8-08	1924:52	-2.8	DATA ON 0.077" Al
90-04	8-08	1937:14	-2.4	DATA ON 0.077" Al
90-05	8-08	1951	-2.4	NO LIGHTNING
90-06	8-09	1905:58	-5.2	STREAMER ONLY; SPOT ON AL
90-07	8-09	2013:48	-4.5	DATA ON 0.077" Al
90-08	8-09	2026:22	-3.2	DATA ON 0.077" Al
90-09	8-09	2041:14	-3.1	DATA ON 0.077" Al
90-10	8-11	2054:56	-4.4	NO LIGHTNING
90-11	8-11	2055:19	-4.8	NO LIGHTNING
90-12	8-11	2057:15	-3.8	DATA ON 0.035" STEEL
90-13	8-11	2116	-3.5	NO LIGHTNING
90-14	8-11	2126:33	-4.0	DATA ON 0.035" STEEL
90-15	8-11	2131:54	-3.2	STREAMER ONLY; SPOT ON STEEL
90-16	8-11	2136:32	-3.5	WIRE BURN ONLY

TABLE 2
COMPARISON OF STROKE CURRENT MEASUREMENTS

SHOT NO.	STROKE NO.	SANDIA I_p (kA)	KSC I_p (kA)
90-07	1	24.5	22.6
	2	18.0	17.2
	3	23.5	22.3
90-08	1	13.8	14.4
90-09	1	16.5	16.0
	2	4.1	4.2
90-12	1	3.9	3.9
	2	15.8	13.4
	3	27.5	22.4
90-14	1	17.0	15.0

the inherent noise level on the data, the accuracy achievable this way is limited. The resulting differences between the two sets of measurements had a mean of 7.4% with a standard deviation of 5.9%. In general, the SATTLIF data yielded the higher value when there was a difference. The KSC data were sampled every 50 ns, while those of Sandia were sampled every 80 ns. Both rates are more than adequate to resolve the rise time of the current front. For comparison, Figure 25 shows the three constituent strokes of Flash 90-07 as measured by both KSC and Sandia and plotted on the same time scale.

Plots of each flash current recorded by the SATTLIF are presented in Appendix B, organized by flash ID number. In each case, the full incident flash current appears first, followed by the individual return strokes, where available, plotted out to approximately 200 μs. Finally, a plot of each return stroke is given on an expanded time scale to permit examination of its current front. In the latter plots, the sampled data points are shown.

The plots of the full flash appearing in Appendix B are those that were recorded on the Dymec FM channel described in Section 5.1.1 that was designed specifically to record the continuing current accurately. In order to provide good resolution of these relatively low-level currents, full-scale response was set to 1 kA. A detailed identification of the major peaks appearing in these plots required a frame-by-frame analysis of the 16-mm films supported by correlation with the analog tape recordings of the NanoFast channel data. In this way it was possible to sort out which major pulses corresponded to return strokes and to identify which portions of the current actually attached to the tops of the samples.

7.2 APS DOWN CONDUCTOR CURRENT MEASUREMENTS

Successful measurements of the return-stroke currents flowing in two separate down conductors of the APS array were obtained during flashes occurring on August 9 and 11. The version of the APS on which these measurements were made had a total of 40 down conductors,

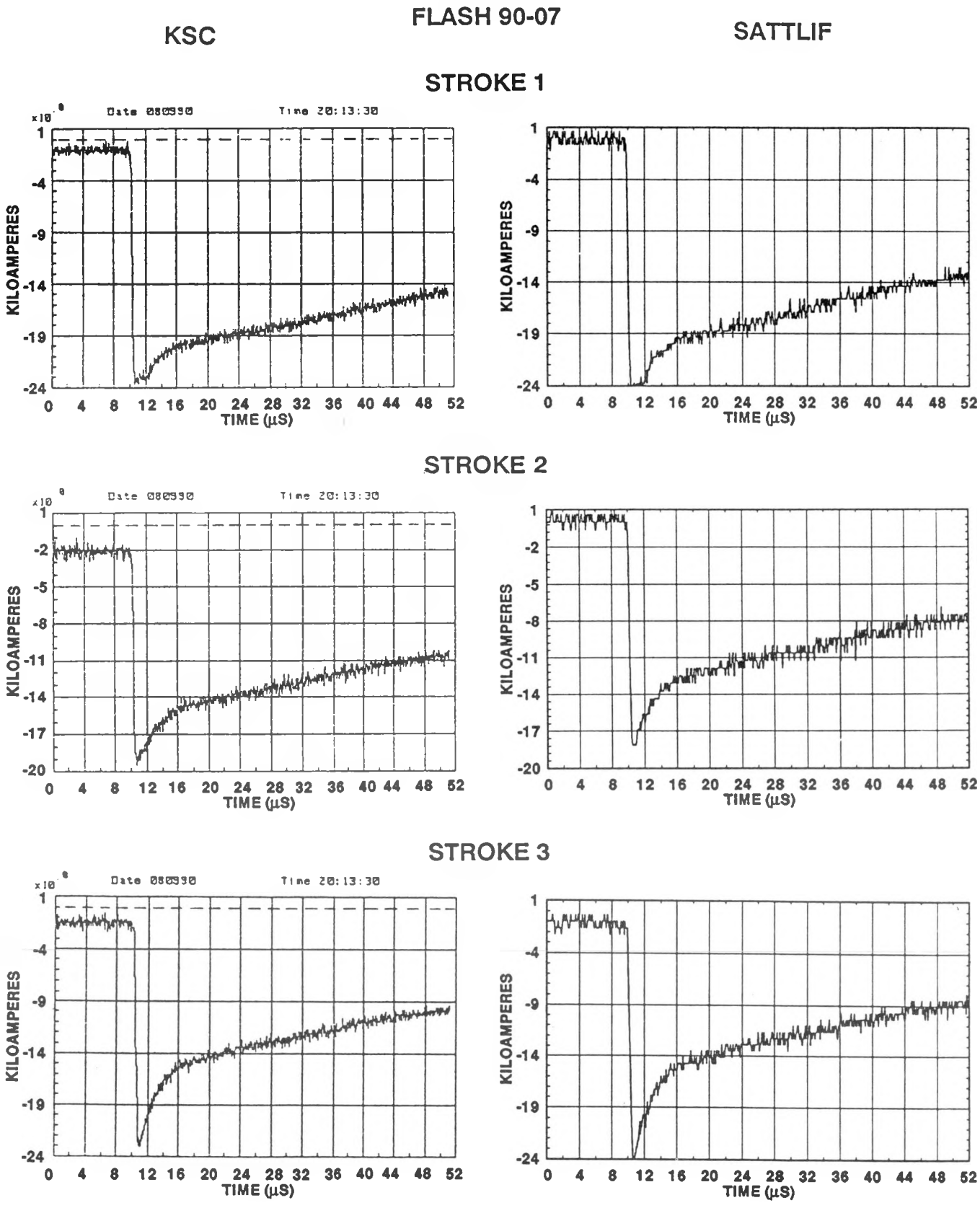

Figure 25. Stroke Currents Measured by KSC and SATTLIF Instrumentation on Flash 90-07

10 on each of the 4 sides of the array. The conductors were of stranded steel wire cable. The measurements were made by physically and electrically inserting the sensor package described in Section 5.1.2 in series between the bottom of the cable and the horizontal counterpoise cable that runs around the perimeter of the APS at a depth of 18 inches in the sandy ground (Figure 26).

On August 9 the sensor was installed on the first cable on the north side of the array next to the northwest corner post. On August 11 it was moved to the middle cable on the same side.

Given the symmetry and dimensions of the structure in comparison with the component wavelengths of the lightning return-stroke currents, the current division among the array conductors would be expected to be about equal, with each carrying approximately 1/40 or 0.025 of the total current incident on the strike rod. Because of modifications to the original structure, various cables have slightly differing diameters. The diameters of the corner cables were 0.42 in, while those of the others alternated around the perimeter between 0.32 and 0.25 in. These variations, plus possible differences in the resistances at connection nodes throughout the array, might alter the expected ratios somewhat. Table 3 gives the results of this set of measurements, and Figure 27 shows an example of the incident stroke current and its corresponding cable current. Per the above discussion, they ought to both have the same waveshape. Appendix C contains plots of the full set of these measurements along with the corresponding incident stroke currents for easy reference.

As was discussed briefly in Section 5.1.2, the cable instrumentation incorporated an experimental amplifier with a dual-gain response function (Figure 9). The advantage of this concept is that, in principle, it increases the effective dynamic range of the channel by selectively amplifying the lower-level portion of the input signal by a larger factor than the higher-amplitude portion. Unfolding is done by multiplying the raw digitized data by the inverse of the gain function.

Figure 26. Sensor and FOL Instrumentation Installed on APS Cable Current Measured on Flash 90-14

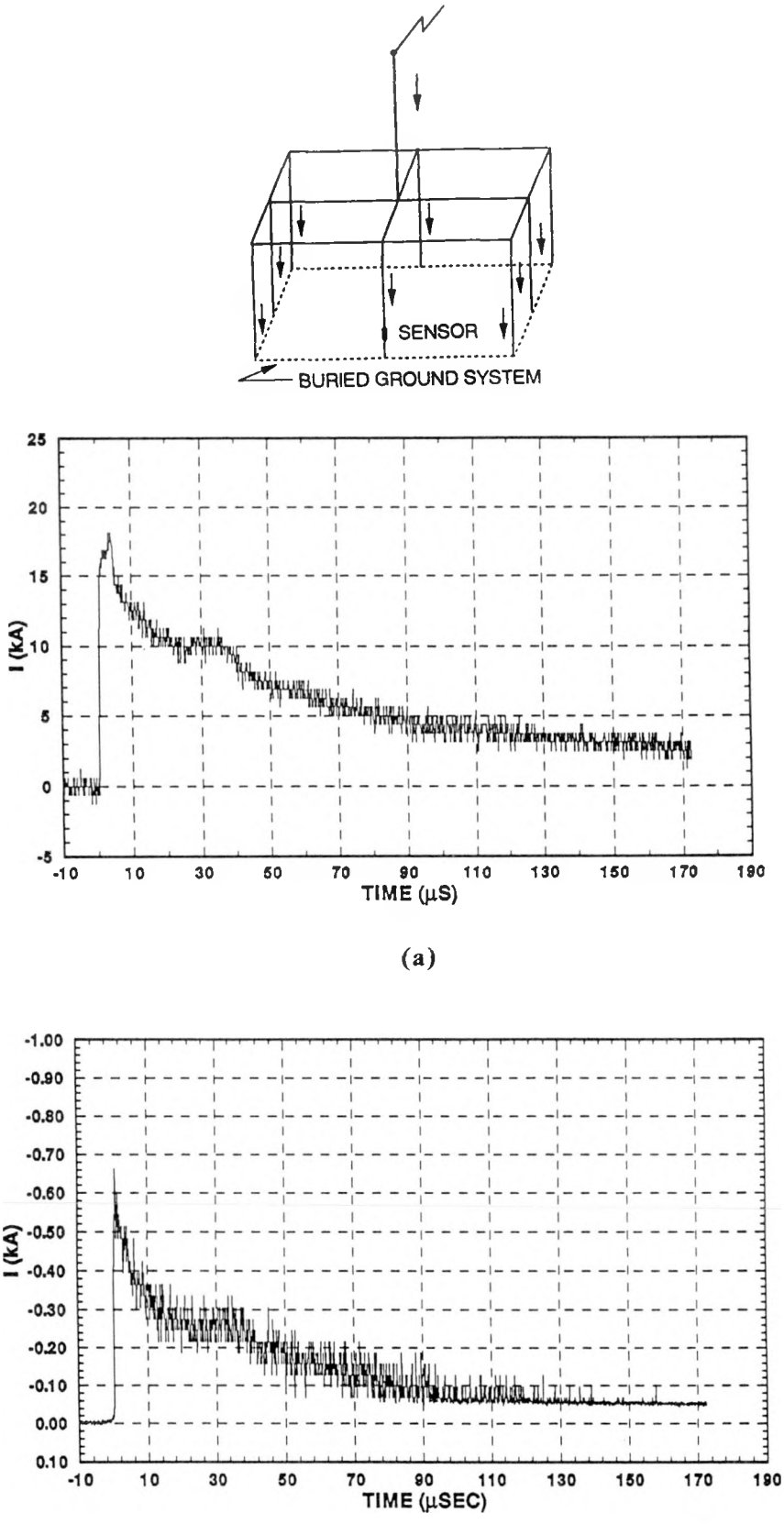

Figure 27. (a) Incident Stroke Current and (b) Corresponding APS Cable Current Measured on Flash 90-14

TABLE 3
APS CONDUCTOR CURRENT DATA SUMMARY

SNL FLASH ID	DATE	TIME	STROKE NO.	I_p CHANNEL (kA)	I_p CABLE (A)	RATIO
90-07	8-9	20:13:48	1	24.5	660	0.027
			2	18.0	500	0.028
			3	23.8	600	0.025
90-09	8-9	20:14:14	1	16.5	420	0.025
			2	4.1	80	0.020
90-12	8-11	20:57:15	2	15.8	520	0.033
			3	28.0	870	0.031
90-14	8-11	21:26:33	1	17.5	600	0.034

In practice it was found that baseline drift in the amplifier corrupted the raw data in a complicated way so that iterative processing was required on each individual recording to recover the true waveform. The procedure involved adjusting the baseline of the raw data until the baseline of the unfolded data fell at zero just prior to the breakpoint of the waveform. The tedium and degree of operator judgement inherent in this process make it unattractive.

A second artifact of the dual-gain amplifier can be observed in Figure 27. Since the final waveform is derived by multiplying the raw data by the inverse of the gain function, the noise on the higher amplitude portion of the waveform becomes artificially amplified, while that on the remainder of the record is suppressed.

The experience gained at KSC indicates that adequate dynamic range for the bulk of the data can be achieved without resorting to any type of nonlinear modification. Use of the gain compression provision will therefore be eliminated.

7.4 MATERIALS DAMAGE DATA

Witness data spots along with the incident currents that produced them were obtained on samples of 2024-T3 aluminum and 4130 ferrous steel. A matrix of materials and thicknesses was part of the test plan covering these experiments. In addition to the aluminum and steel, the materials included copper, stainless steel, and titanium. In setting the priority of each material, aluminum was first, both because of its widespread use in Sandia products and because much of the laboratory test data base in the existing literature is on aluminum. Steel was next in priority because of its use in some Sandia weapon designs of current interest. The thickness of the tested aluminum samples was nominally 80 mils, which corresponds to the thickness of many aircraft wings and is therefore well represented for comparison reasons in the existing laboratory test data base. Had further opportunities for data occurred, the priorities would have been copper (for comparison with available samples of copper exposed to unrecorded lightning currents in a previous experiment by Uman [1]), stainless steel, and titanium.

Through detailed examination of the 16-mm films, flash currents recorded on the various channel types, and the samples themselves, it was possible to correlate individual spots on many of the samples with the streamer, return-stroke, and continuing currents that produced them. These data provide a definitive set of reference benchmarks against which to improve and quantify the fidelity of laboratory burnthrough simulation. Table 4 summarizes the important flash parameters measured on the currents that were verified by the 16-mm films to have passed through the samples.

TABLE 4
DATA SUMMARY
OF STRIKES TO MATERIAL SAMPLES

FLASH ID	STROKE	I_p (kA)	T_r (μs)	CC	DURATION[1] (ms)	CHARGE (C)
90-02	LAST[2]	13	1.3[3]	Y	50	7.6
90-03	1	13	<1	Y	120	13.6
	2	5.3	<1	Y	3	0.5
90-04	LAST	19	<1	Y	40	5.5
	LAST-1	13	<1	N	---	0.4
	LAST-2	5.4	1.9	Y	30	1.8
90-07	1	24.5	0.4	Y	6	0.5
	2	18	0.3	Y	10	2.3
	3	23.8	0.5	Y	10	2.7
90-08	1	13.8	0.5	N	3	0.01
90-09	1	16.5	0.5	Y	6	0.76
	2	4.1	1.1	Y	2	0.42
90-12	1	3.2	~3	Y	20	5.8
	2	15.8	0.7	Y	32	7.8
	3	28	0.6	Y	175	49
90-14	1	17.5	0.5	Y	25	7.8

[1] Approximate

[2] Only the last stroke of this flash hit the sample.

[3] Due to FOL malfunctioning, no high time resolution data were recorded for strokes in flashes 90-02,03,04 on 8-8-90. Peak currents I_p and 10-90% rise times T_r in this table are as read from plots of the KSC records for these shots.

Photographs of each of the samples for which significant results were obtained are presented in Appendix D. Each photograph is accompanied by a plot of the total current that passed through the specimen. Also given at the beginning of Appendix D is a table of summary comments on each sample. Several examples of particular interest are presented. In this discussion, all quoted dimensions of the damage spots are approximate and were obtained with the aid of a millimeter scale only. Observational comments reflect only what could be visually noted with the aid of a hand-held magnifying lens.

Figure 28a shows the aluminum sample that was exposed on Flash 90-02. Figure 28b is a plot of the current that was recorded on that event. These data illustrate the importance of the 16-mm high-speed films. In this case, the film clearly reveals that during the flash the wind carried the ICC channel across the front of the three samples that were lying horizontal prior to being erected for exposure. As a result, the first seven strokes of the flash attached to one or more of these samples, and only the current appearing to the right of the indicated line in Figure 28b passed through the sample. The spot labeled RS#8 in Figure 28a can therefore be deduced to have been caused unambiguously by the indicated current in Figure 28b, which transferred ~7.6 coulombs of charge.

The two most dramatic results are indicated in Figures 29 and 30, corresponding to Flashes 90-03 and 90-12, respectively. Flash 90-03 was comprised of two strokes, both of which were photographically confirmed to have attached to the top of the erected aluminum sample. The first stroke was followed by a continuing current that transferred approximately 13.6 coulombs of charge at a sustained level of 100 A. The corresponding spot on the sample is concluded to be the large one, labelled "1" in the photograph. This spot has a diameter of ~8 mm. On the back side of the specimen directly behind the spot is an area of slight discoloration and a raised "dot" of 1.5-mm diameter and 0.1-mm height.

Correlation of the other two major spots appearing in the photograph is less definitive due to the clear photographic evidence that only a total of two strokes attached to the sample during this flash. The second stroke of Flash 90-03 was a weak one with no continuing current. It is therefore doubtful that it is responsible for the rather significant spot, labelled "2." The spot immediately to the right of number 1, while fairly large in diameter, is only a surface scar that shows no discoloration whatever from heating. It is therefore postulated that this mark corresponds to the second return stroke of Flash 90-03 shown in Figure 29b. That leaves the larger number 2 spot to be accounted for. It is speculated that it may have resulted from the attachment of one of the "wayward" strokes from Flash 90-02 discussed earlier. (Resolution of the 16-mm records is unfortunately inadequate, partly because of the obscuring smoke of the rocket plume, to establish which of the horizontal pole(s) was struck during Flash 90-02.) This possible explanation for the source of spot number 2 is supported by the fact that its appearance and size is very similar to the single unambiguous spot appearing on sample 90-02. It is just such a spot that would have resulted from the attachment of the second return-stroke and continuing current combination shown in Figure 28b, for example. The remainder of the minor spots on the 90-03 sample clearly correlate with streamer currents that did not result in return-stroke attachments.

Returning to spot number 1 on 90-03, it is noted that the damage it represents is both significant in extent and was produced by a continuing current of quite modest severity. According to the Cianos and Pierce lightning data base compilation [17], for example, both the 100-A magnitude and 120-ms duration of the continuing current fall at approximately the

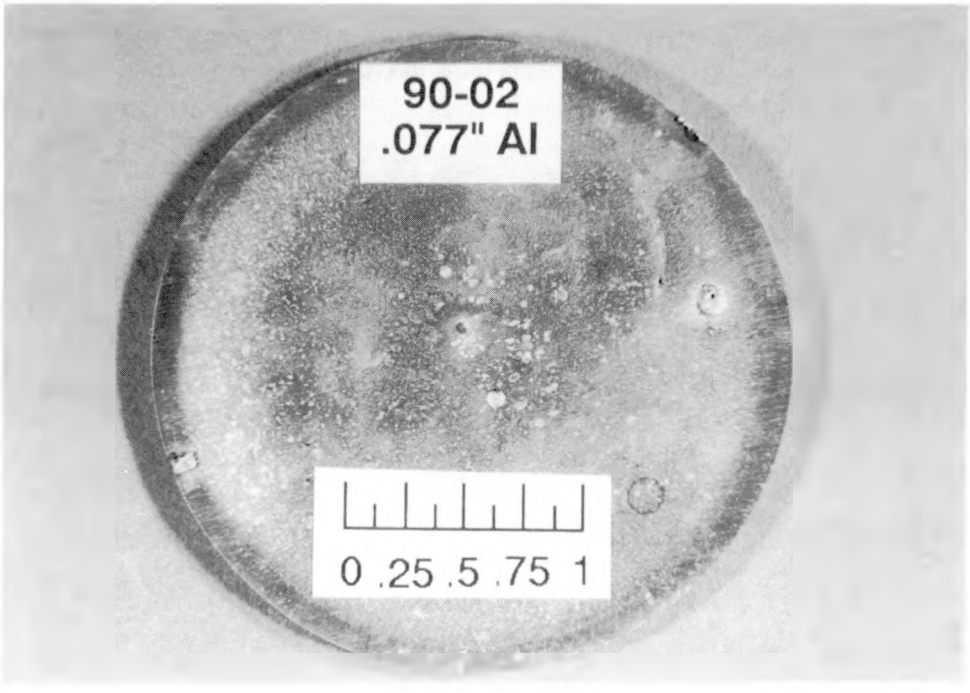

(a)

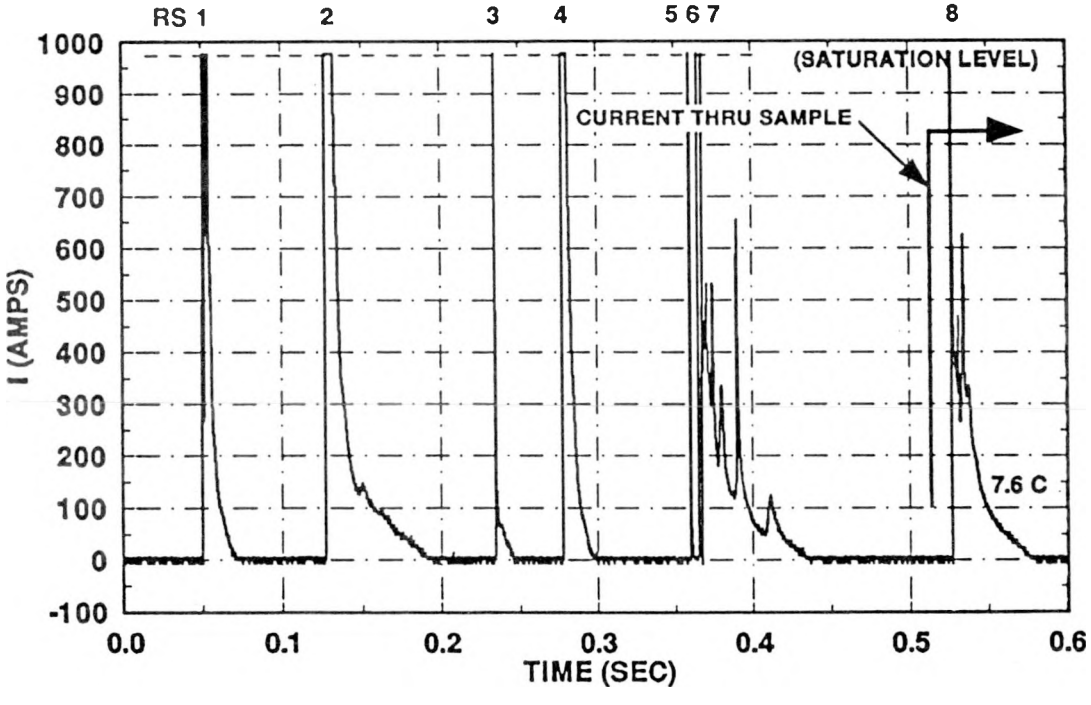

(b)

Figure 28. (a) 77-mil Aluminum Sample Following Exposure on Flash 90-02, (b) Measured Current Through the Sample

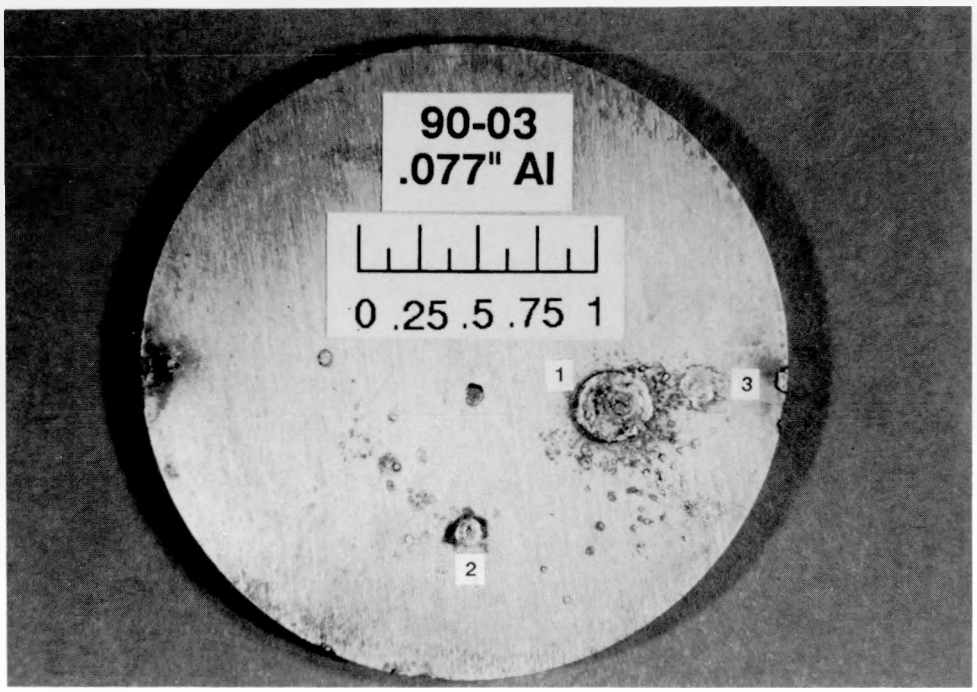

(a)

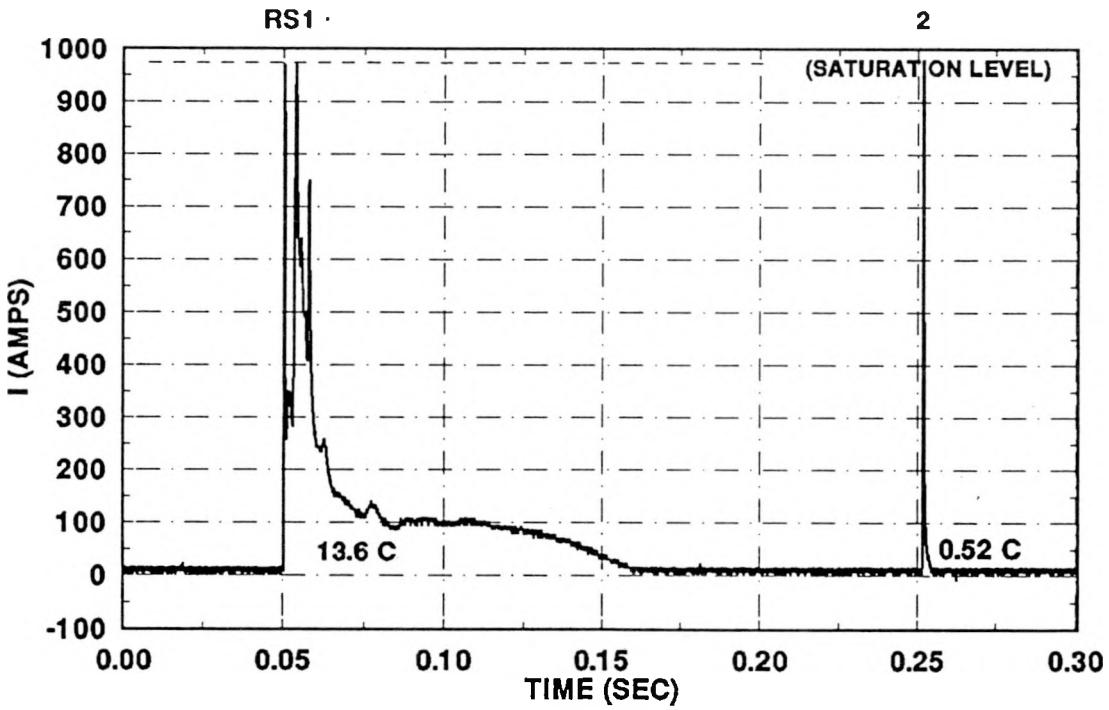

(b)

Figure 29. (a) 77-mil Aluminum Sample Following Exposure on Flash 90-03, (b) Measured Current Through the Sample

(a)

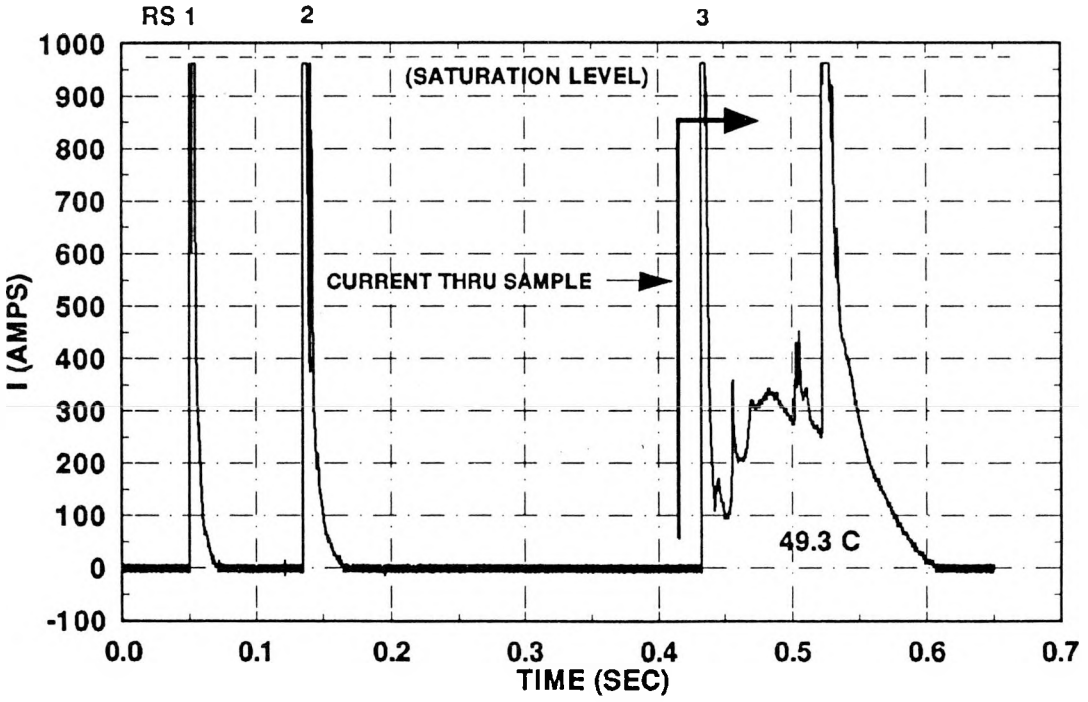

(b)

Figure 30. (a) 35-mil Steel Sample Following Exposure on Flash 90-12, (b) Measured Current Through the Sample

thirtieth percentile points on their respective frequency distributions. That is, the amplitude and duration of continuing currents fall below those levels in only 30% of all cases. Furthermore, the 13-coulomb charge transfer falls at only the twelfth percentile point on that distribution. From either point of view, the present current was not even of median severity.

Figure 30a shows the damage produced on a steel sample during Flash 90-12. Again, as confirmed by the 16-mm record, the first two strokes indicated in Figure 30b terminated on one of the horizontal samples. Only the current starting at approximately 430 ms in the figure attached to the upraised specimen. That portion of the current consists of a single return stroke of 28-kA peak amplitude followed by a rather severe continuing current. By virtue of its position within an established continuing current and its very slow rise time (>400 μs), the broad peak occurring at 520 ms is not a return stroke. It is simply one of a series of relatively large surges of current observed on several occasions within continuing currents. (See, for example, Flash 90-04 in Appendix D.) From correlation with the NanoFast channel record of this flash, it can be deduced that the peak of this particular surge was <1.5 kA. A plausible explanation of these surges, which are plainly evident on the film records, would appear to be that they are associated with contact of the lightning channel with locally large pockets of available charge within the cloud.

According to Cianos and Pierce, 300 A and 49 coulombs fall at approximately the ninety-third and eightieth percentiles of their respective frequency distributions. This event, therefore, represents a fairly severe, but by no means extreme, continuing current, and it produced commensurate results on the 35-mil steel sample. The cluster of three large overlapping spots at the 8:00 position in the photograph appear to result from some migration of the attachment point during the course of the continuing current. At some point in time, the spot stuck at the center, where it effectively burned through the full thickness. The small spot in the middle of the center one is a miniature crater with its rim raised up ~0.5 mm above its surrounding material. Within this crater is a penetration approaching 1 mm in depth. Figure 31 shows the back side of the same sample. The central feature in the darkened area corresponds to the pin-hole location on the front side. There is no residual line-of-sight penetration at this point, but it appears evident that, during the current flow, the metal was fully molten.

Following the same process of examination of all the recorded data, a number of other data points have been established, with varying degrees of confidence, to correspond to individual strokes and continuing currents. In subsequent laboratory work using the Sandia Lightning Simulator (SLS) in Albuquerque, attempts will be made to replicate the damage under simulated conditions. In each case, the link back to real lightning will be the applied current, which will be adjusted to correspond in amplitude and shape to what was measured in the present experiments. Other parameters of the test configuration, such as the geometry and material of the SLS output electrode, electrode spacing, use of a fine starter wire, etc., will then be varied until the best duplication of the present data spots is achieved. Detailed metrology, possibly including sectioning, will then be carried out to quantify the correspondence and, consequently, the degree of simulation fidelity that has been achieved. From that point, use of the optimum technique will be employed in all such testing.

7.5 VIDEO OBSERVATIONS OF STREAMERS AND CHANNEL FEATURES

The video records of several of the flashes reveal upward-going streamers from the top of the samples. Such streamers before strokes preceded by dart leaders have not previously been

Figure 31. Back Side of Steel Sample Exposed on Flash 90-02

reported. Since, as mentioned in Section 3.0, the strokes of triggered lightning are normally initiated by dart leaders, the present records are of interest in this context. Figure 32 shows one example of this phenomenon. The original video frame reproduced in Figure 32a shows two individual streamers, only one of which is evident in the reproduction. Figure 32b occurs two frames later (time resolution is ~30 ms per frame) and shows both streamers as well as the return stroke's attachment to the sample. The return stroke channel overlays the faint streamer that did not reproduce very well in Figure 32a, while the streamer that does show in Figure 32a overlays the lower streamer in the second figure. Unfortunately, the limited 30-ms time resolution of the video leaves some degree of uncertainty in the interpretation of these observations.

Figure 33 is of interest in that the bright segment of channel about a foot above the sample appears to be the junction of the upward streamer with the downward traveling dart leader. (The scale was determined from separate records in which an included scaling device was visible.)

Finally, Figure 34 illustrates not only upward streamers, but also the attachment of a return stroke to the sample through the 1/2-inch water drain hole on the side of the dielectric shield

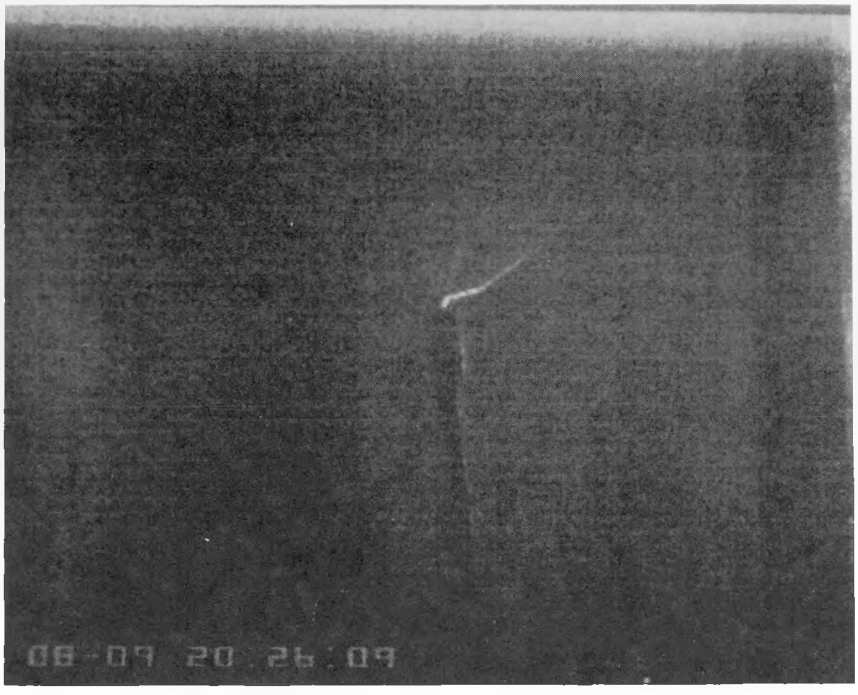

(a)

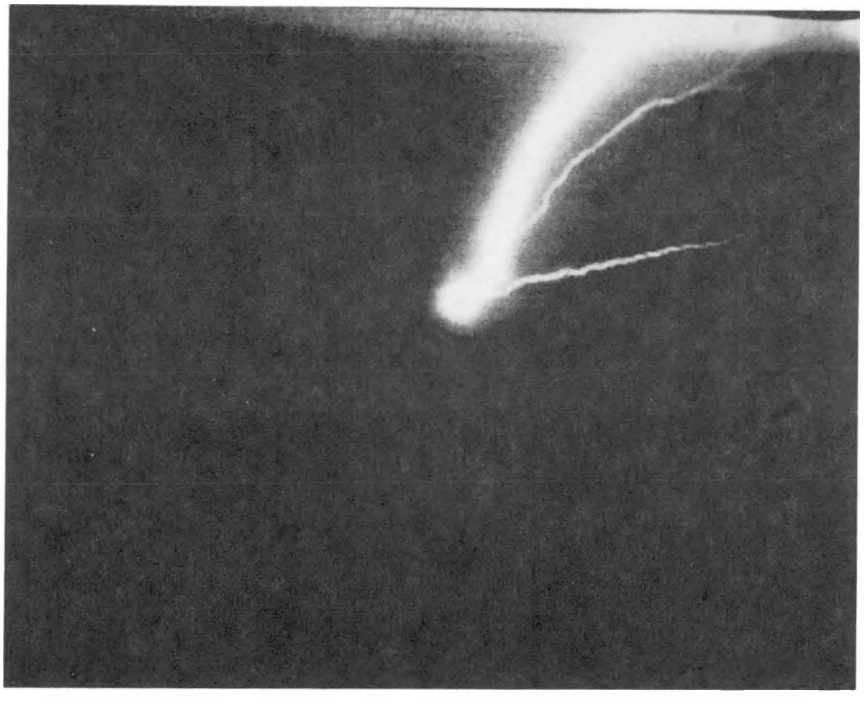

(b)

Figure 32. (a) Upward Streamers from Sample During Flash 90-08, (b) Streamers and Return Stroke Recorded Two Frames Later

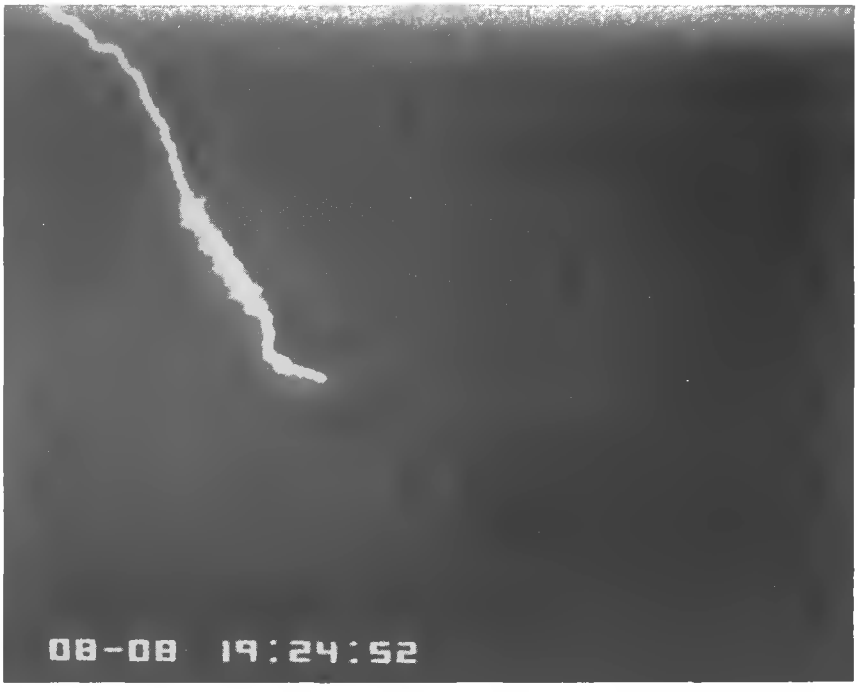

Figure 33. Return Stroke to Sample on Flash 90-03 Showing Leader/Streamer Junction

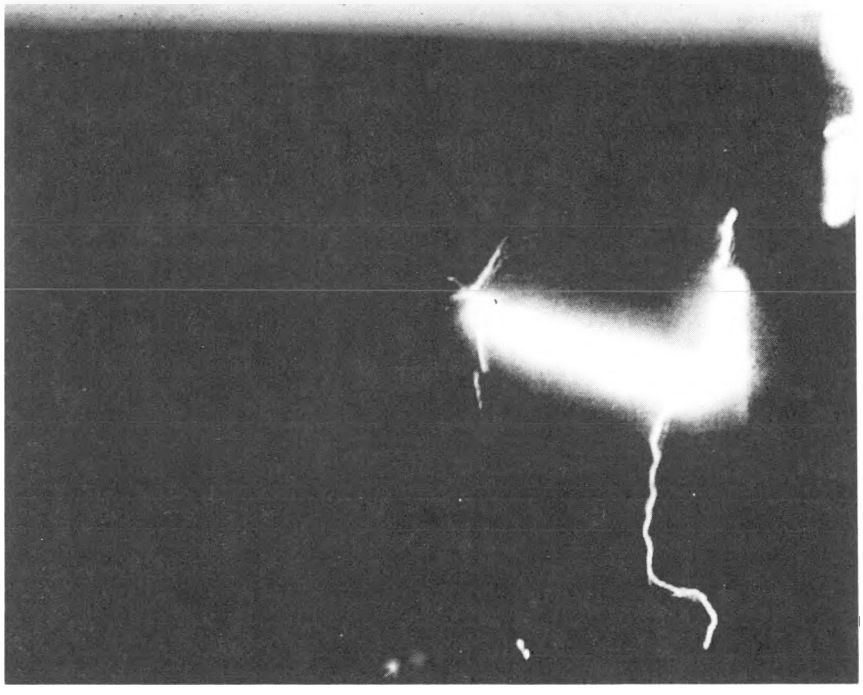

Figure 34. Return Stroke Attachment to Sample During Flash 90-09

over the fixture. This example demonstrates the perverse and largely unpredictable nature of lightning that must be considered during the design and assessment of systems that can be exposed to lightning. These experiments were purposely designed to provide every inducement for attachment to the exposed flat upper surface of the samples. Nevertheless, the attachment took place through a circuitous route that passed through a small aperture in a 1-inch-thick dielectric sleeve. As indicated in Section 6.1, this occurred in several instances, and a modified design for the fixture will be used in the future for such experiments. Given the 30-ms resolution of the video frame, the nature of the additional vertical channel section below the bright horizontal portion cannot be established directly from the photo. It is probable that it is the decaying channel from either the ICC or a previous return stroke that terminated below the sample.

8.0 REFERENCES

1. Fisher, R. J. and M. A. Uman, *Simulation Fidelity in Lightning Penetration Studies*, SAND89-3051, February 1990.

2. Brook, M., G. Armstrong, R. Winder, B. Vonnegut, and C. Moore, "Artificial Initiation of Lightning Discharges," *J. Geophys. Res.*, Vol. 66, No. 11, November 1961.

3. Newman, M. M., J. R. Stawman, J. D. Robb, E. A. Lewis, S. G. Martin, and S. V. Zinn, "Triggered Lightning Strokes at Very Close Range," *J. Geophys. Res.*, Vol. 72, No. 18, September 15, 1967.

4. Fieux, R., C. Gary, and P. Hubert, "Artificial Triggering of Lightning above Ground," *Proc. Int. Conf. on Lightning and Static Electricity*, April 1975.

5. Laroche, P., A. Eybert-Berard, P. Richard, P. Hubert, G. Labaune, and L. Barret, "A Contribution to the Analysis of Triggered Lightning: First Results Obtained During the TRIP82 Experiment," *Proc. 8th Int. Aerospace and Ground Conf. on Lightning and Static Electricity*, June 1983.

6. Eybert-Berard, A., L. Barret, J. P. Berlandis, P. Laroche, C. Leteinturier, and W. Jafferis, "Current Waveforms Analysis of Lightning Flashes Triggered by the Rocket and Wire Technique," *Proc. Int. Conf. on Lightning and Static Electricity*, April 1988.

7. Horii, K., "Experiment of Artificial Lightning Triggered with Rocket," *Memoirs of the Faculty of Engineering*, Nagoya University, Vol. 34, No. 1, May 1982.

8. Steuber, T. F., *Artificially Triggered Cloud-to-Ground Lightning Exhibiting Characteristics of Natural Lightning*, SAND82-0745, May 1982.

9. Luette, J. P., *Sandia 1982 Triggered Lightning Experiment Conducted at Langmuir Laboratory*, SAND83-04444, May 1983.

10. Johnson, J. P., J. M. Arellano, R. T. Hasbrouck, and J. W. Lamb, "Computer Controlled Data Acquisition System for the NASA 1986 Rocket Triggered Lightning Program," *Proc. Int. Conf. on Lightning and Static Electricity*, April 1988.

11. Uman, M. A., *The Lightning Discharge*, Academic Press, New York, 1987.

12. Uman, M. A. and E. P. Krider, "Natural and Artificially Initiated Lightning," *Science*, October 27, 1989.

13. Richmond, R. D., "Rocket Triggered Lightning: A Comparison with Natural Flashes," *Proc. Int. Conf. on Lightning and Static Electricity*, June 1984.

14. LeVine, D. M., J. C. Willet, and J. C. Bailey, "Comparison of Fast Electric Field Changes from Subsequent Return Strokes of Natural and Triggered Lightning," *J. Geophys. Res.*, Vol. 94, No. D11, September 30, 1989.

15. Willet, J. C., J. C. Bailey, V. Idone, A. Eybert-Berard, and L. Barret, "Submicrosecond Intercomparison of Radiation Fields and Currents in Triggered Lightning Based on the Transmission Line Model," *J. Geophys. Res.*, Vol. 94, No. D11, September 30, 1989.

16. Orville, R. E., R. B. Pyle, and R. W. Henderson, "An East Coast Lightning Detection Network," *IEEE Trans. on Power Systems*, PWRS-1, No. 4, November 1986.

17. Cianos, N. and E. T. Pierce, *A Ground-Lightning Environment for Engineering Use*, SRI Report, Project 1834, August 1972.

APPENDIX A

CENG ROCKET SPECIFICATIONS

PROPELLANT

Type :	Black cartridge, 930 g
Initiation :	Electrical safety squib
Transport Classification :	1.3.C, with special air flight cargo crate: UNO number 0186

PHYSICAL

Length :	84 cm
Body Diameter :	6.5 cm
Fin Area :	320 cm^2
Mass (without propellant) :	1908 g

INITIATOR

Firing Voltage :	9 V
All-Fire Current :	6.5 A
No-Fire Current :	2.5 A
Resistance :	1.5 Ω

FLIGHT PERFORMANCE

Maximum Vertical Range :	1300 m
Maximum Velocity :	250 m/s
Maximum Acceleration :	40 g
Burn Duration :	11 s, maximum thrust occurs 1.1 s after ignition
Flight Duration :	20 s, typical
Ground Impact Zone :	Circular area, 500 m

APPENDIX B

RECORDED LIGHTNING FLASH CURRENTS

Presented in this appendix are plots of the flash currents as recorded on both the return-stroke (sampled every 80 ns) and continuing-current (FM, bandwidth 0-500 kHz) instrumentation channels. During the storm on August 8, the NanoFast fiber optic receiver malfunctioned, and no digitized recording of the individual return strokes (other than those made by KSC) were acquired. For the flashes obtained on August 9 and 11, the full flash currents are shown, followed by plots of each return stroke on two time scales. On the fast time scale plots, the filled dots indicate the sampled points.

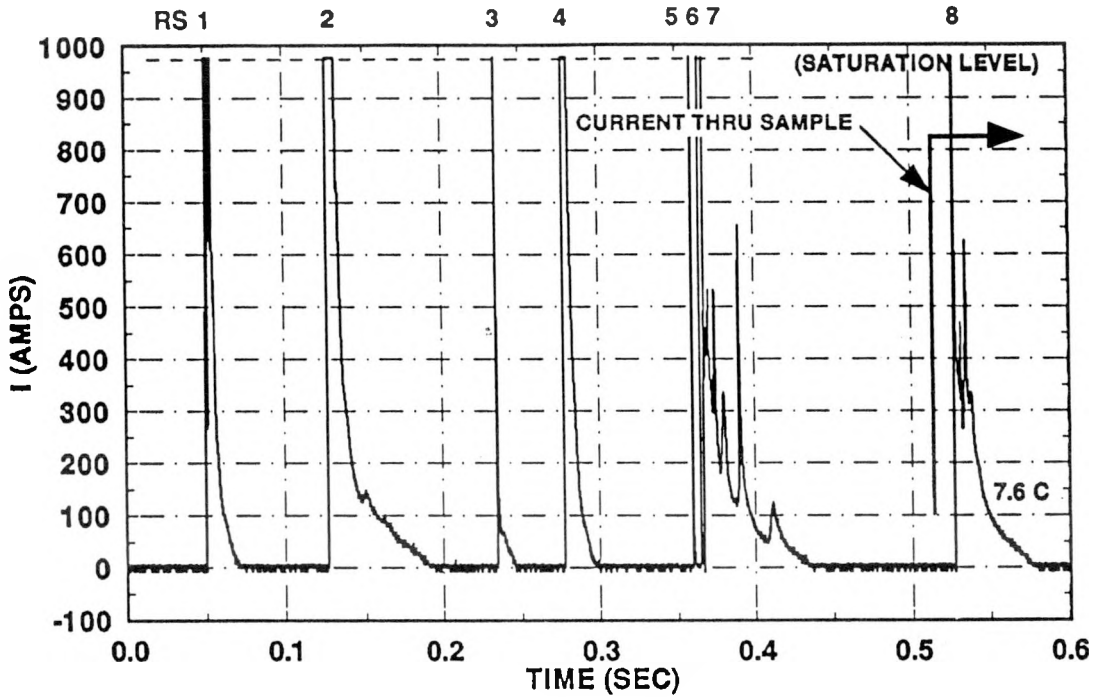

Figure B-1. FM Channel Record, Flash 90-02

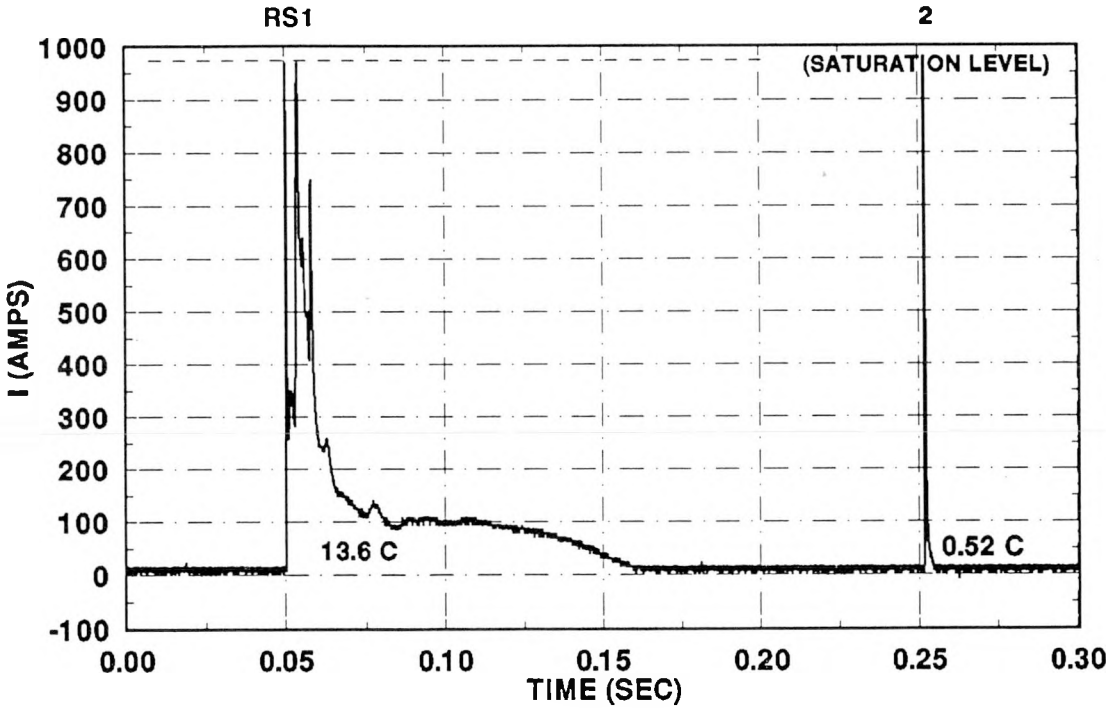

Figure B-2. FM Channel Record, Flash 90-03

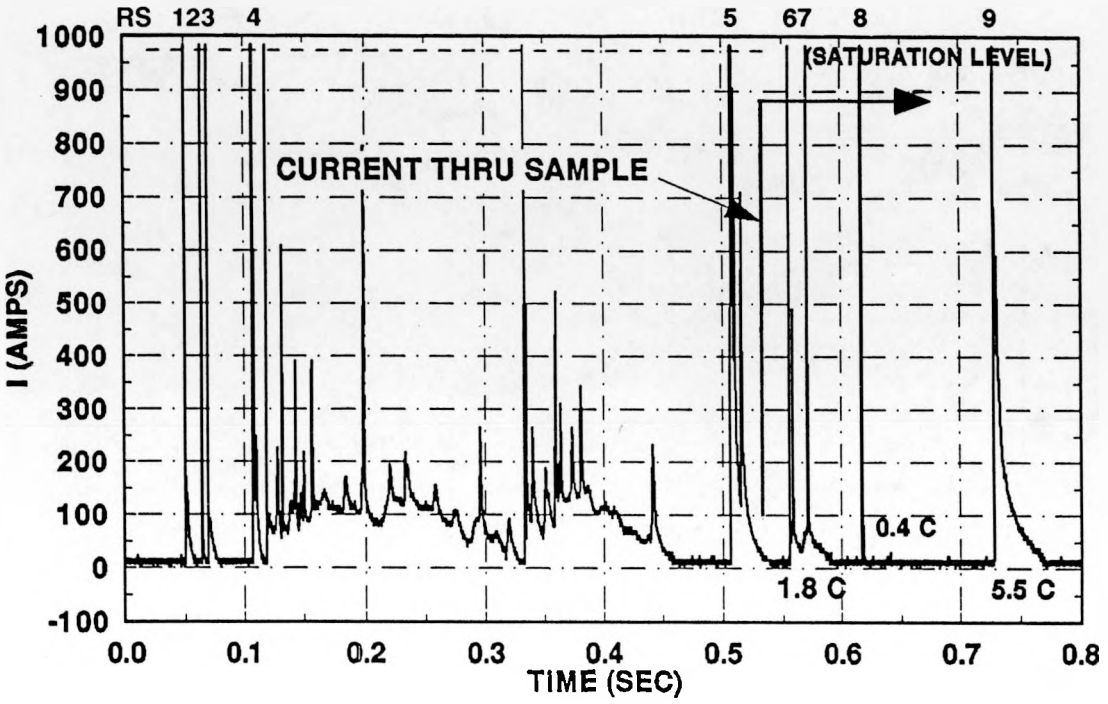

Figure B-3. FM Channel Record. Flash 90-04

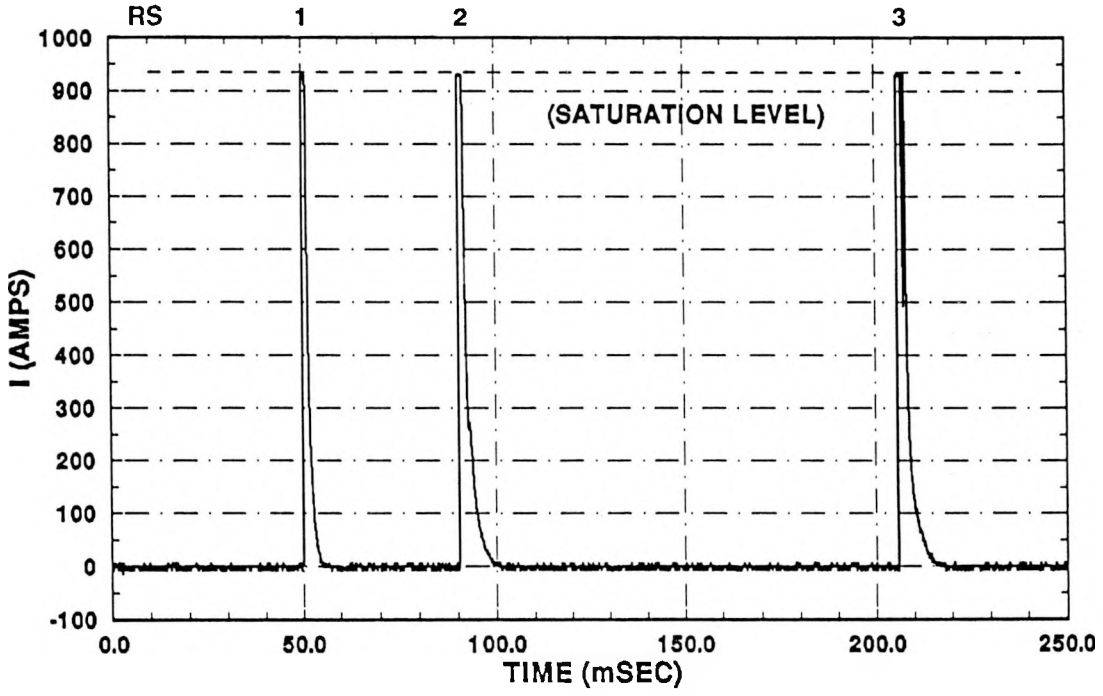

Figure B-4. FM Channel Record, Flash 90-07

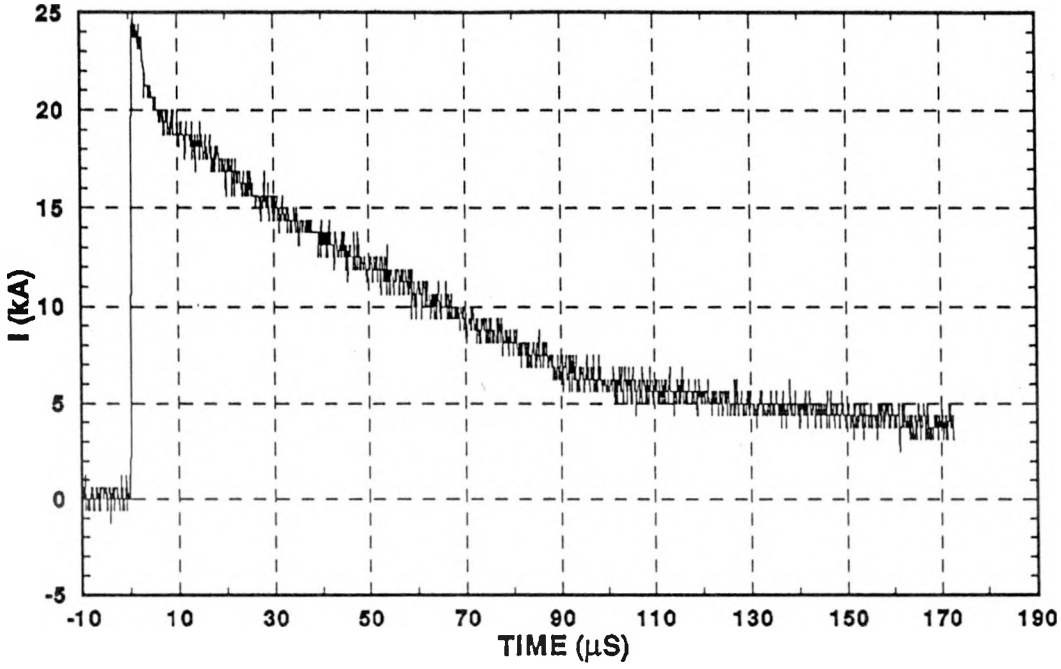

(a) Full Record

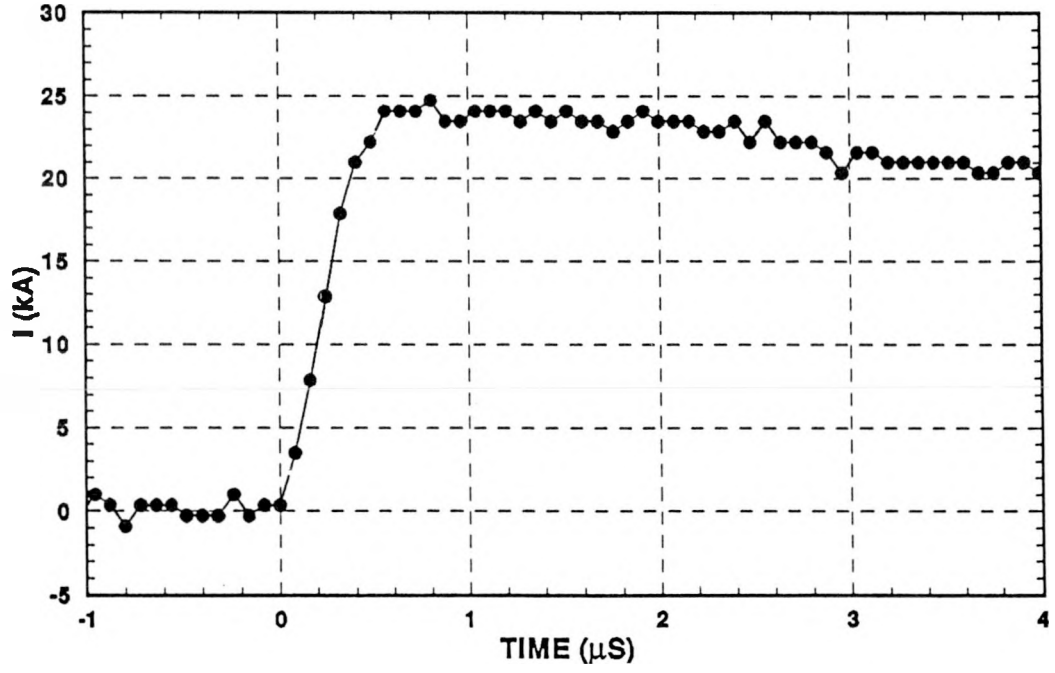

(b) Fast Time Scale

Figure B-5. Flash 90-07, Return Stroke No. 1

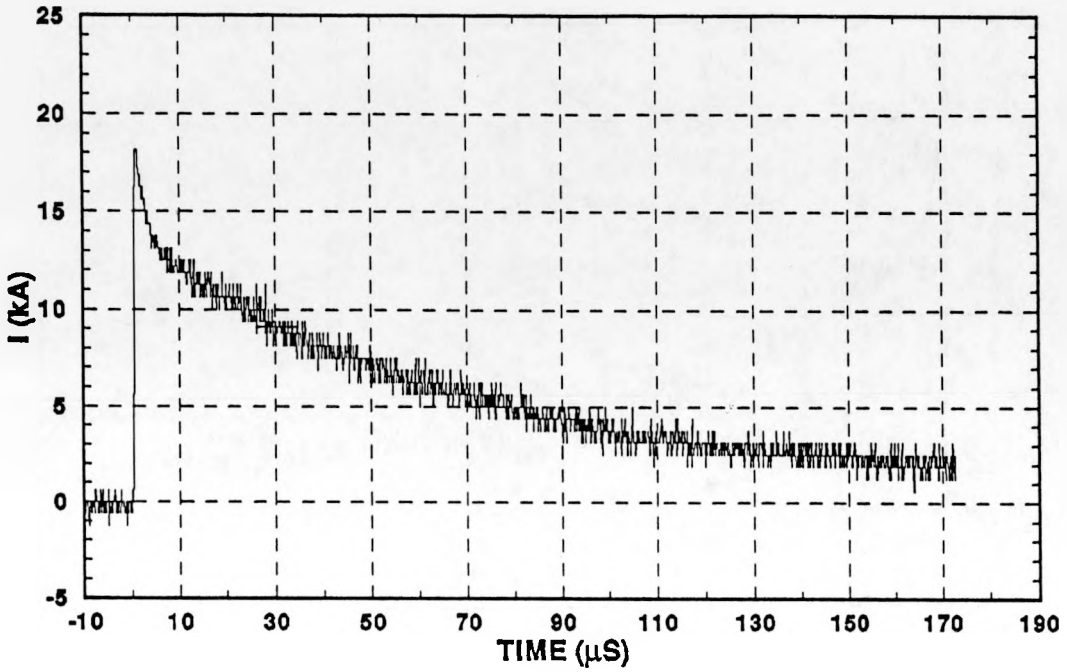

(a) Full Record

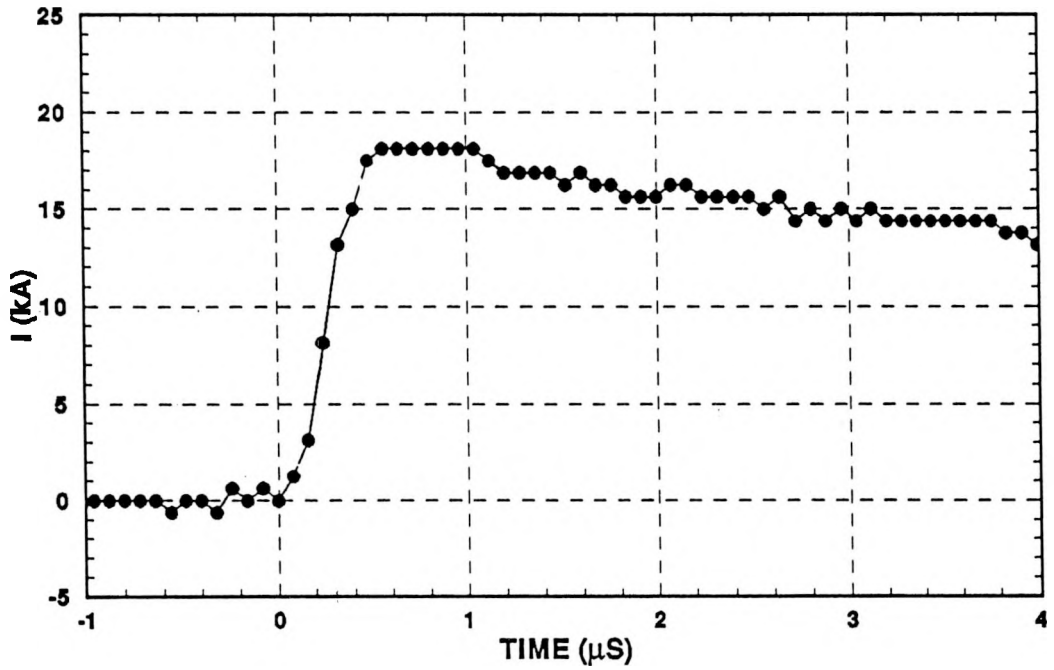

(b) Fast Time Scale

Figure B-6. Flash 90-07, Return Stroke No. 2

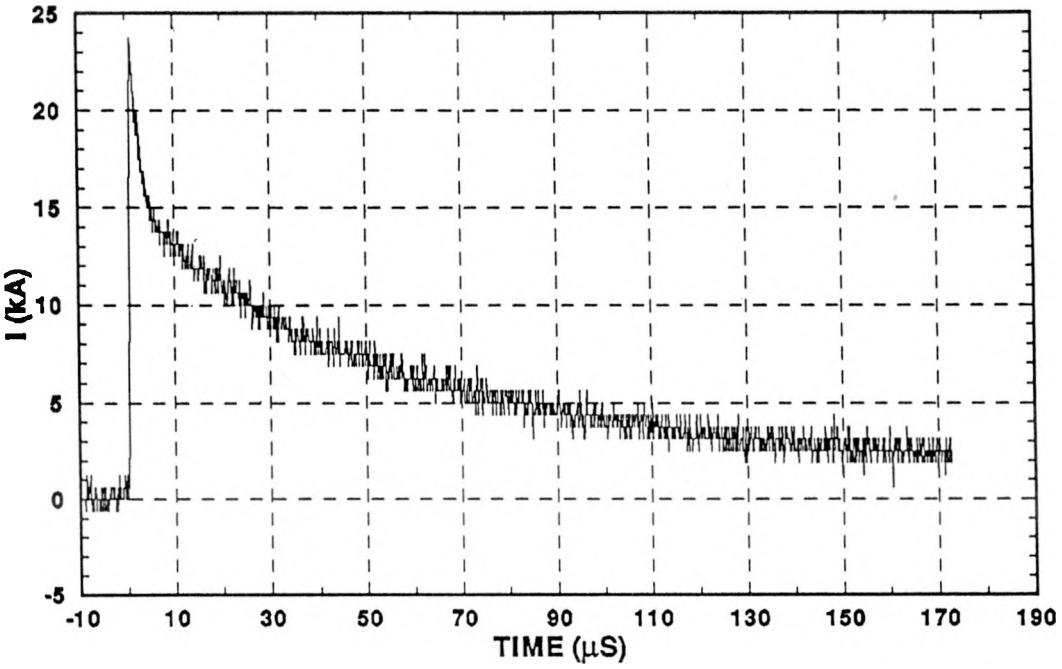

(a) Full Record

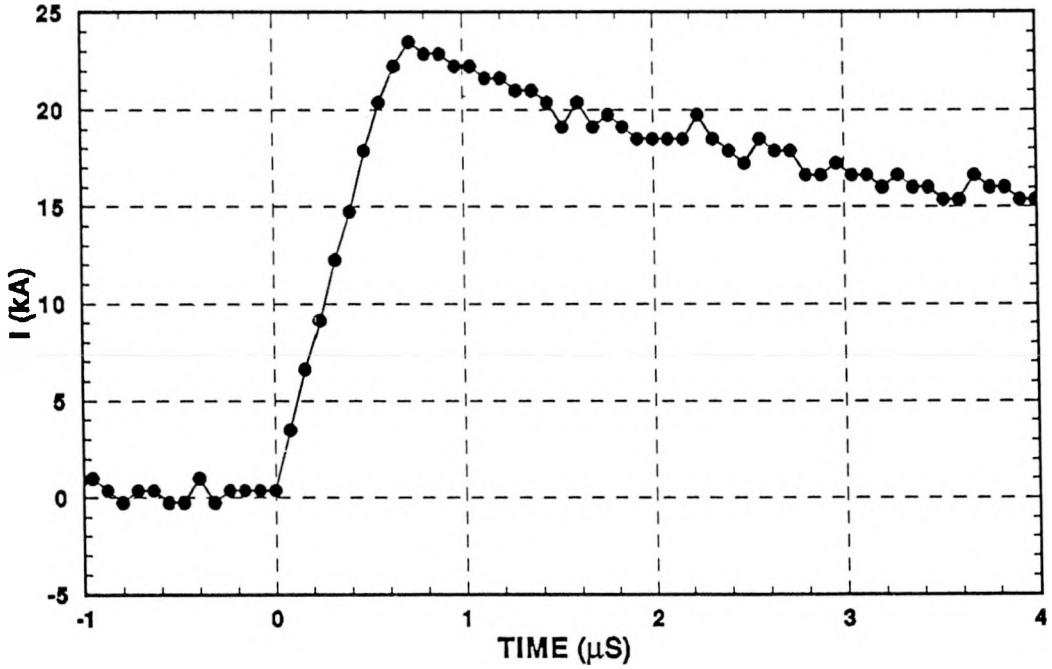

(b) Fast Time Scale

Figure B-7. Flash 90-07, Return Stroke No. 3

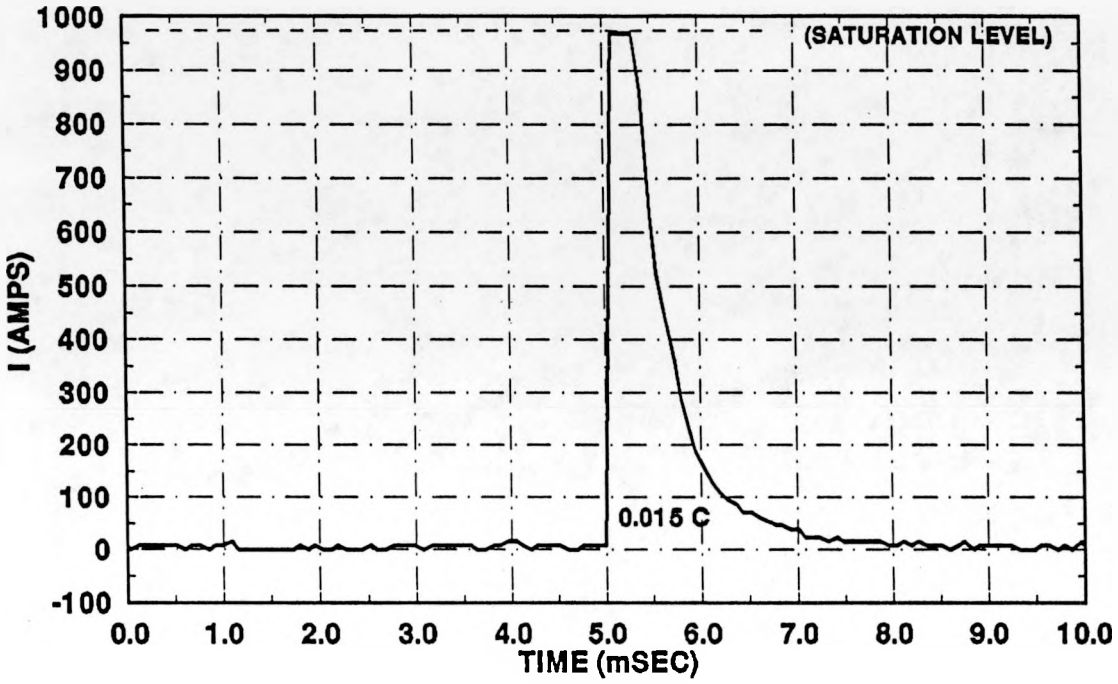

Figure B-8. Flash 90-08 FM Channel Record. (Digitized return stroke data lost during post-test processing.)

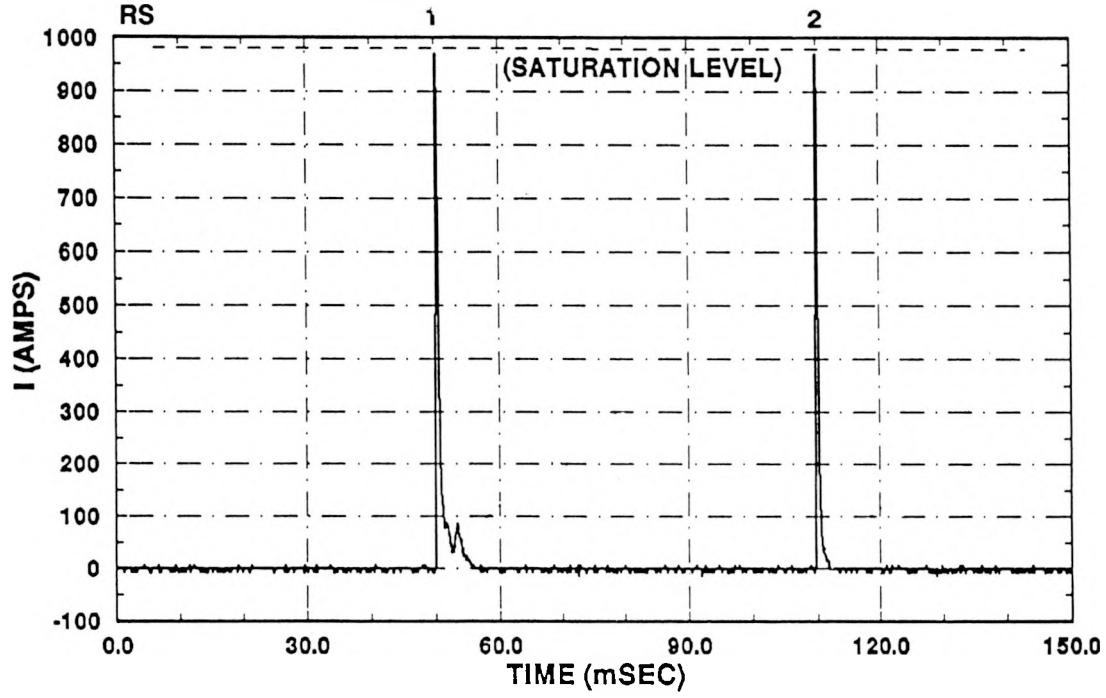

Figure B-9. Flash 90-09 FM Channel Record

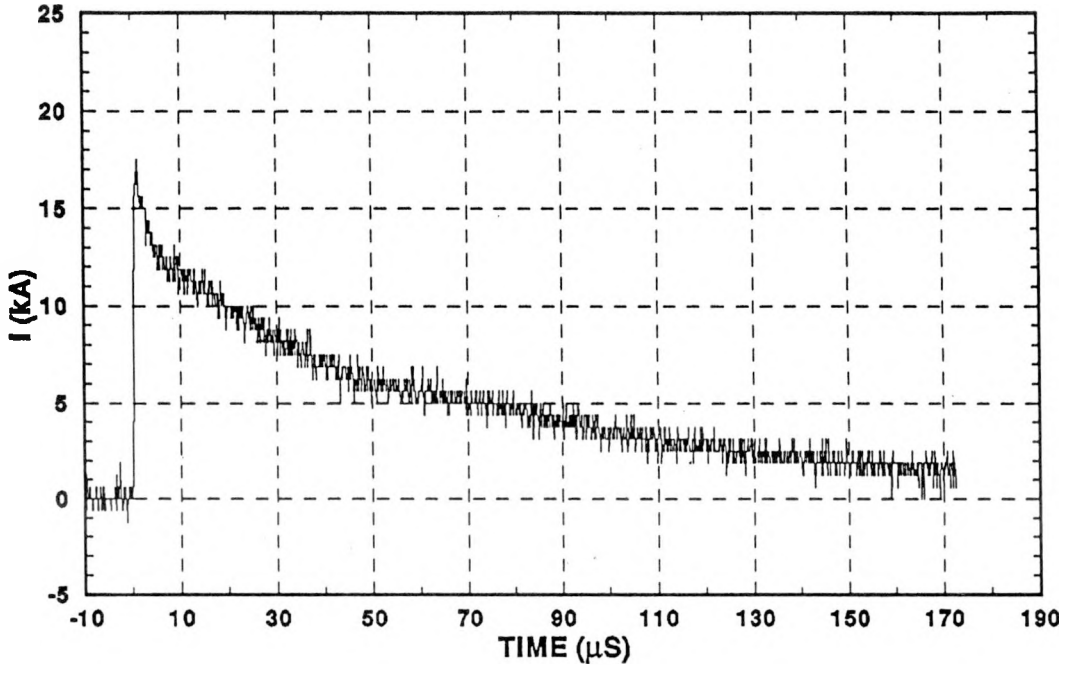

(a) Full Record

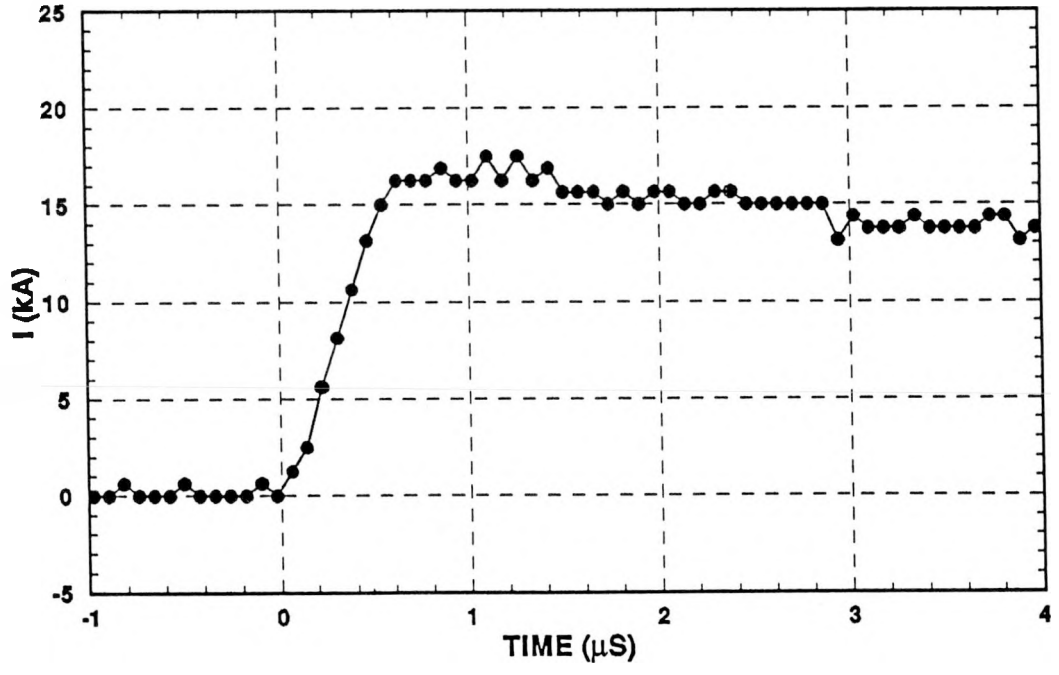

(b) Fast Time Scale

Figure B-10. Flash 90-09, Return Stroke No. 1

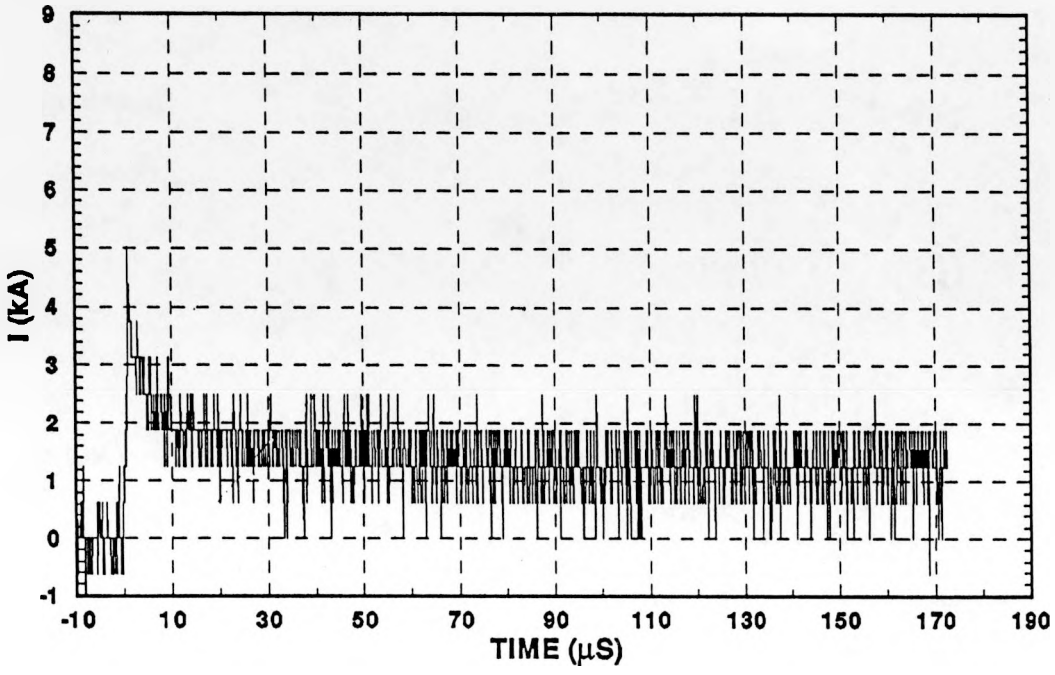

(a) Full Record

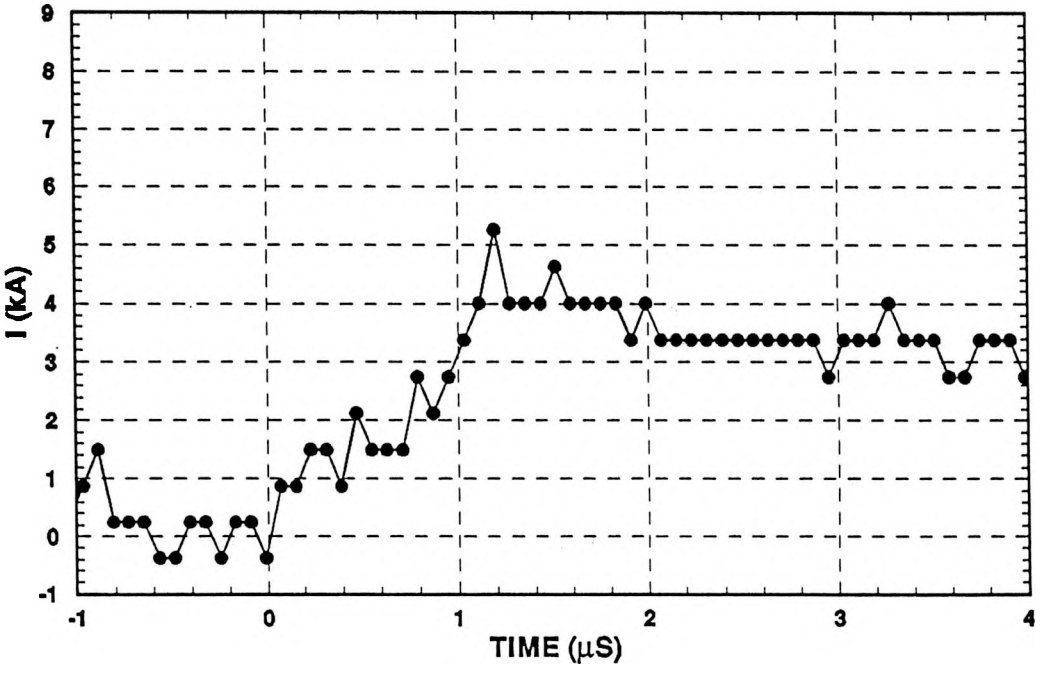

(b) Fast Time Scale

Figure B-11. Flash 90-09 Return Stroke No. 2

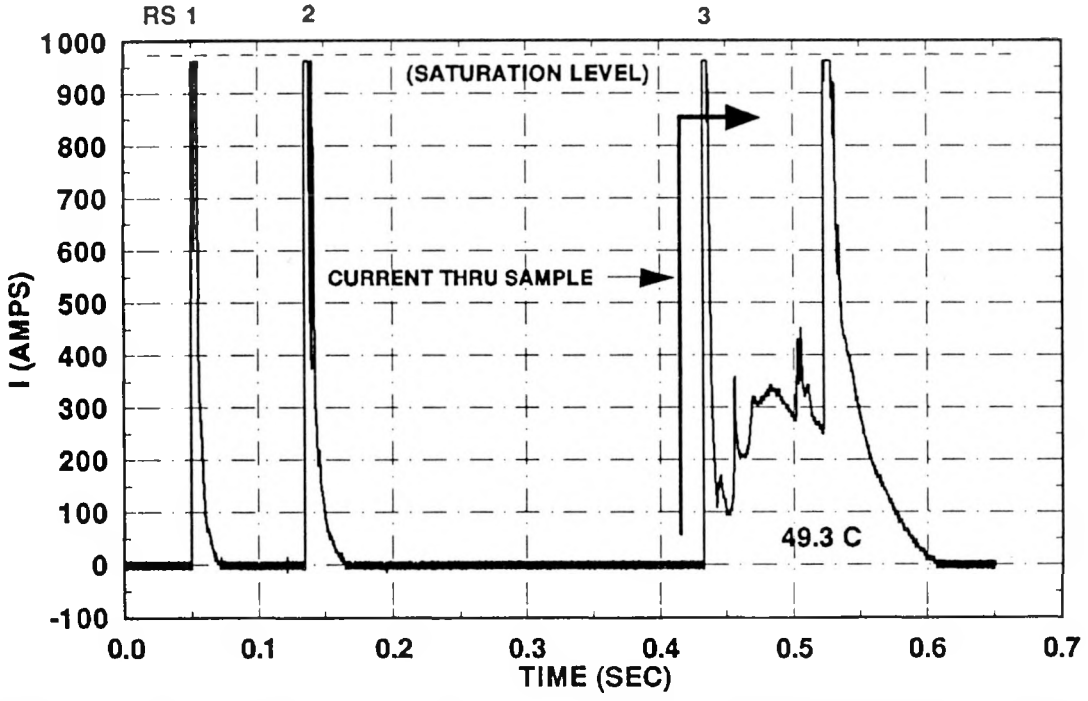

Figure B-12. Flash 90-12 FM Channel Record

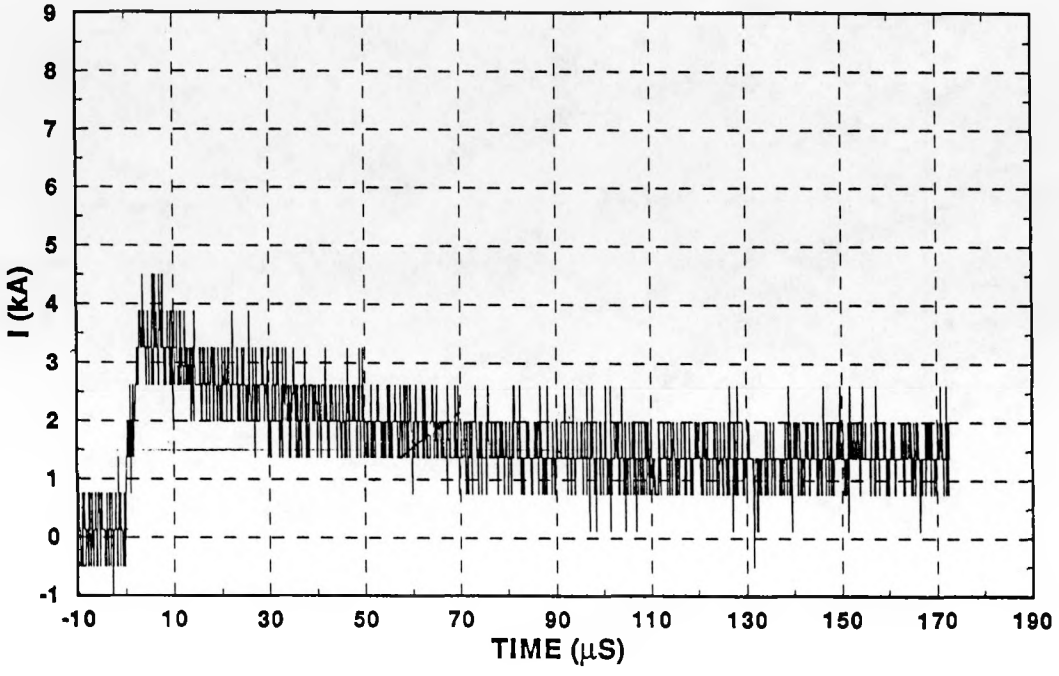

(a) Full Record

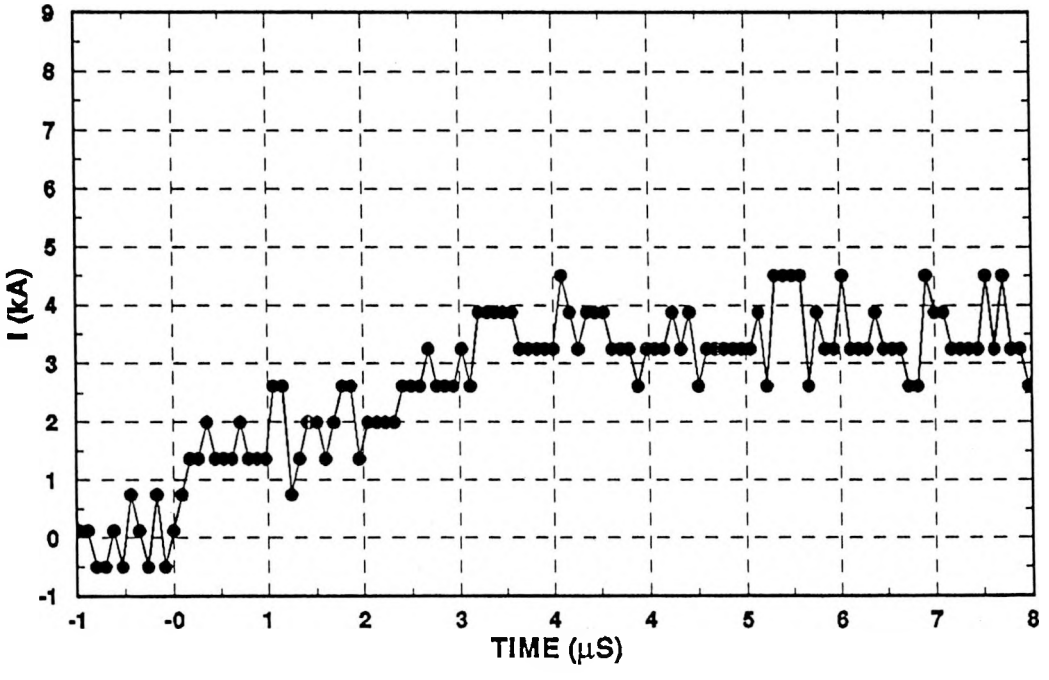

(b) Fast Time Scale

Figure B-13. 90-12 Return Stroke No. 1

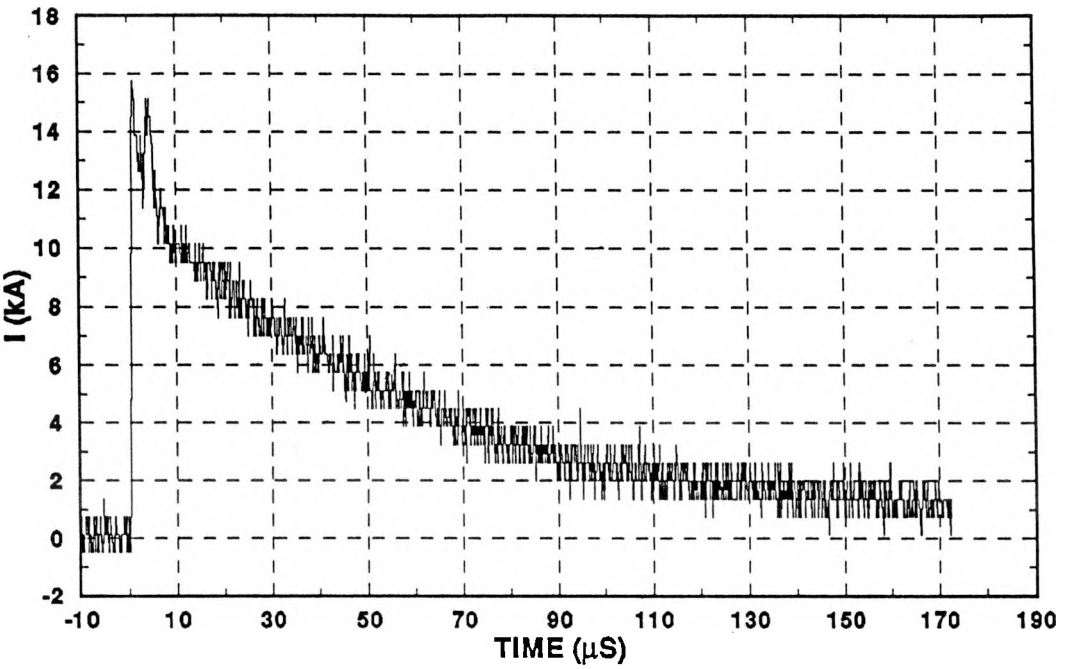

(a) Full Record

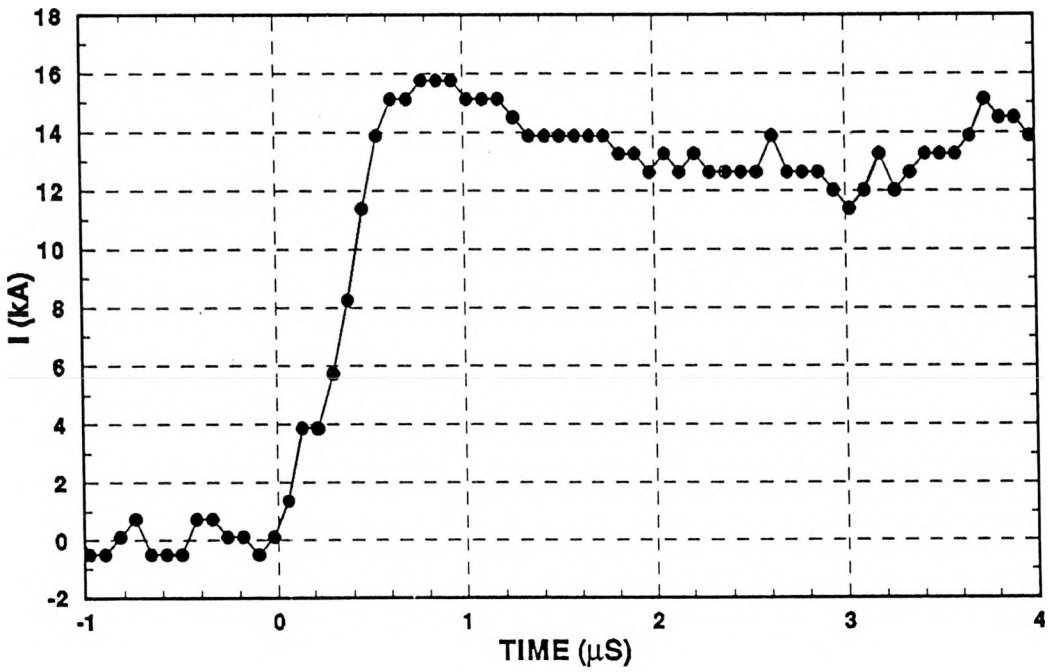

(b) Fast Time Scale

Figure B-14. Flash 90-12, Return Stroke No. 2

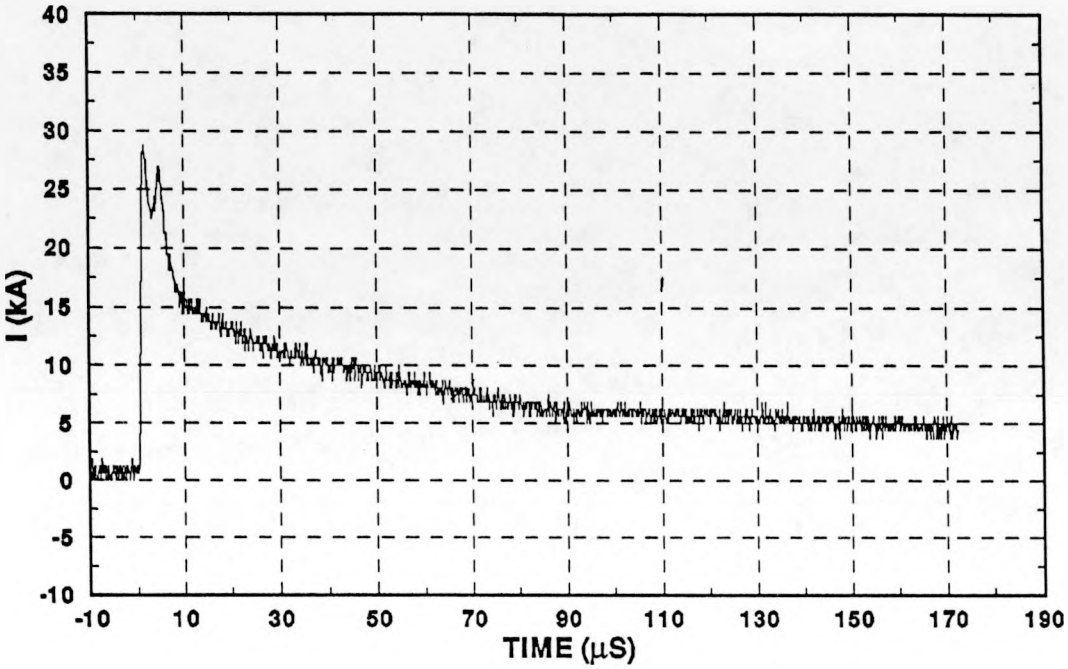

(a) Full Record

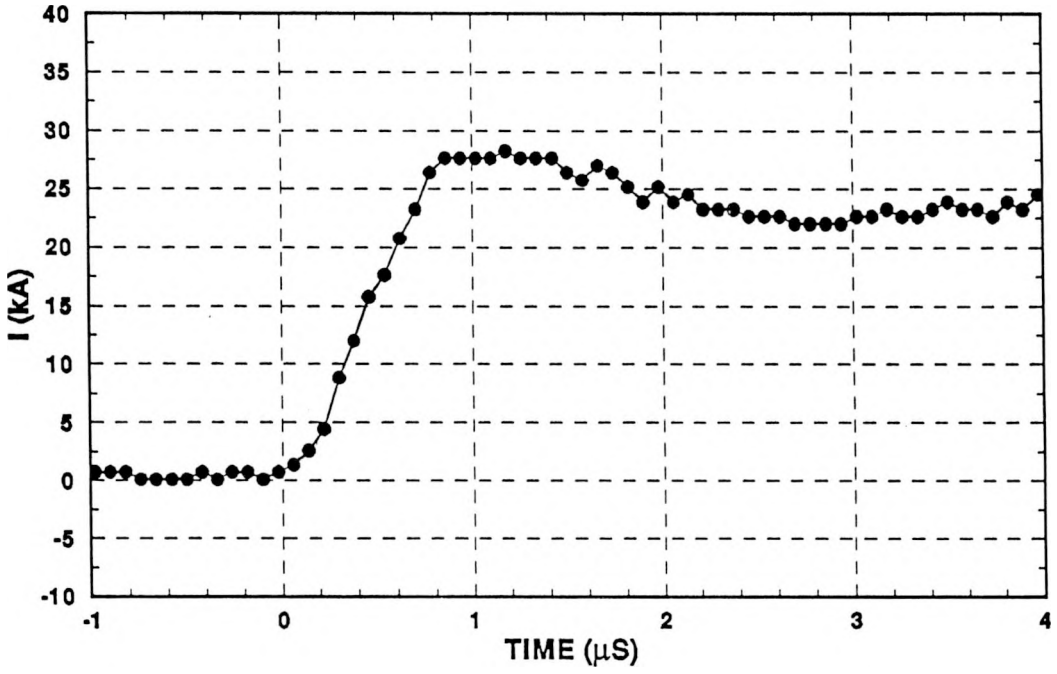

(b) Fast Time Scale

Figure B-15. Flash 90-12, Stroke 3

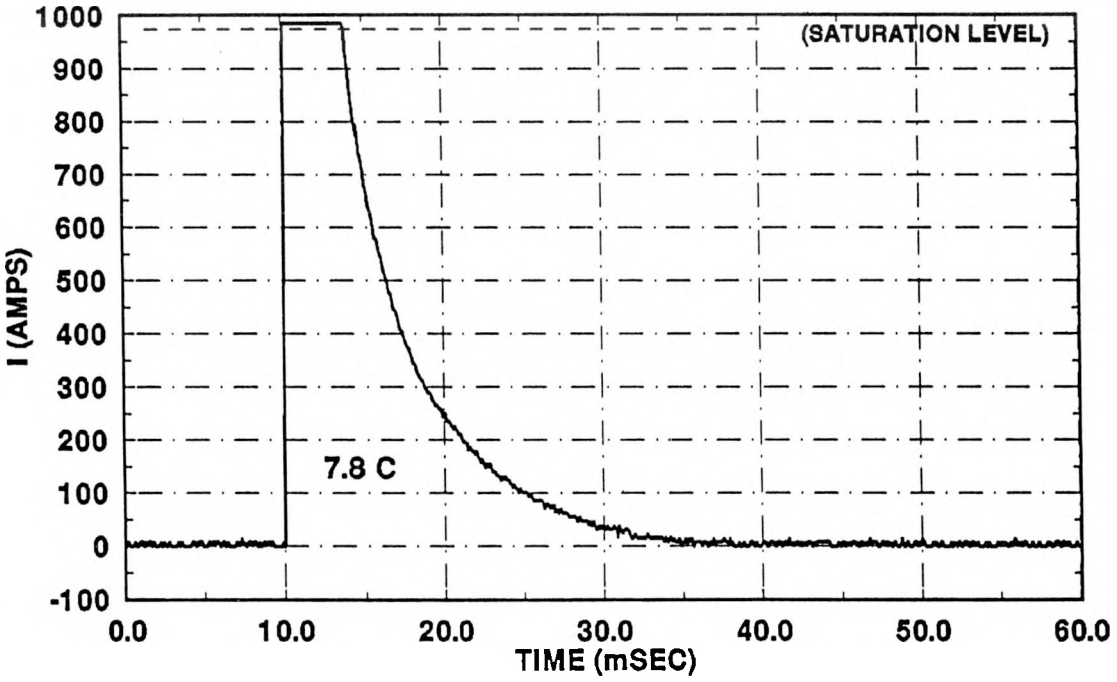

Figure B-16. Flash 90-14 FM Channel Record

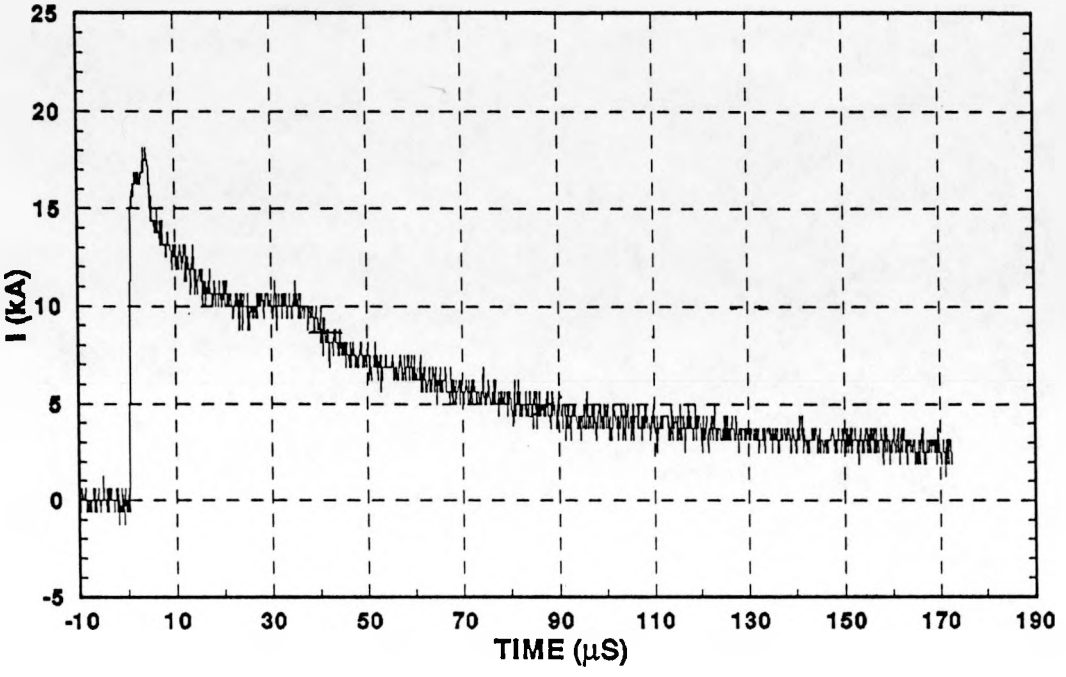

(a) Full Record

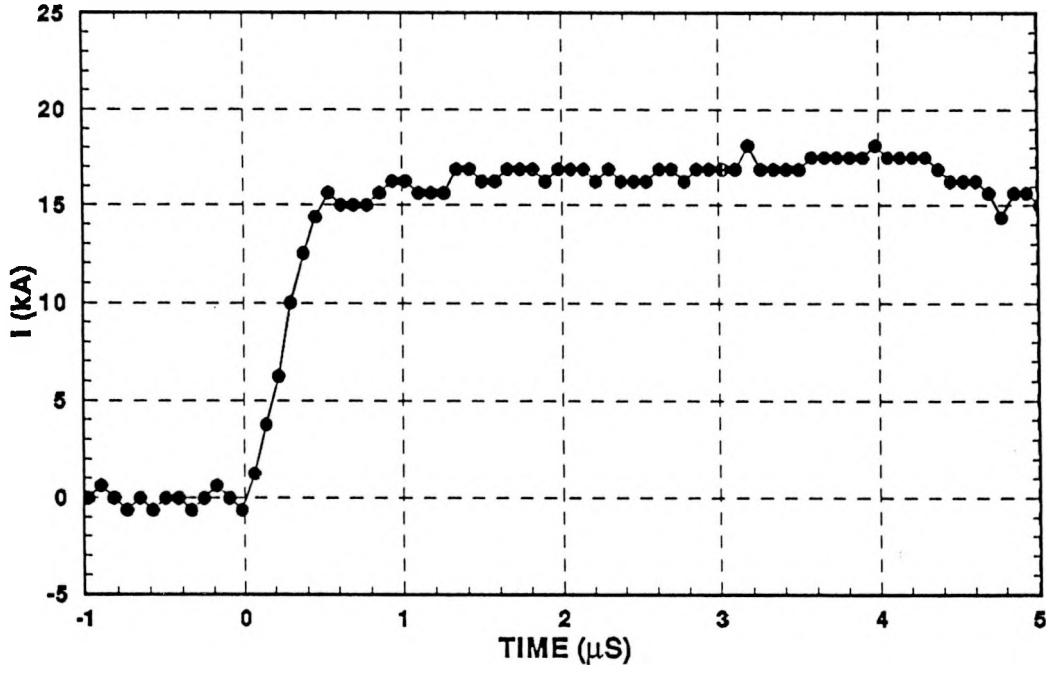

(b) Fast Time Scale

Figure B-17. Flash 90-14 Return Stroke

APPENDIX C

KSC AREA PROTECTION SYSTEM STRUCTURAL CURRENT MEASUREMENTS

Presented in this appendix are plots of the incident lightning current on the APS structure followed by the corresponding currents measured on the instrumented down conductors. In each case the currents are presented on two time scales.

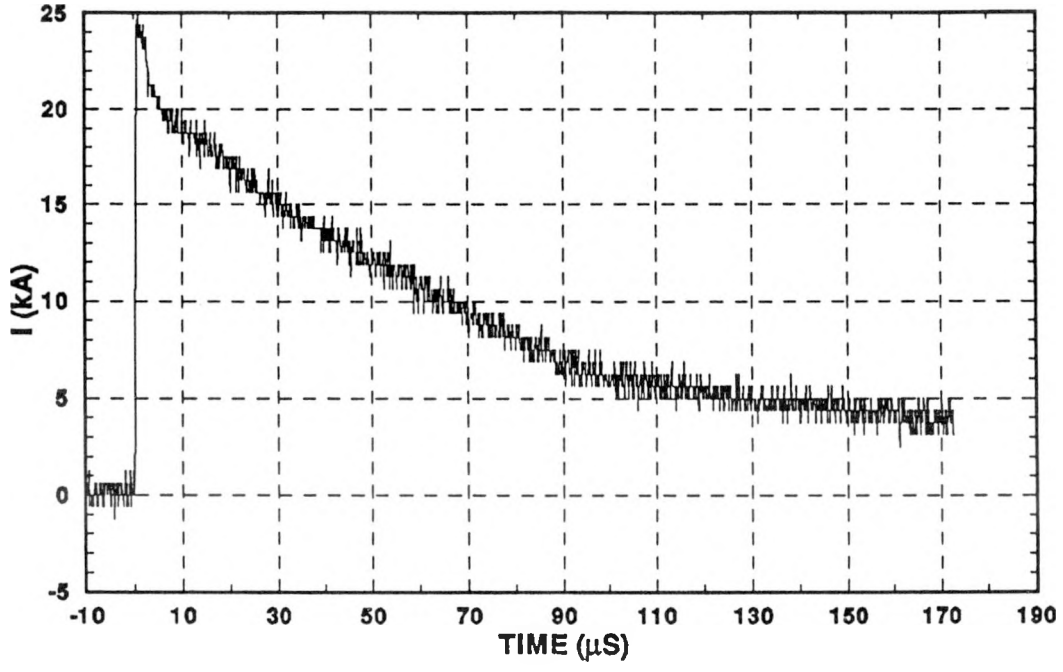

Figure C-1. Lightning Current Incident on APS, Slow Time Scale. Flash 90-07, Stroke 1.

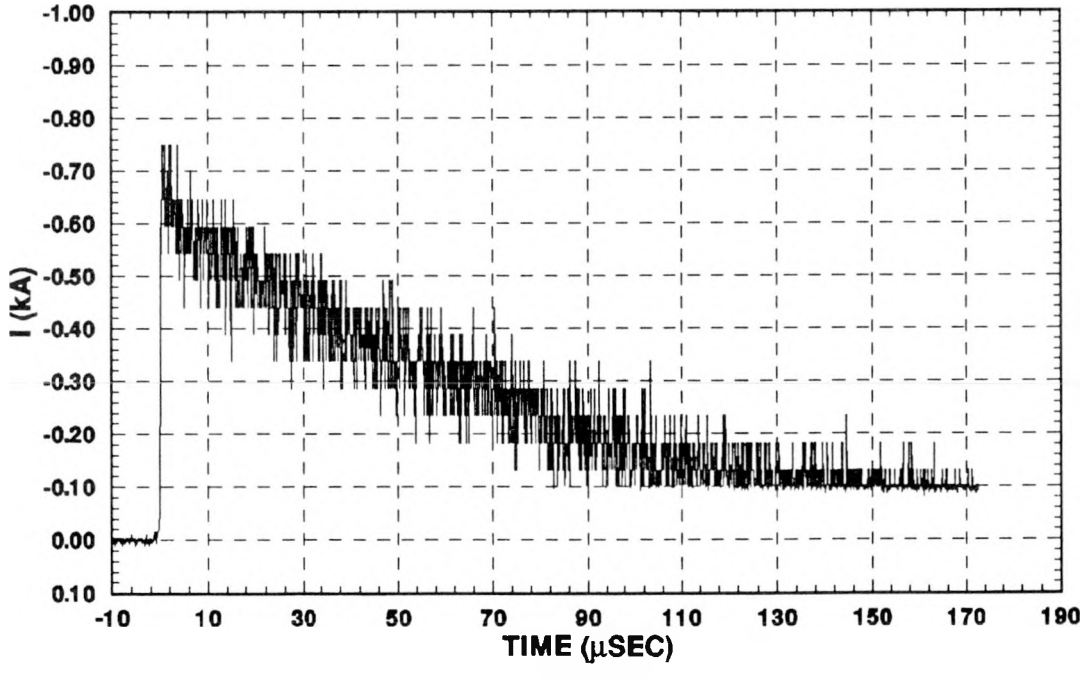

Figure C-2. Lightning Current Measured in One Down Conductor, Slow Time Scale. Flash 90-07, Stroke 1.

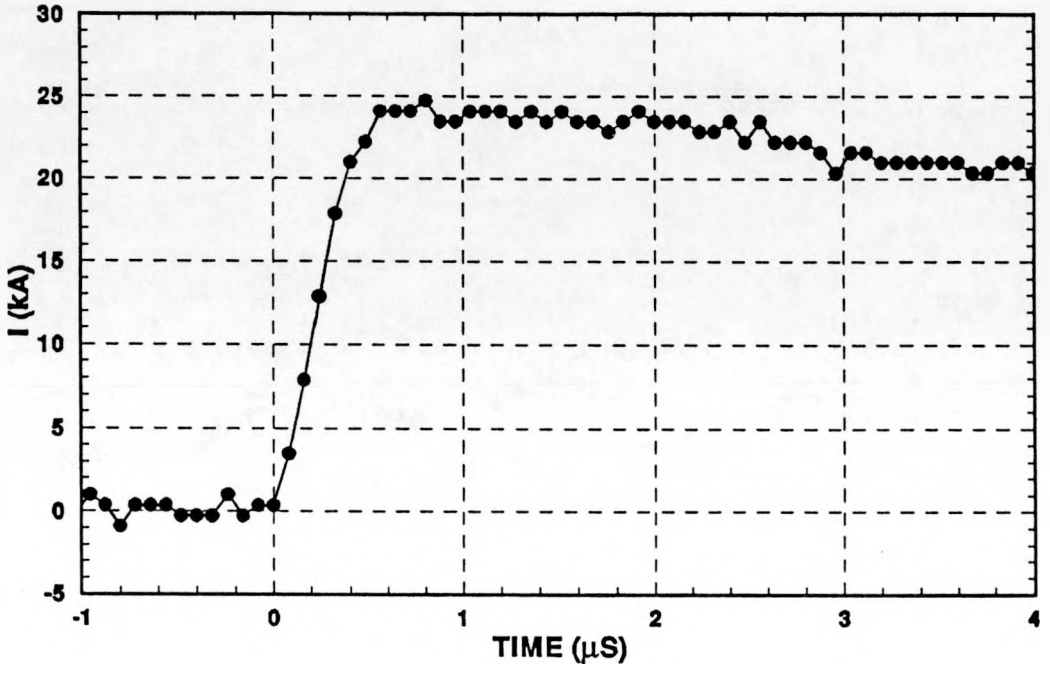

Figure C-3. Lightning Current Incident on APS, Fast Time Scale. Flash 90-07, Stroke 1.

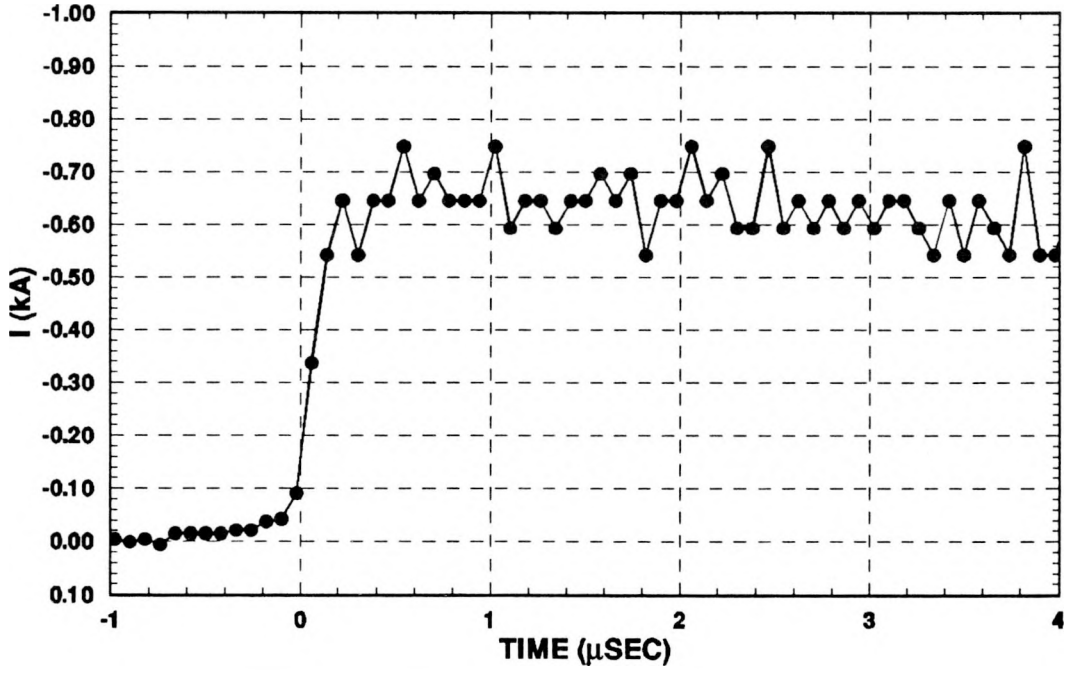

Figure C-4. Lightning Current Measured in One Down Conductor, Fast Time Scale. Flash 90-07, Stroke 1.

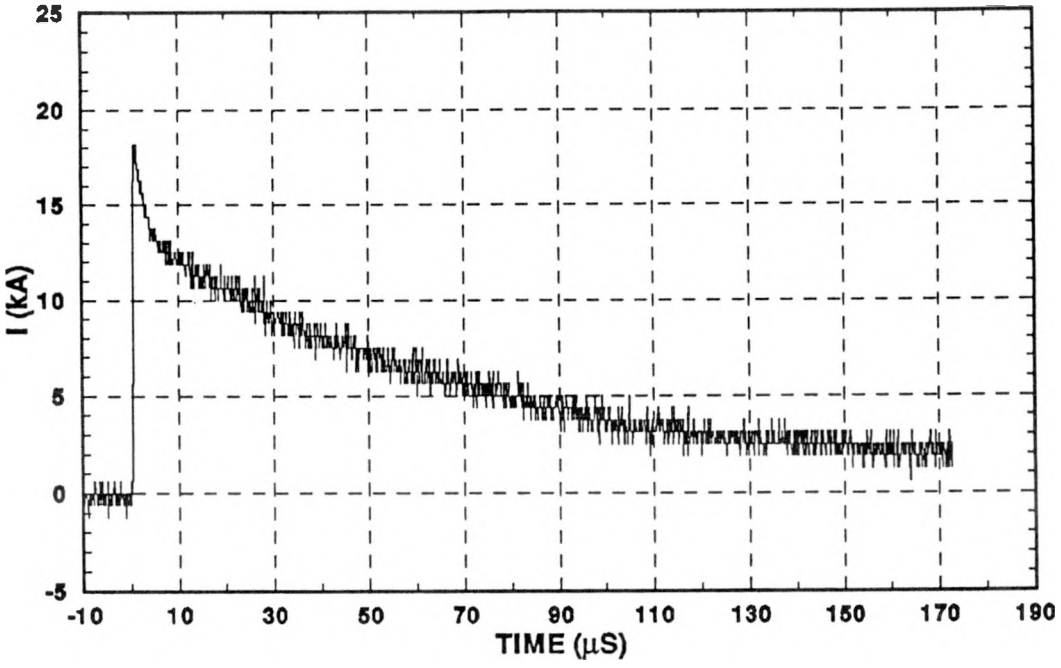

Figure C-5. Lightning Current Incident on APS, Slow Time Scale. Flash 90-07, Stroke 2.

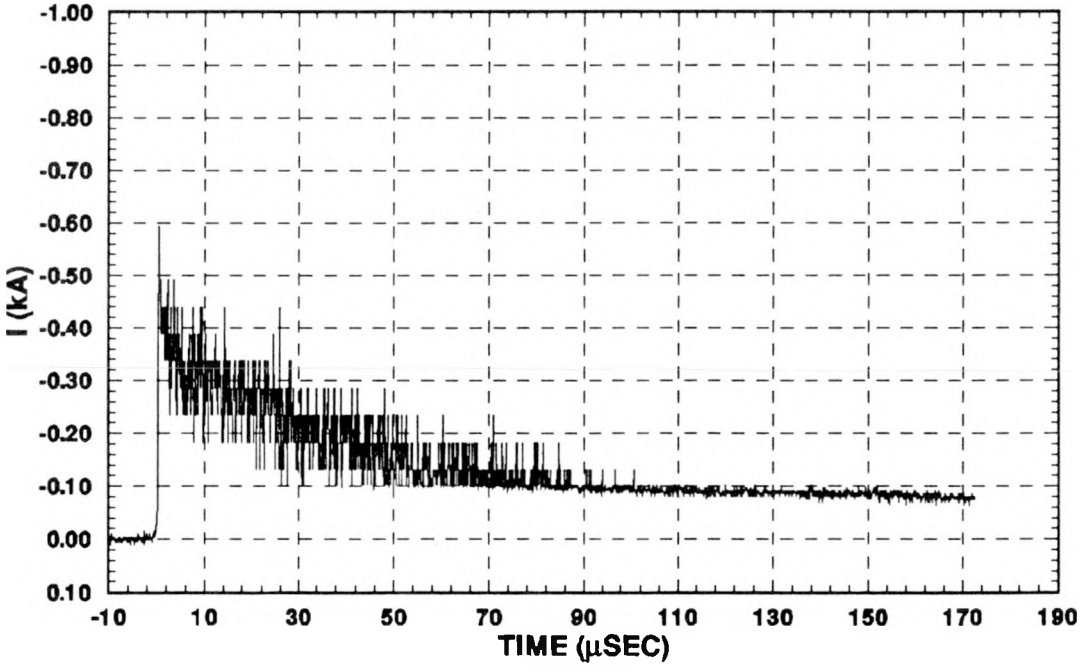

Figure C-6. Lightning Current Measured in One Down Conductor, Slow Time Scale. Flash 90-07, Stroke 2.

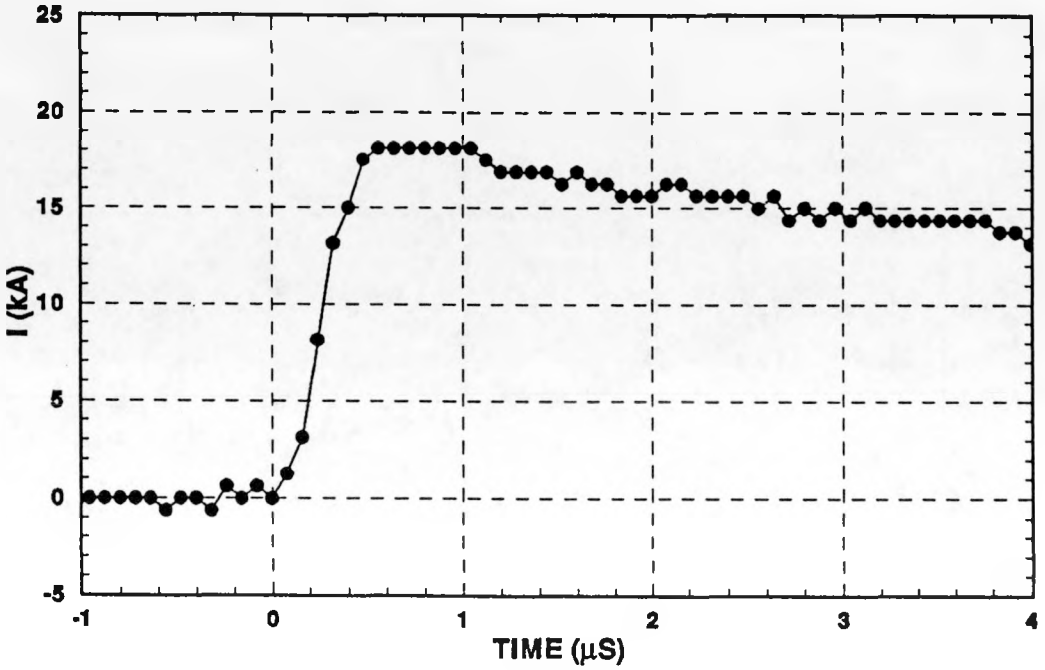

Figure C-7. Lightning Current Incident on APS, Fast Time Scale. Flash 90-07, Stroke 2.

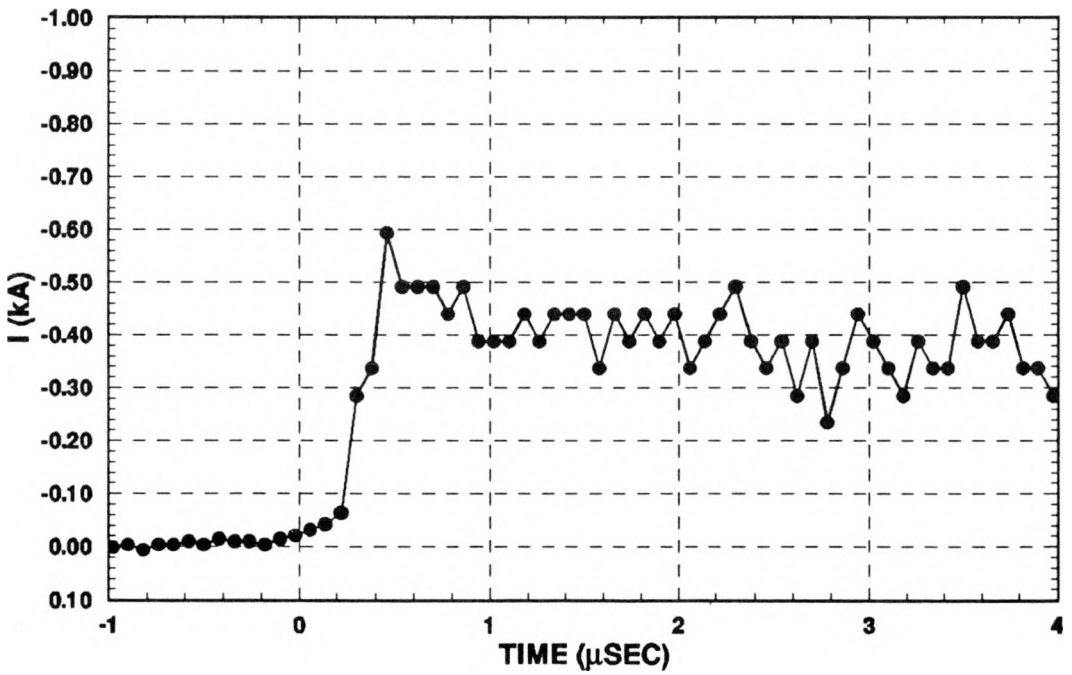

Figure C-8. Lightning Current Measured in One Down Conductor, Fast Time Scale. Flash 90-07, Stroke 2.

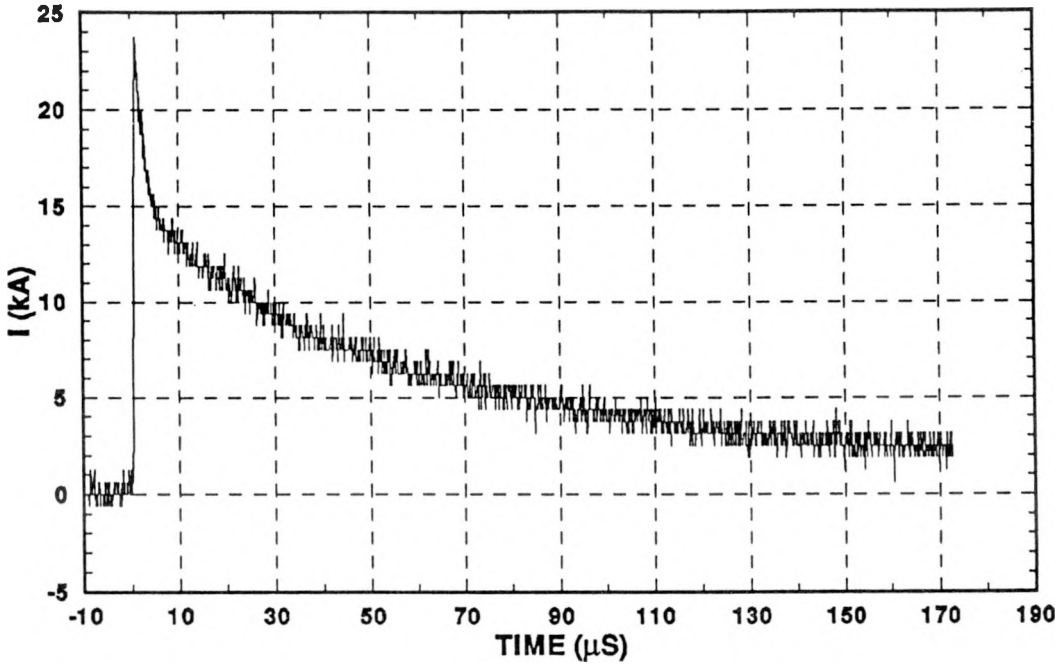

Figure C-9. Lightning Current Incident on APS, Slow Time Scale. Flash 90-07, Stroke 3.

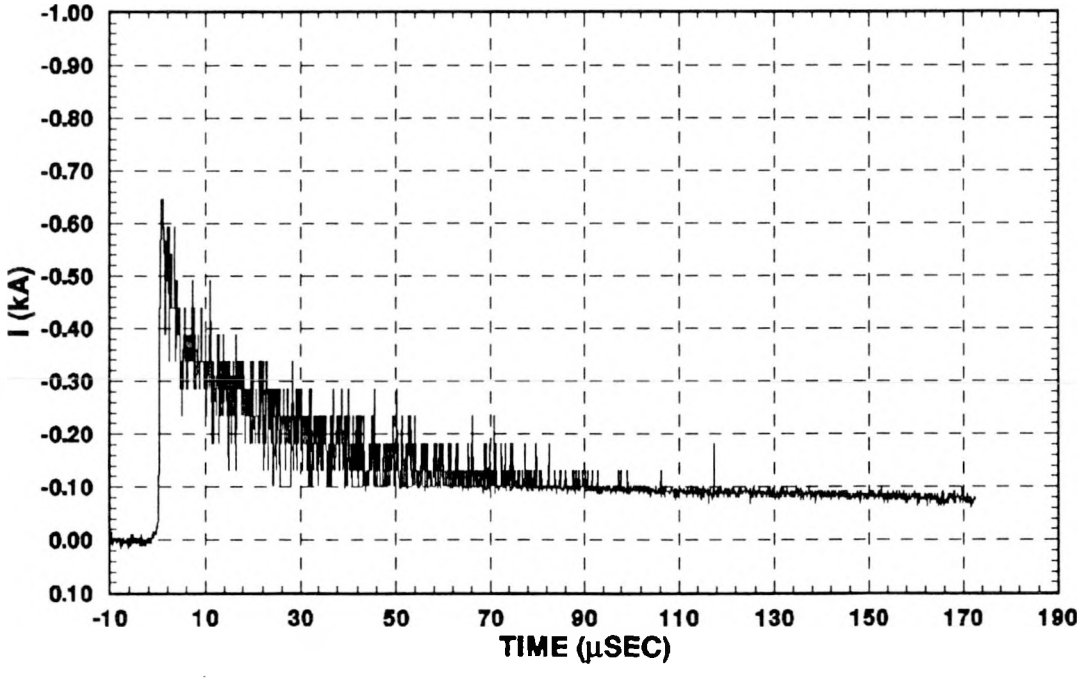

Figure C-10. Lightning Current Measured in One Down Conductor, Slow Time Scale. Flash 90-07, Stroke 3.

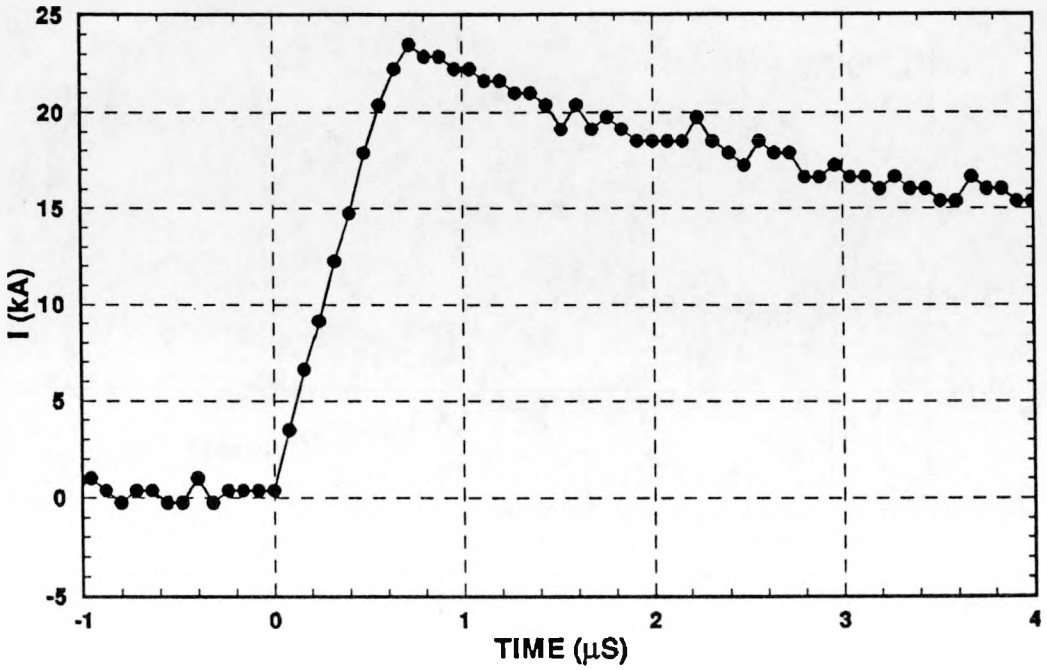

Figure C-11. Lightning Current Incident on APS, Fast Time Scale. Flash 90-07, Stroke 3.

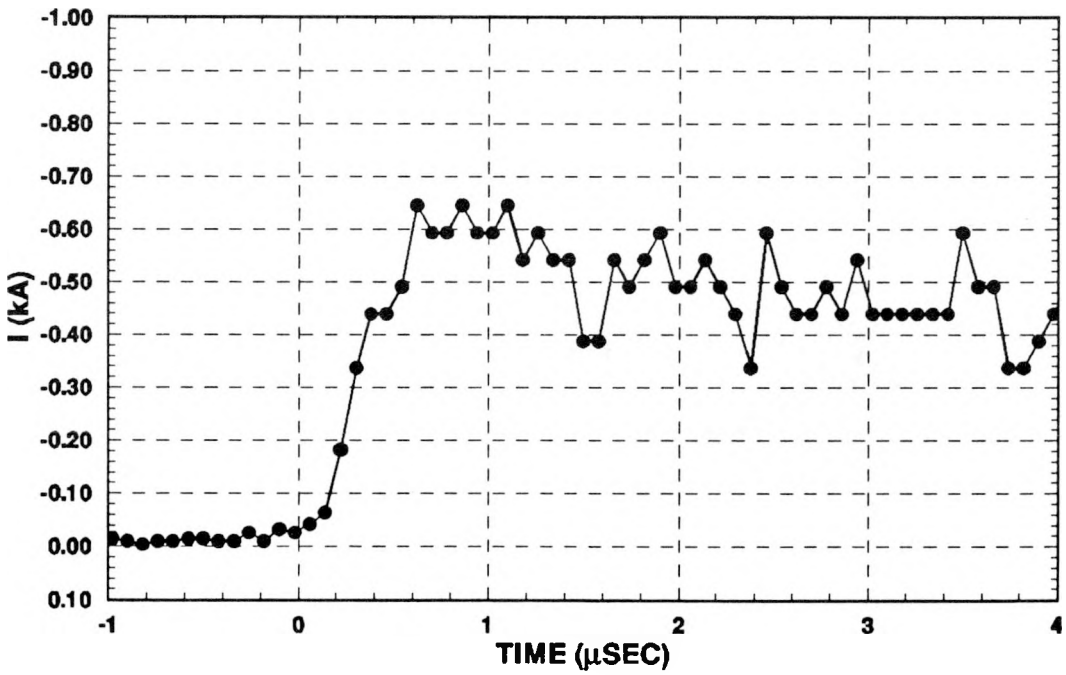

Figure C-12. Lightning Current Measured in One Down Conductor, Fast Time Scale. Flash 90-07, Stroke 3.

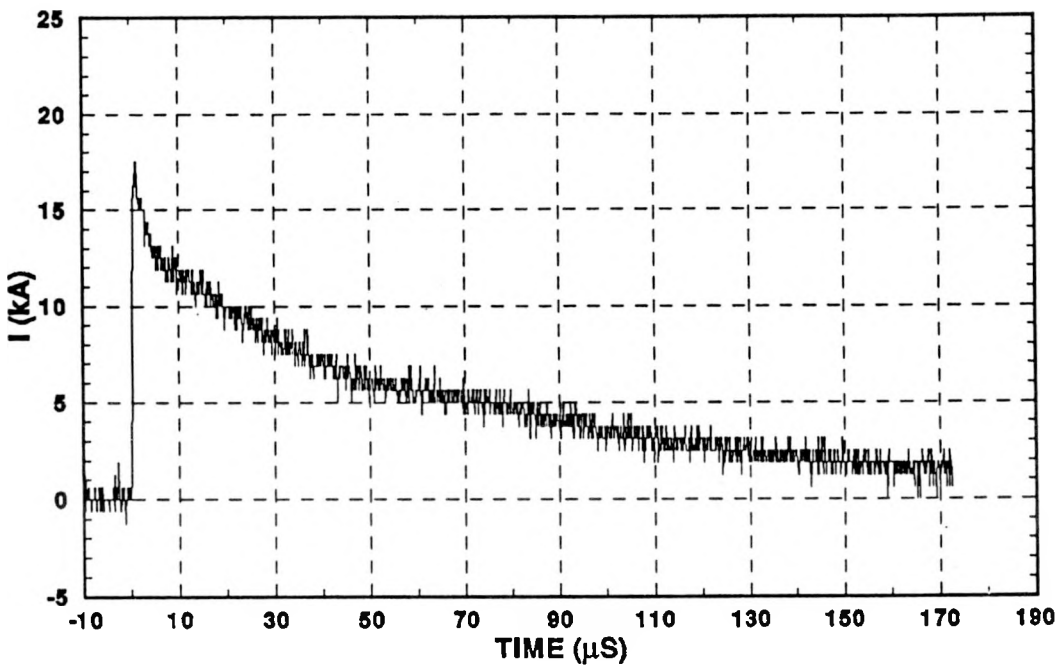

Figure C-13. Lightning Current Incident on APS, Slow Time Scale. Flash 90-09, Stroke 1.

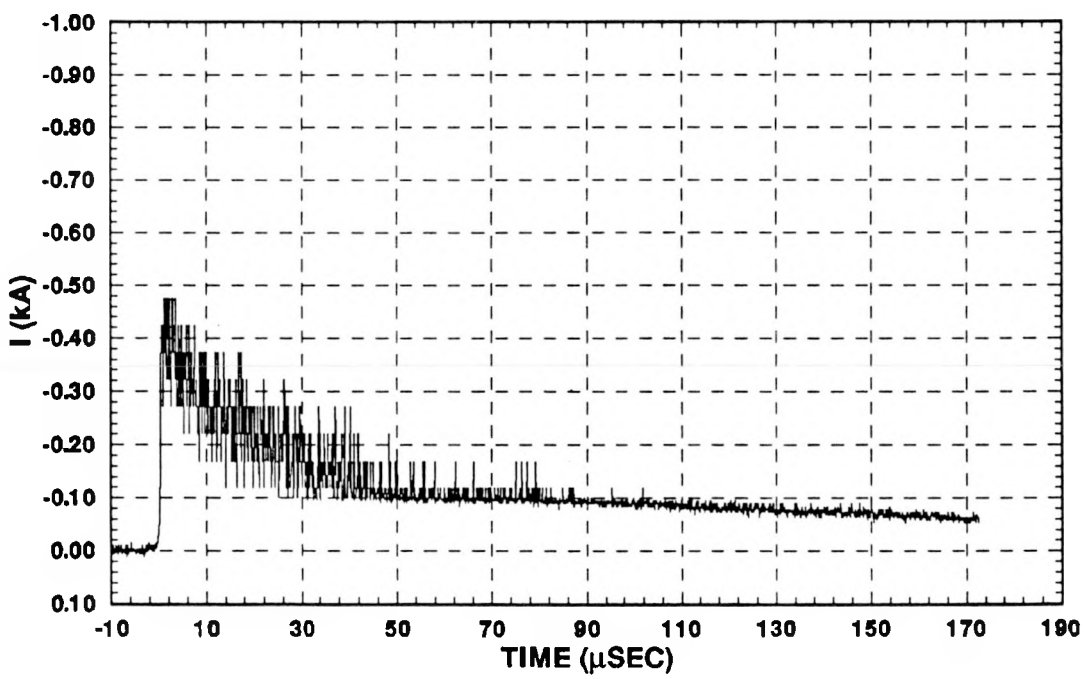

Figure C-14. Lightning Current Measured in One Down Conductor, Slow Time Scale. Flash 90-09, Stroke 1.

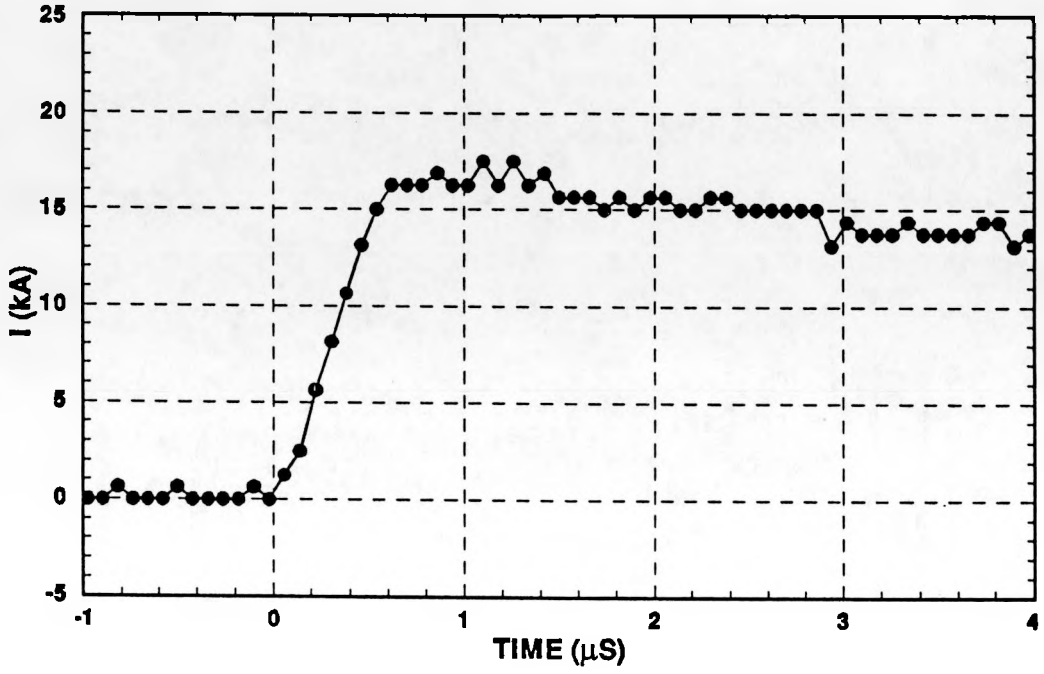

Figure C-15. Lightning Current Incident on APS, Fast Time Scale. Flash 90-09, Stroke 1.

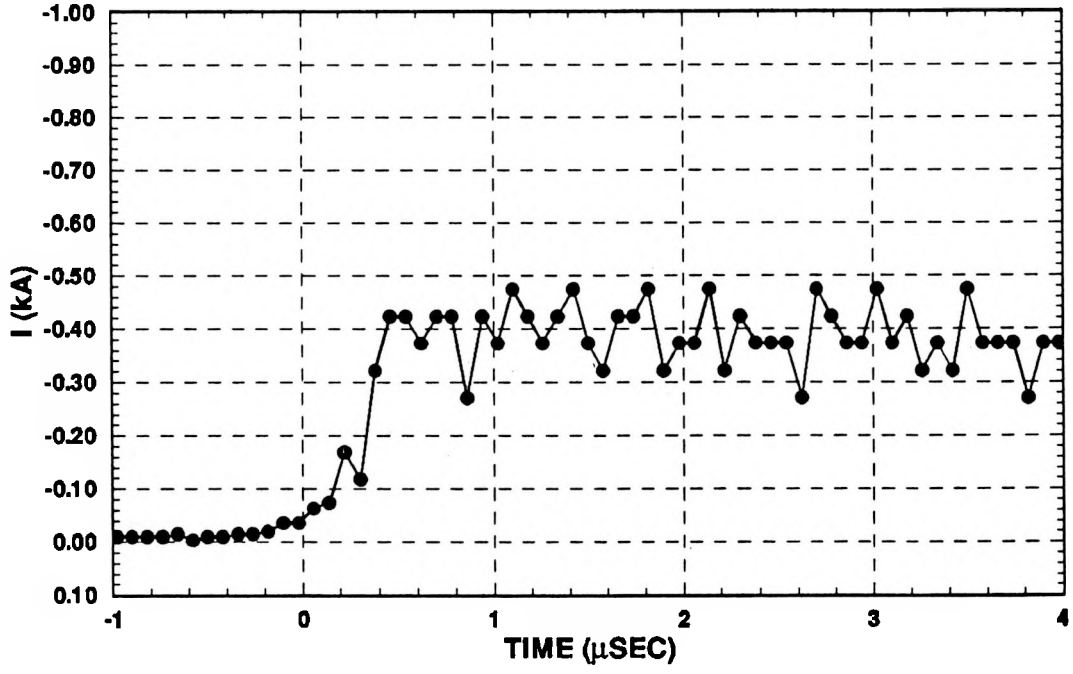

Figure C-16. Lightning Current Measured in One Down Conductor, Fast Time Scale. Flash 90-09, Stroke 1.

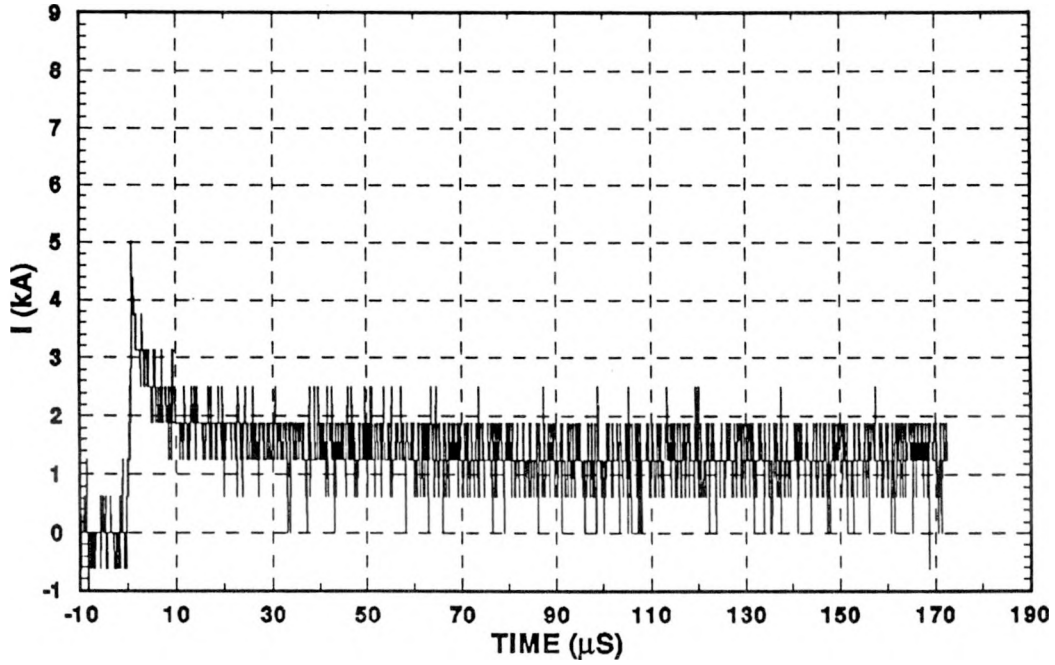

Figure C-17 Lightning Current Incident on APS, Slow Time Scale. Flash 90-09, Stroke 2.

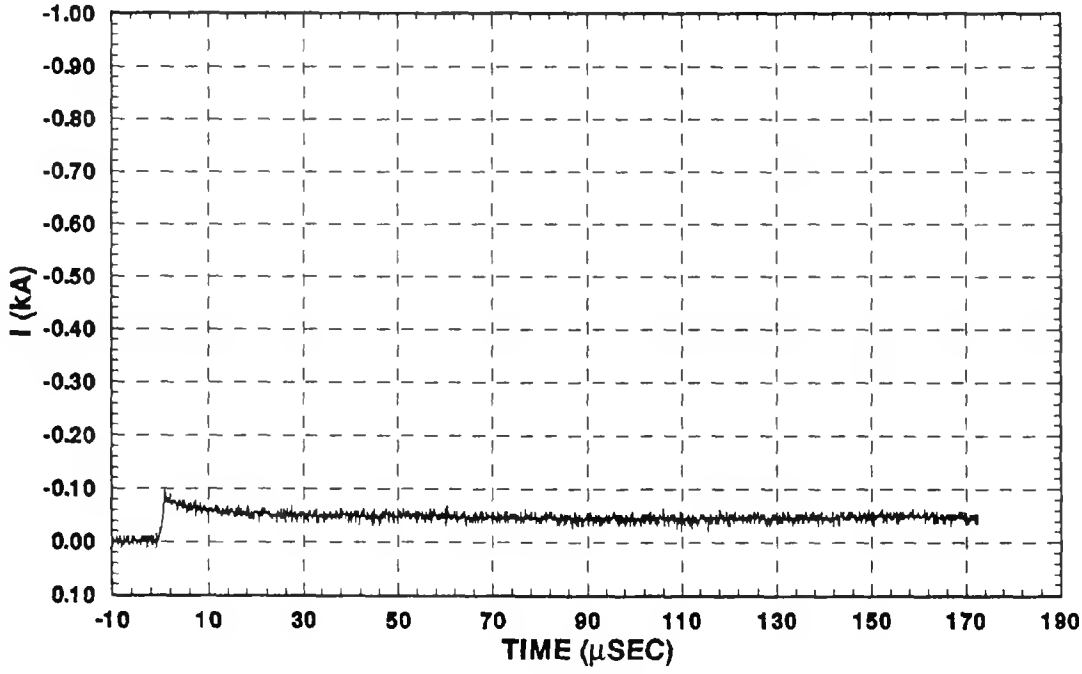

Figure C-18. Lightning Current Measured in One Down Conductor, Slow Time Scale. Flash 90-09, Stroke 2.

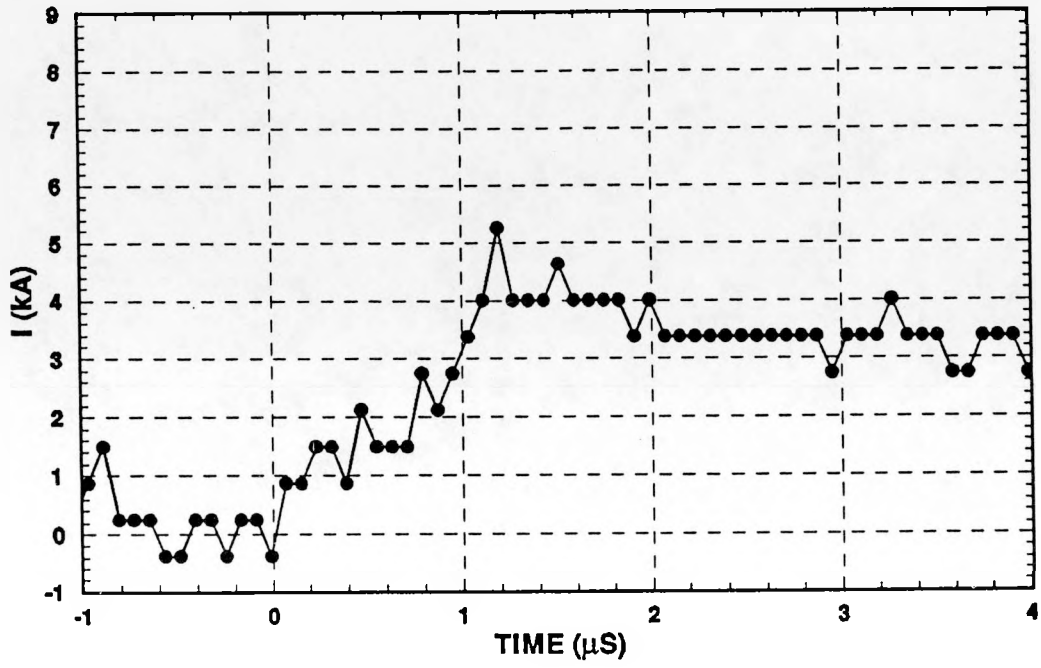

Figure C-19. Lightning Current Incident on APS, Fast Time Scale. Flash 90-09, Stroke 2.

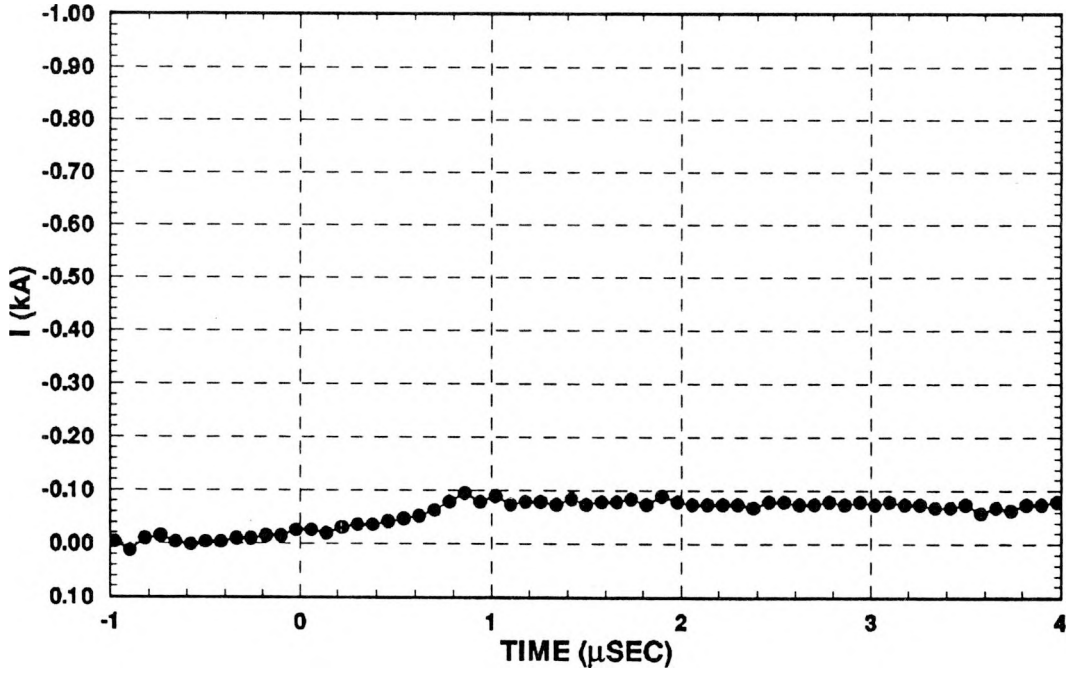

Figure C-20. Lightning Current Measured in One Down Conductor, Fast Time Scale. Flash 90-09, Stroke 2.

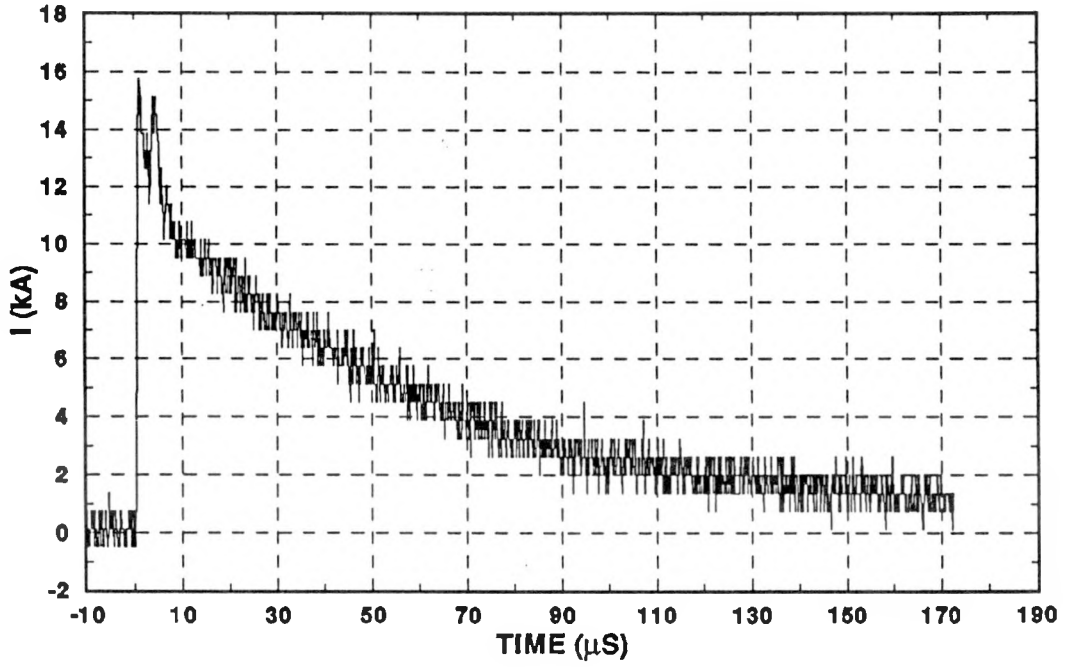

Figure C-21. Lightning Current Incident on APS, Slow Time Scale. Flash 90-12, Stroke 2.

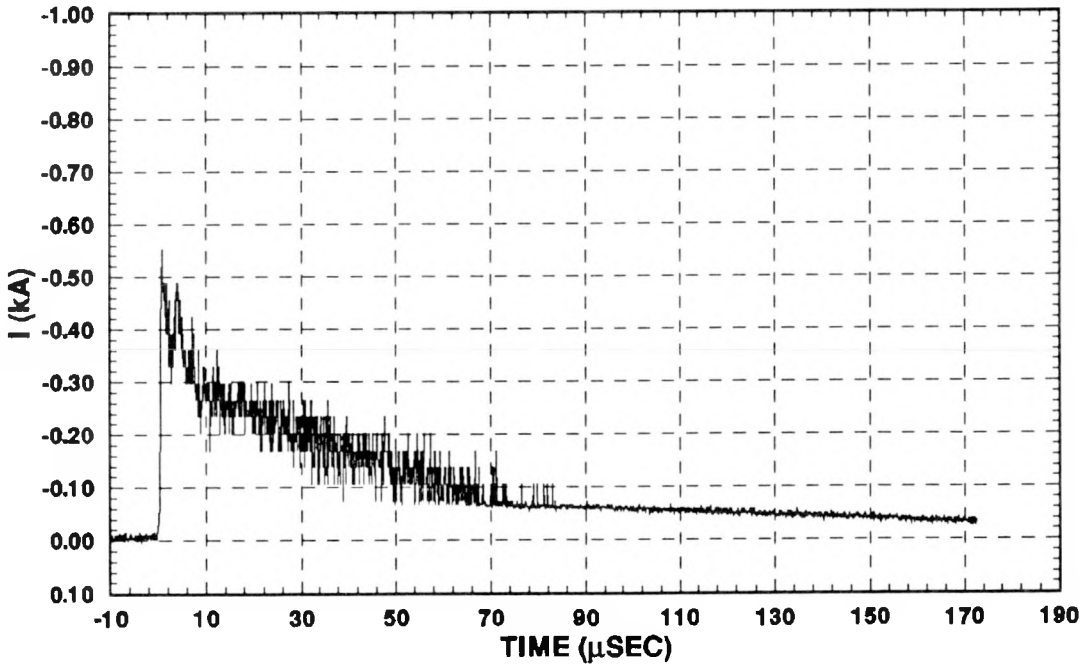

Figure C-22. Lightning Current Measured in One Down Conductor, Slow Time Scale. Flash 90-12, Stroke 2.

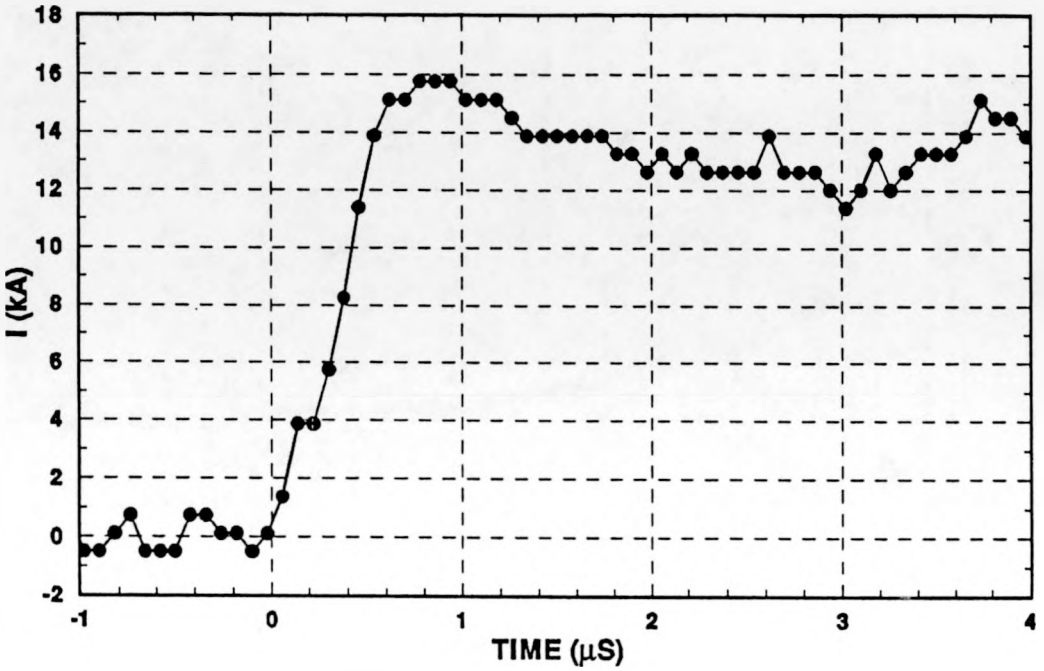

Figure C-23. Lightning Current Incident on APS, Fast Time Scale. Flash 90-12, Stroke 2.

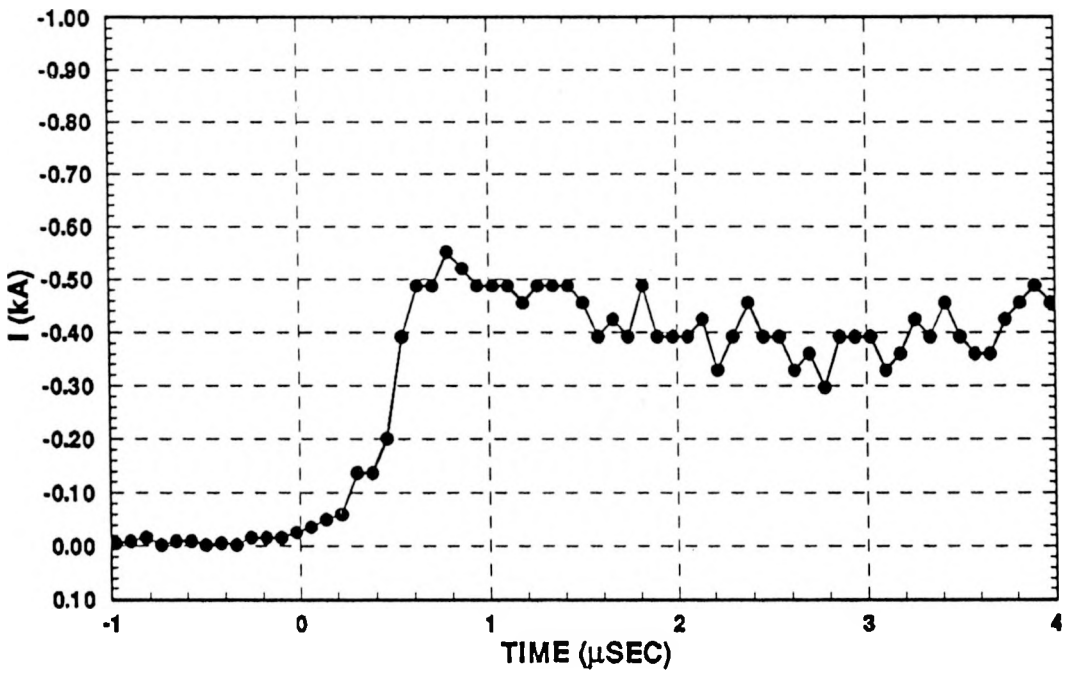

Figure C-24. Lightning Current Measured in One Down Conductor, Fast Time Scale. Flash 90-12, Stroke 2.

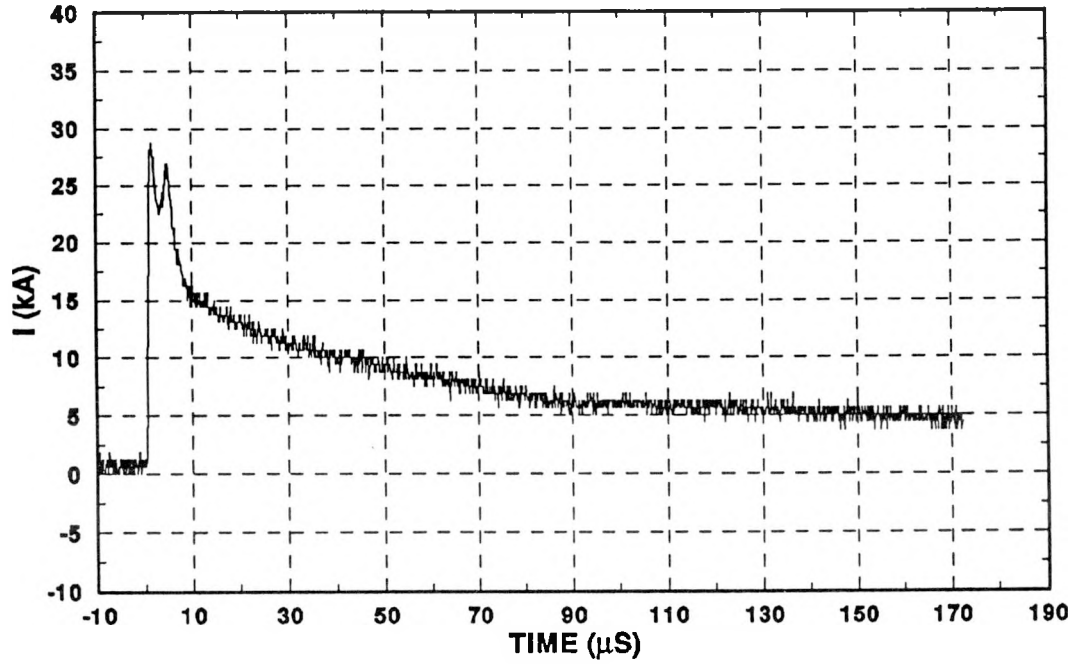

Figure C-25. Lightning Current Incident on APS, Slow Time Scale. Flash 90-12, Stroke 3.

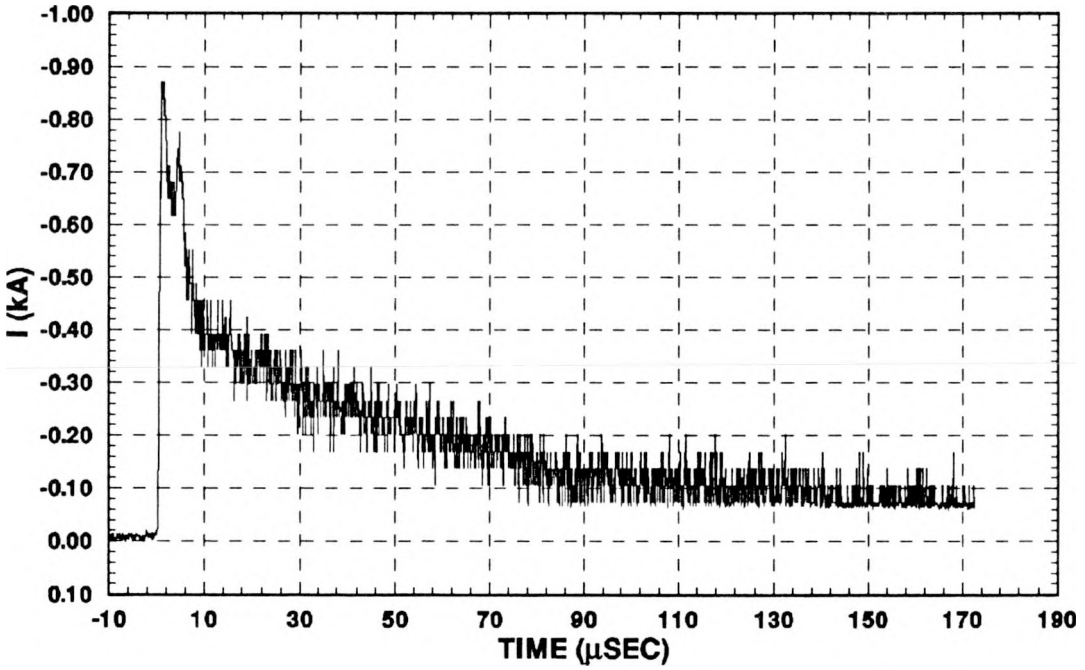

Figure C-26. Lightning Current Measured in One Down Conductor, Slow Time Scale. Flash 90-12, Stroke 3.

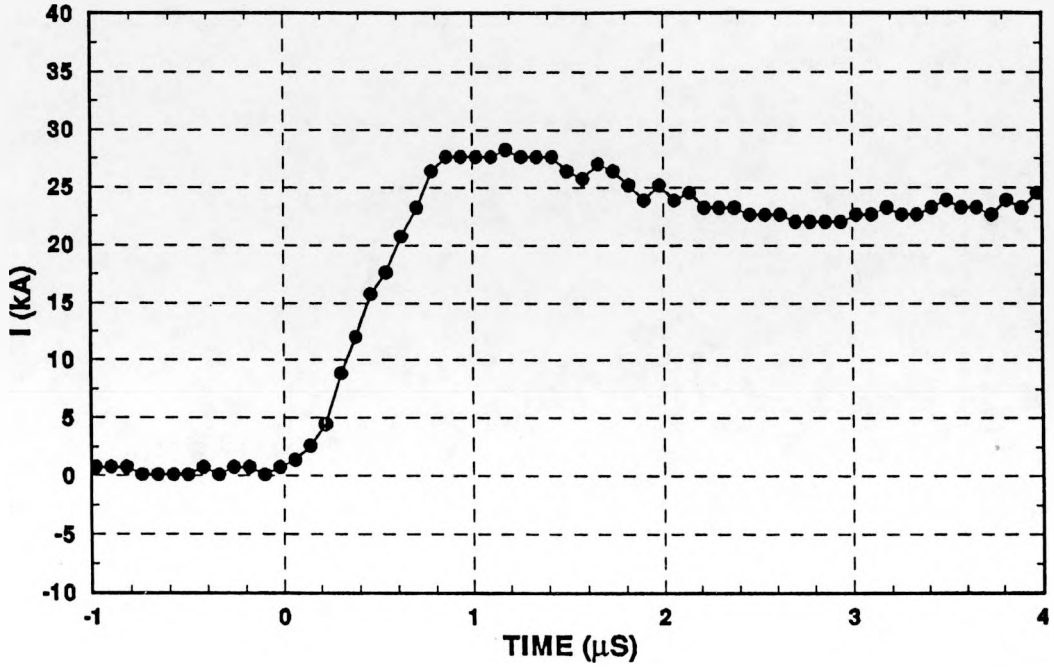

Figure C-27. Lightning Current Incident on APS, Fast Time Scale. Flash 90-12, Stroke 3.

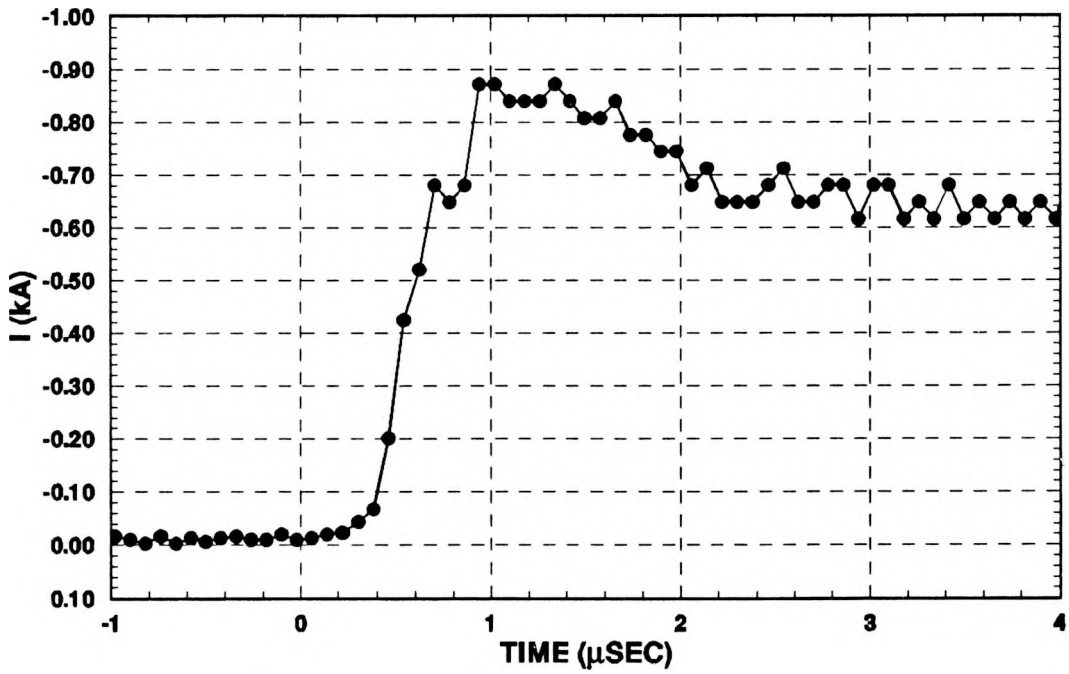

Figure C-28. Lightning Current Measured in One Down Conductor, Fast Time Scale. Flash 90-12, Stroke 3.

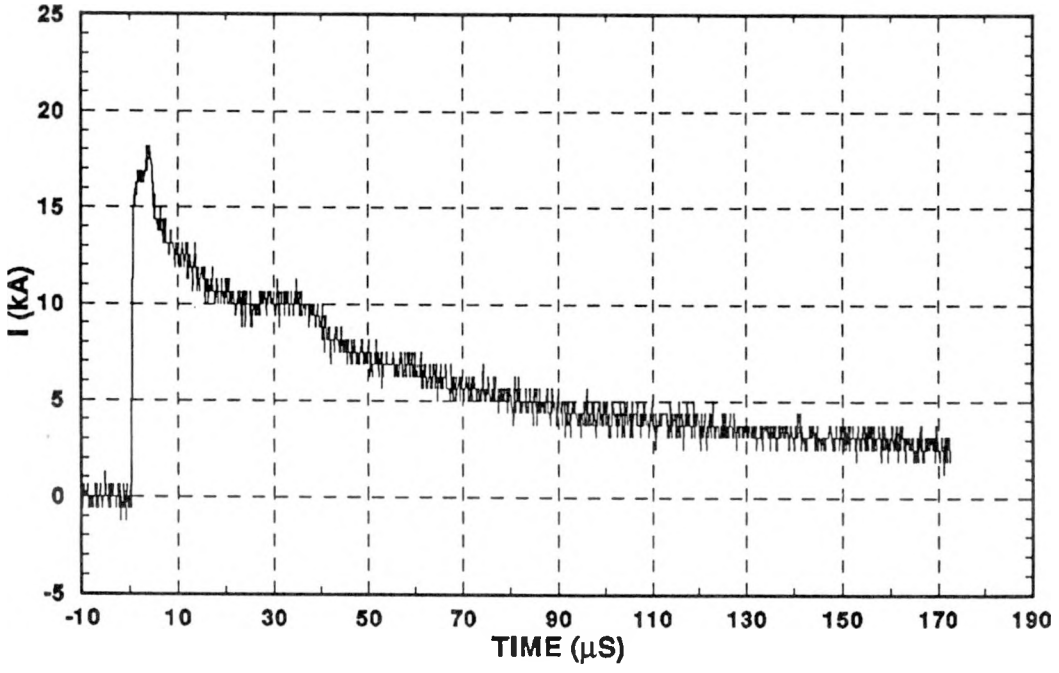

Figure C-29. Lightning Current Incident on APS, Slow Time Scale. Flash 90-14, Stroke 1.

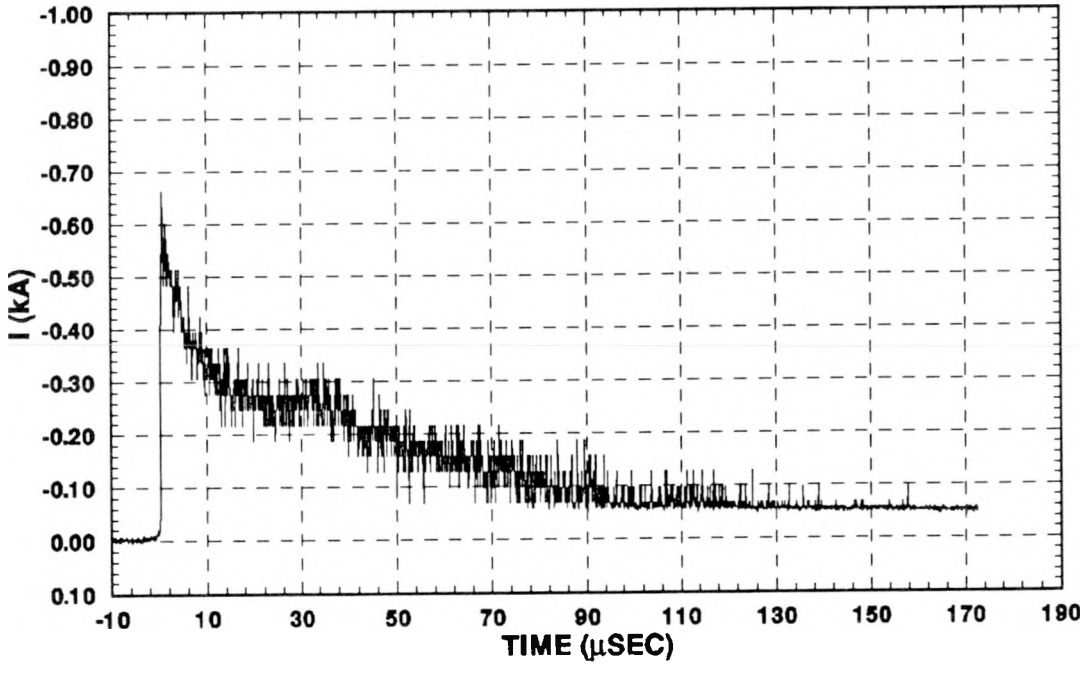

Figure C-30. Lightning Current Measured in One Down Conductor, Slow Time Scale. Flash 90-14, Stroke 1.

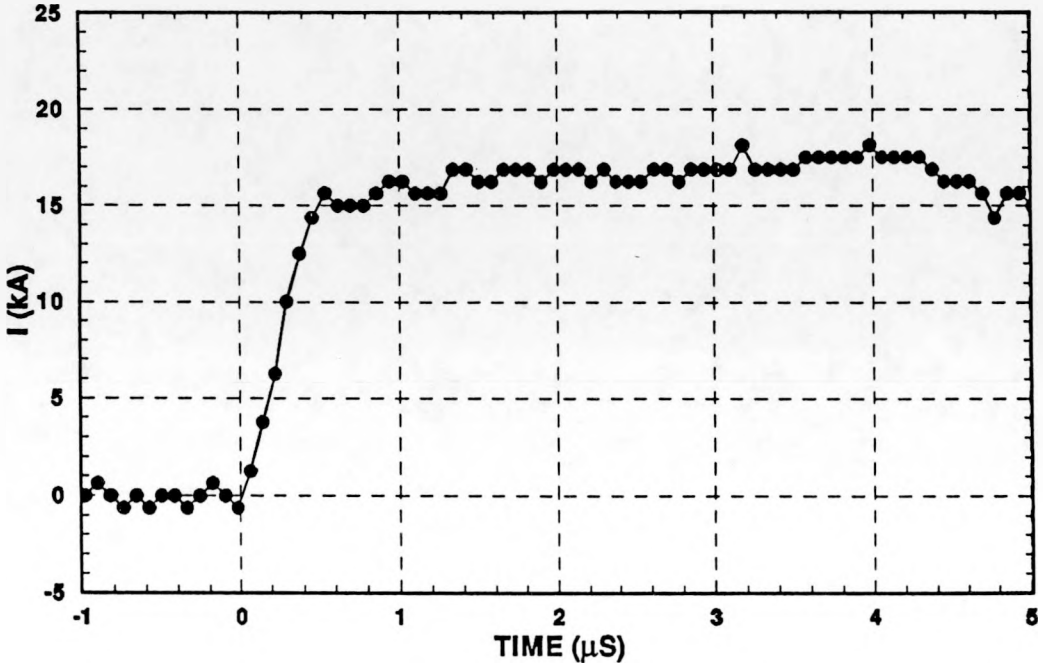

Figure C-31. Lightning Current Incident on APS, Fast Time Scale. Flash 90-14, Stroke 1.

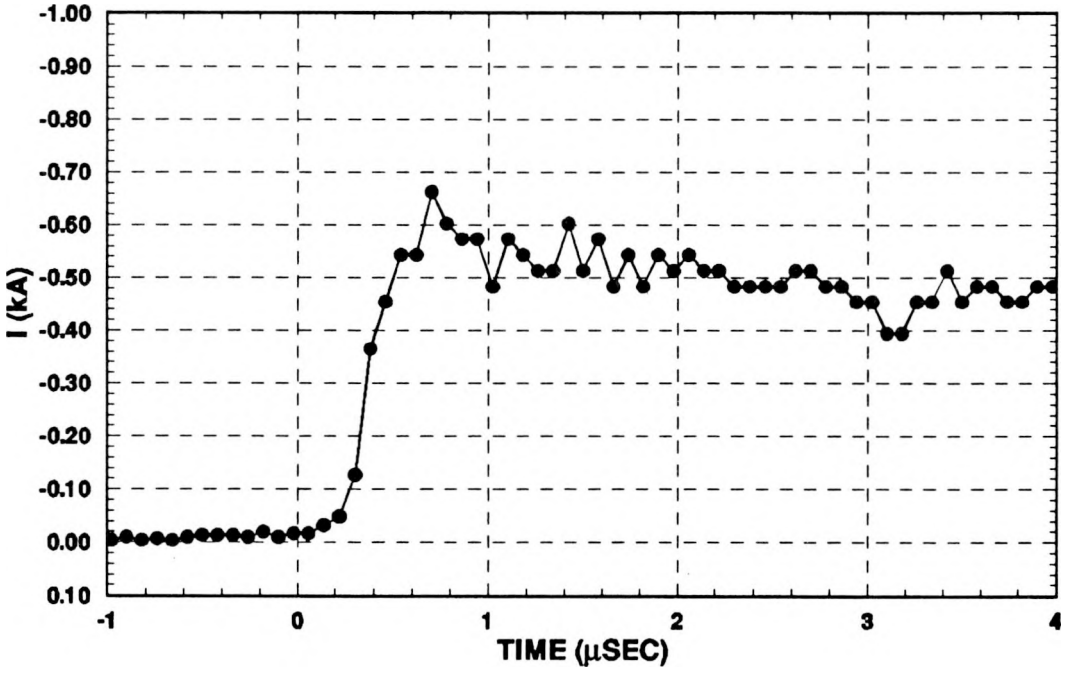

Figure C-32. Lightning Current Measured in One Down Conductor, Fast Time Scale. Flash 90-14, Stroke 1.

APPENDIX D

MATERIALS DAMAGE DATA

Presented in this appendix are photographs of each sample for which data spots were acquired. Accompanying each photograph is a plot of the current on the corresponding flash as recorded by the Dymec FM continuing-current instrumentation channel. High-resolution plots of the associated return-stroke components of these flashes are given, when available, in Appendix B.

Table D-1 summarizes observations obtained by visual inspection of the samples with the aid of a magnifying lens and measurements of the spot dimensions made with a millimeter scale. No destructive metrology will be conducted until after laboratory efforts to replicate these data spots are completed.

TABLE D-1
MATERIALS DAMAGE DATA SUMMARY

SHOT ID	MATERIAL/ THICK. (mm)	DAMAGE DESCRIPTION
90-02	Al, 1.96[1]	Sample hit by one stroke plus CC, charge 7.6 C. Corresponding spot of raised, crystalline material, 0.5 mm high and 4 mm in diameter. Depression in center of lump with pin hole in its center. Pin hole penetrates ~0.5 mm below flat surface. Good data point for future simulation reference. Moderate erosion at 3 spots on edge (lengths of 8, 5, 3 mm) where arcing to fixture cup occurred.
90-03	Al, 1.96	Raised lump of melted, crystalline material, 3-mm diameter, 0.75 mm high. Pin hole in center, ~.2 mm deep. Major damage spot, 8-mm diameter, with 5-mm diameter raised spot inside, slightly off-center. Two pin holes, one in center of raised lump, one on its edge in the crater surrounding the lump. Lump raised about 1 mm above the surface; crater depth ~0.25 mm at deepest point. No discoloration on back side of large spot, but a 1.5-mm diameter "dot" raised about 0.1 mm. 2 spots, each 5 mm across and of depth ~0.1 mm adjacent to the large crater. Somewhat irregular, slightly crystalline raised portion in center. Largest spot correlates to RS plus 120 ms CC transferring 13.6 C. Good data point for simulation reference. Edges show significant erosion at points where arcing to the fixture cup occurred. Five areas of same with lengths of 14, 20, 11, 16, and 13 mm.
90-04	Al, 1.96	Crater, with appearance somewhat different from the others. Diameter of 3.5 mm. Crater surrounded by rim raised about 0.3 mm. Deep penetration (>1 mm). Non-discolored "dot" on back. Difficult to measure diameter, but can be clearly felt. 2 other typical spots of raised, crystalline material, 3 mm and 1.7 mm. No significant penetration. From the 16 mm film, the initial series of strokes and CC of the flash hit through the water drain hole on the dielectric shield. This is corroborated by a large patch of carbon deposit on the side of the top of the sample, and by the erosion of the brass fixture cup there. The last three strokes and CC hit the sample via a new channel and look like they hit directly on the top. Therefore, we associate the first spot above with the final RS+CC (5.5 C), and the other two with the preceding 2 strokes (1.8 and 0.4 C).

		The first spot represents the deepest penetration obtained. Since it seems reasonable to associate it with the final stroke and CC, it is a good data point for simulation reference.
90-06/07	Al, 1.96	No RS to the sample, although an upward-going streamer was photographed. A portion of the starter wire is still intact and is surrounded by numerous small, shiny pits caused by streamer electrode spots. No significant erosion. Strikes through the water drain hole to edge of sample on 90-07.
90-08	Al, 1.96	Single return stroke. Sample shows an irregularly shaped surface mark (like a splatter) adjacent to the spot of the starter wire. No significant erosion. A second spot, 3.5-mm diameter, with a smaller raised center. Felt to correspond to the single return stroke (13.8 kA, 0.015 C). Good data point for simulation reference for RS.
90-09	Al, 1.96	Some streamer marks near the edge along with carbon blackening. Strike was through the water drain hole on the side of the fixture.
90-12	Steel, 0.89[2]	Major damage. There were three strokes in the flash. The first 2 terminated on one of the samples that was not erected. The erected sample took 1 stroke plus a moderate continuing current that transferred 49 C. There are 3 large overlapping spots. (8.5, 10 and 7 mm respectively). The appearance of the melted material is different than in Al. Here it flowed more, and exhibits less of the crystalline appearance. The melted material tends to be gray in color. At the center of the largest spot is a hole of 1-mm diameter surrounded by a well defined rim of material raised about 0.5 mm above the surface. The hole has a depth of more that 1 mm. The back side of the sample has a large gray discoloration of graded gray color about 11 x 17 mm in total. There is a raised lump of melted material about 1.5 mm across. For all practical purposes, this represents a burnthrough of the sample. Good data point for future simulation reference.
90-14	Steel, 0.89	Single RS with CC. Left a large irregular track across the surface with melted gray material surrounded by shiny silver border. Appears to be an example of the RS attaching (leaving a well-defined round spot), and then moving across the surface during the following continuing current. No significant penetration. Total charge : 7.8 C. Back side of sample has elongated slightly discolored mark behind the attachment spot, but nothing that can be felt. Good data point for simulation reference.
90-15/16	Steel. 089	Streamer current marks only.

[1] 2024-T3 aluminum
[2] 4130 ferrous steel

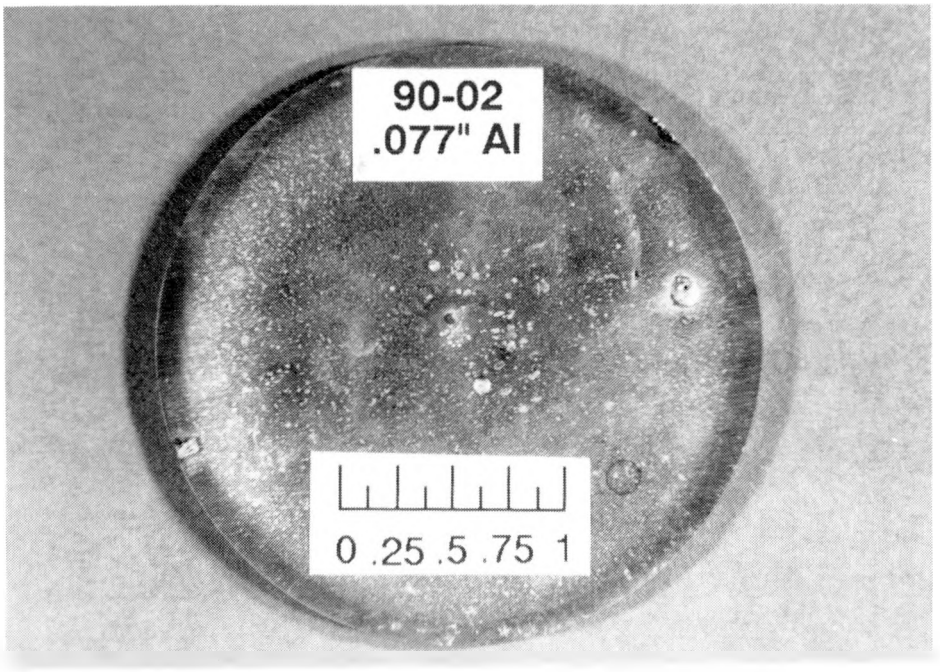

Figure D-1. Sample 90-02

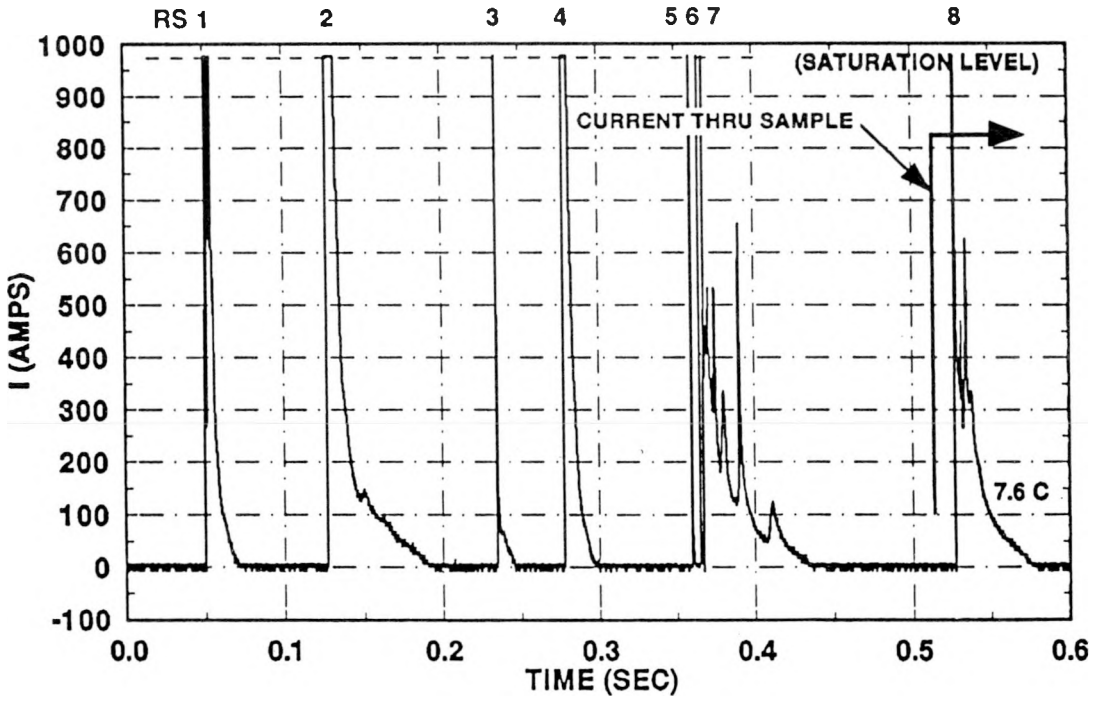

Figure D-2. Recorded Current, Flash 90-02. Only final stroke attached to the top of the sample.

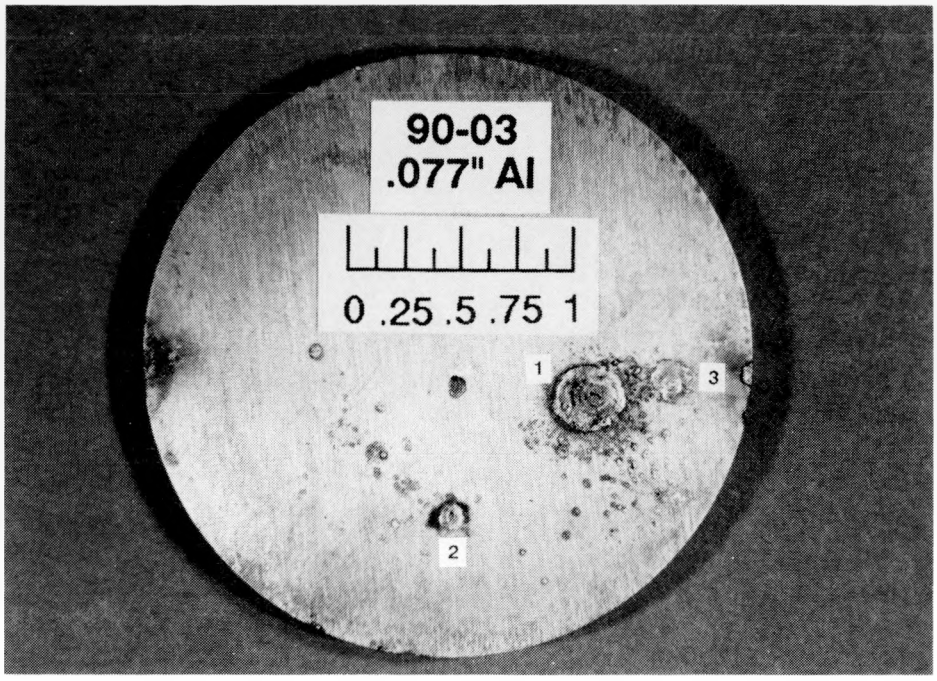

Figure D-3. Sample 90-03

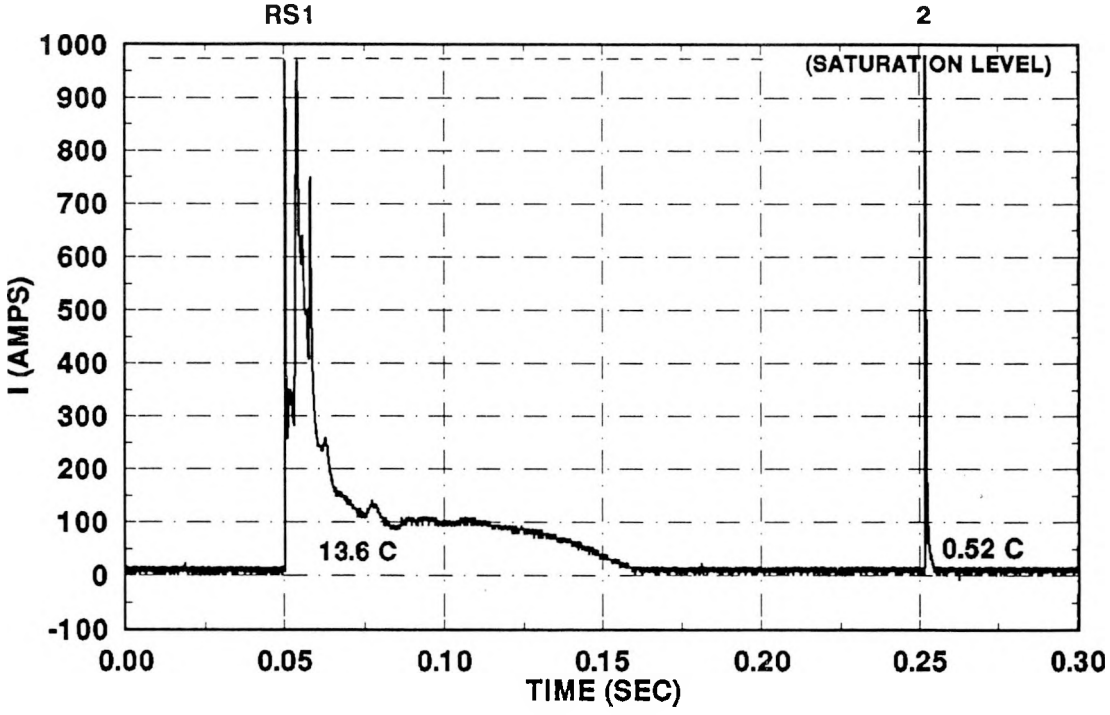

Figure D-4. Recorded Current, Flash 90-03

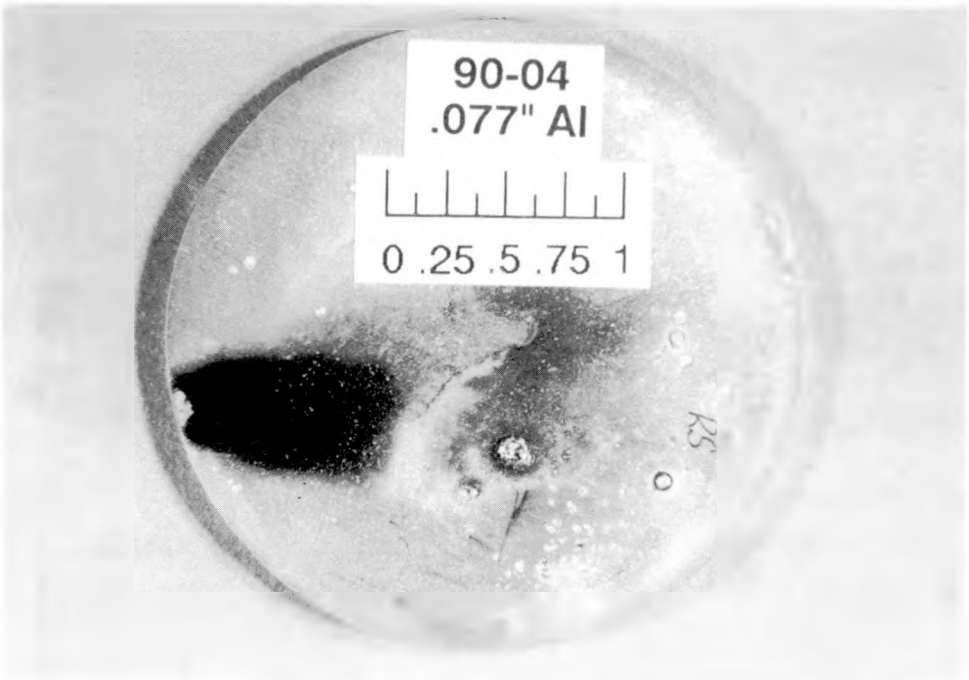

Figure D-5. Sample 90-04

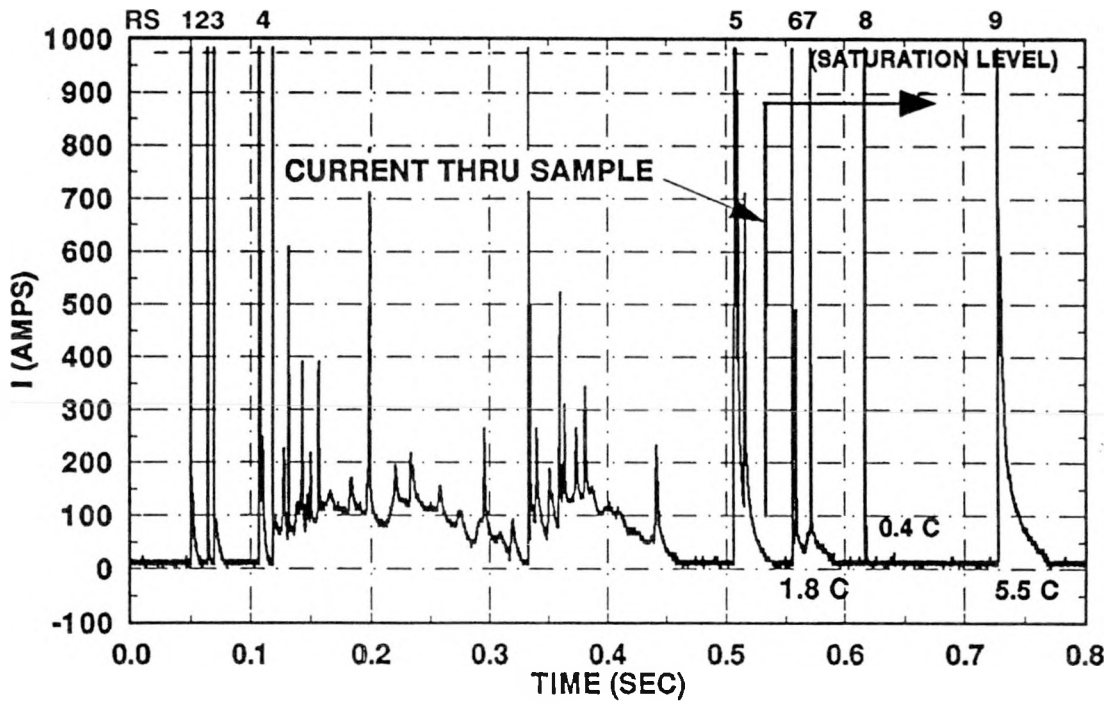

Figure D-6. Recorded Current, Flash 90-04. (Only the indicated portion of the current attached to the top of the sample.)

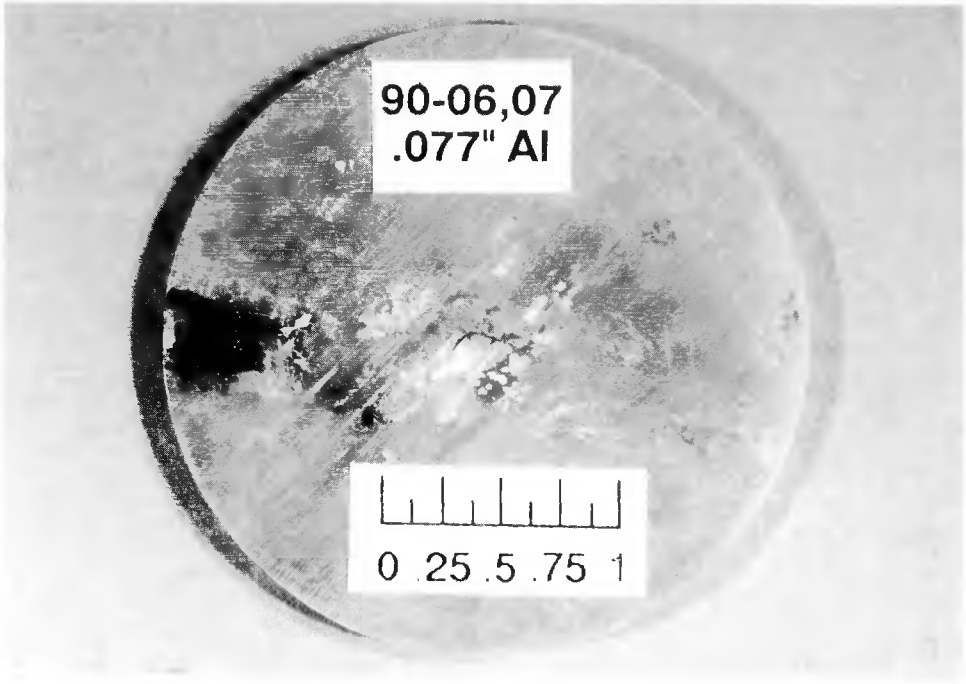

Figure D-7. Sample 90-06/07

(No return-stroke attachment to the top of sample)

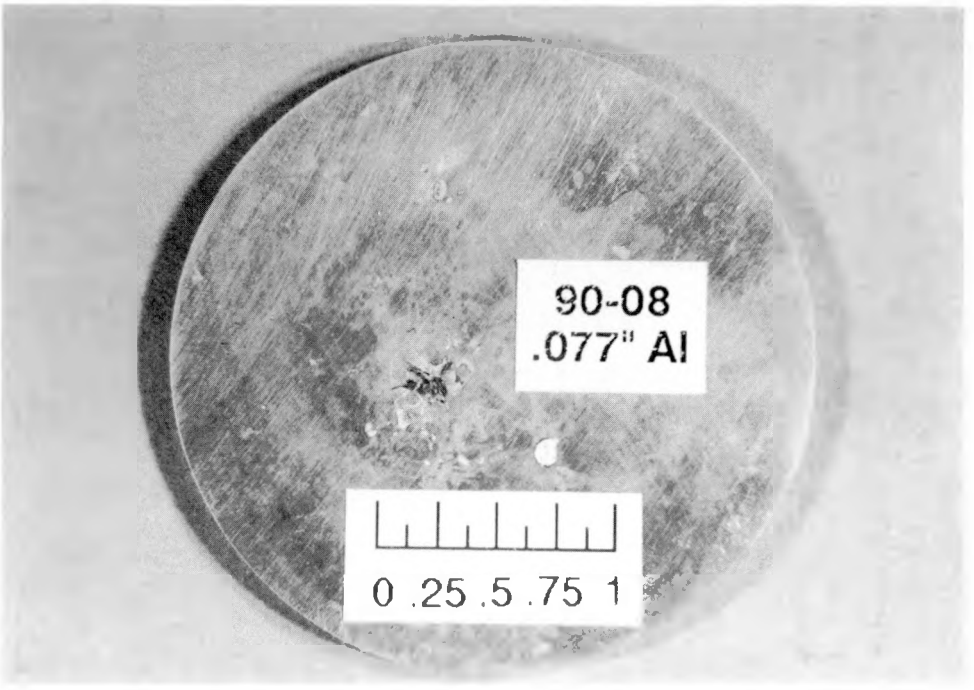

Figure D-8. Sample 90-08

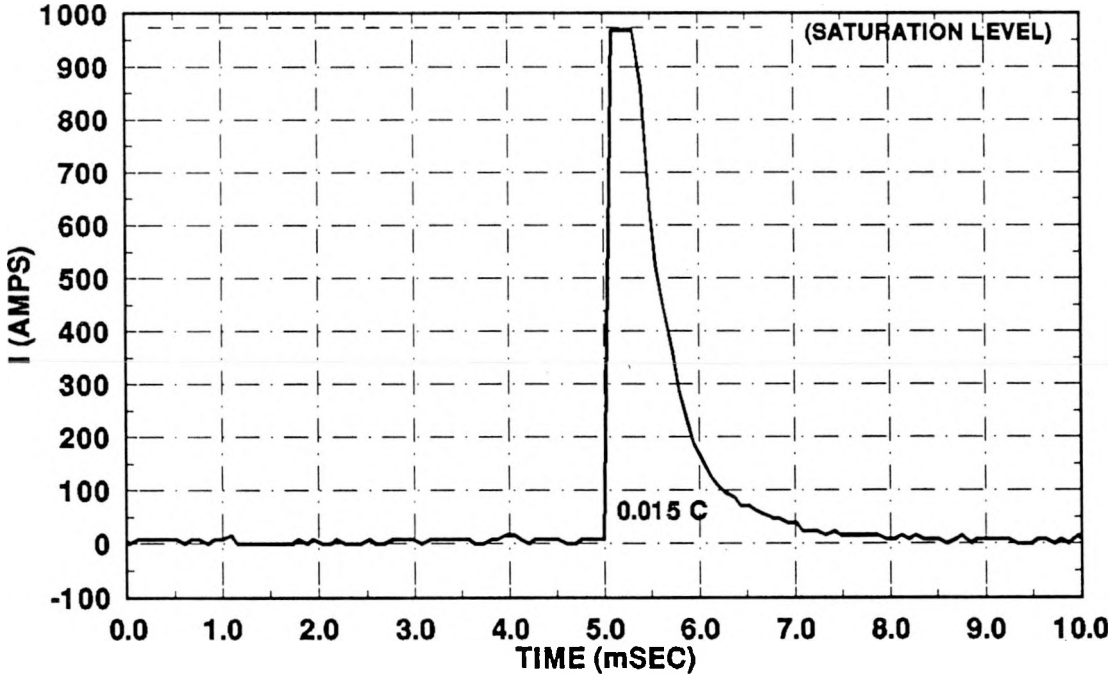

Figure D-9. Recorded Current, Flash 90-08. (Return stroke only; no continuing current.)

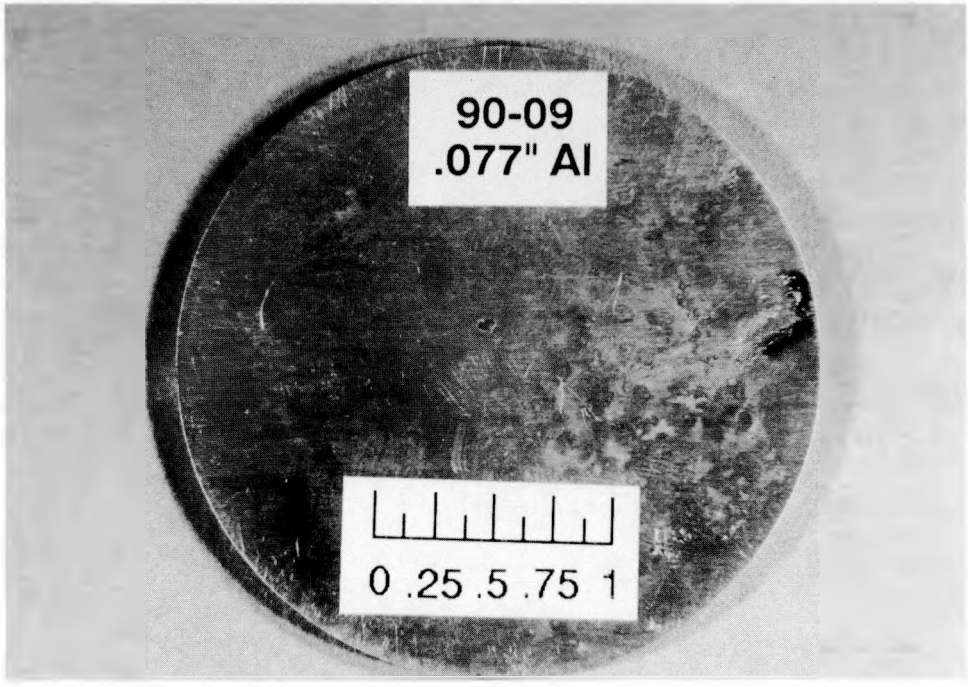

Figure D-10. Sample 90-09

(No return-stroke attachment to top of sample)

Figure D-11. Front Side of Sample 90-12. (See Figure 31 in Section 7.4 for back side of sample)

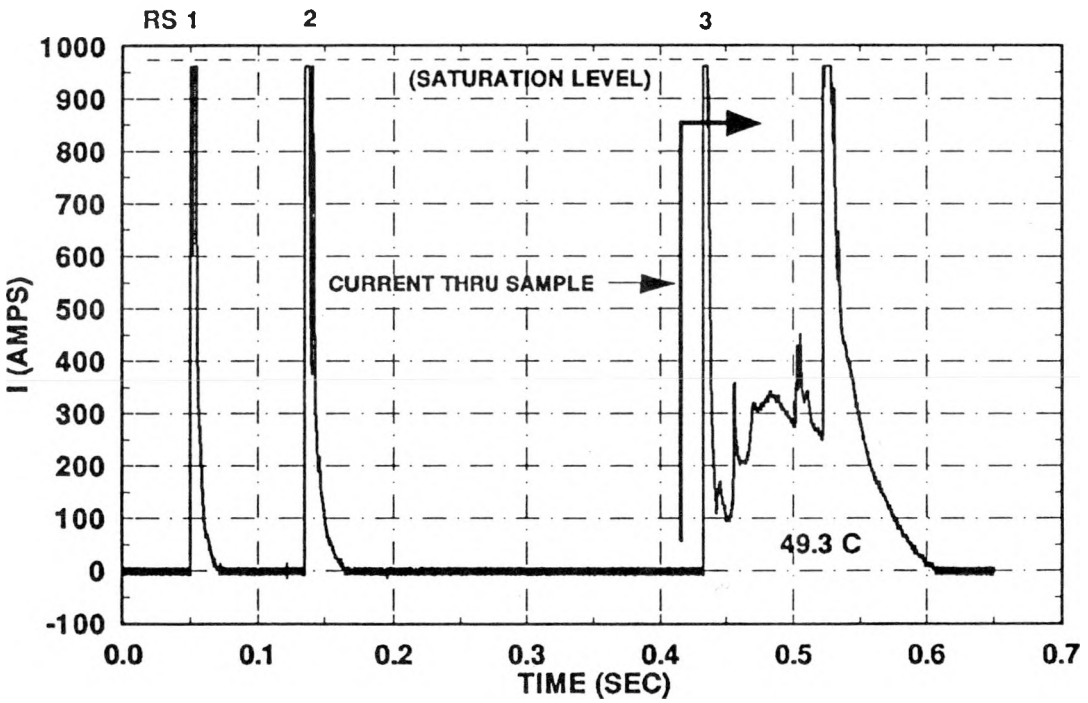

Figure D-12. Recorded Current, Flash 90-12. (Only indicated portion of current attached to the top of the sample.)

Figure D-13. Sample 90-14

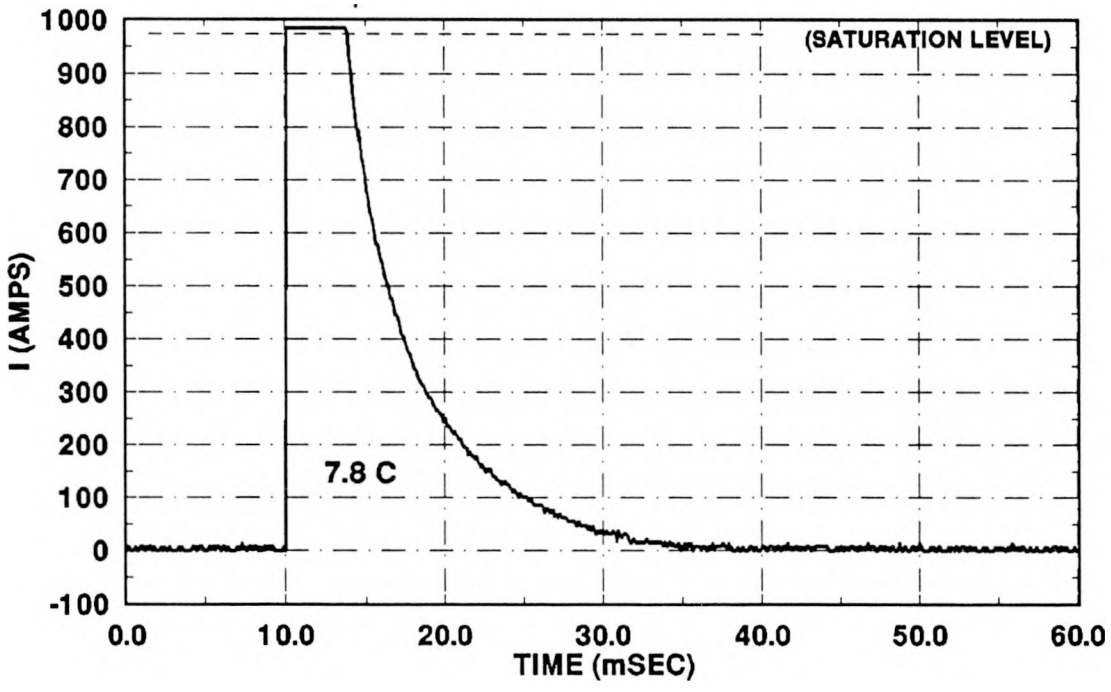

Figure D-14. Recorded Current, Flash 90-14. (Return stroke plus weak continuing current.)

Figure D-15. Sample 90-15/16

(No return stroke attachment)

END
6-7-91

DISTRIBUTION

1 Office of the Assistant to the Secretary
of Defense (Atomic Energy)
Room 3E1074, The Pentagon
Washington, DC 20301-3050

1 Commander, US Army Nuclear and Chemical Agency
7500 Backlick Road
Springfield, VA 22150
Attn: MONA-MS (G. Long)

3 Commander
USA Armament Research, Development,
and Engineering Center
Picatinny Arsenal, NJ 07806-5000
Attn: SMCAR-FSN
SMCAR-AEC-IM
SMCAR-FSN-T

4 Assistant Project Manager for Nuclear Munitions
Picatinny Arsenal, NJ 07806-5000
Attn: AMCPM-NUC-R
AMCPM-NUC
AMCPM-NUC-AFO
AMCPM-NUC-M

1 Commander, White Sands Missile Range
Bldg. 21225
White Sands Missile Range, NM 88002
Attn: Nuclear Effects Division
Troy West

1 Commander, US Army Missile Command
Redstone Arsenal, AL 35898-5690
Attn: AMCPM-PE-EA
C. D. Pond

3 Harry Diamond Labs
2800 Powder Mill Road
Adelphi, MD 20783
Attn: SLCHD-DE-FT
M. Kolodny
SLCHD-IT-EC
SLCHD-TA-ET

1 Commander, Naval Sea Systems Command
Department of the Navy
Washington, DC 20360
Attn: Nuclear Weapons/Munitions
Sec Div (SEA-643)

1 Commander, Naval Sea Systems Command
Theater Nuclear Warfare Program (PMS 423)
Washington, DC 20362-5101
Attn: T. Rosling

1 Commander, US Army Armament, Munitions and Chemical Command
Picatinny Arsenal, NJ 07806-5000
Attn: AMSC-MAY-W

DISTRIBUTION (Continued)

1 Commander, US Army Armament, Munitions and Chemical Command
Rock Island, IL 61299-6000
Attn: AMSMC-ASN-N

1 Commander
NATC
Patuxent River NAS, MD 20670
Attn: M. Whitaker (SY84)

4 Director, Strategic Systems Projects
Department of the Navy
Washington, DC 20376
Attn: B. Hannah
R. M. Jones
M. Whittaker
Ruth Ann Lee

3 Weapons Laboratory
Kirtland AFB, NM 87117-6006
Attn: D. Fattor/NTSW
Capt. Daniel Douthit/NISM
M. Harrison/NTCA

1 US Department of Energy
Office of Military Applications
Washington, DC 20545
Attn: DP-22

1 US Department of Energy
Albuquerque Operations Office
P.O. Box 5400
Albuquerque, NM 87115
Attn: NESD/WSSB

1 Los Alamos National laboratory
P.O. Box 1663
Los Alamos, NM 87545
Attn: Technical Library
M. G. Wheeler, WX-1

3 University of California
Lawrence Livermore National Laboratory
P.O. Box 808
Livermore, CA 94550
Attn: Technical Info. Dept.
R. T. Hasbrouck
Bill Hubbel, L-125
R. A. Woelffer, L-125

3 NASA
Kennedy Space Center, FL 32899
Attn: W. Jafferis (DL-ESS-23)

1 Commander
Naval Surface Weapon Center
Dahlgren, VA 22448
Attn: Ben Franklin

DISTRIBUTION (Continued)

1 Commander
NWEF
Kirtland AFB, NM 87117
Attn: Jeff Stickney

2 Electromagnetic Applications, Inc.
12567 W. Cedar Dr., Suite 250
Lakewood, CO 80228-2091
Attn: R. Perala
R. Collier

1 8100 E. E. Ives
1 8130 J. D. Gilson
1 8133 A. C. Skinrood
1 8133 K. A. Mitchell
1 8150 J. B. Wright
1 8155 R. G. Miller
1 8155 D. L. Gehmlich
1 8155 E. B. Talbot
1 8156 M. E. John
1 8156 J. L. Mitchell
1 8160 D. J. Bohrer
1 8162 C. T. Yokomizo
1 8162 G. E. Dietel
1 8162 D. S. Post
1 8163 D. J. Beyer
1 8163 J. Martinell
1 8163 S. J. Vasey
1 8165 R. A. Pearson
1 8165 G. C. Story
1 8170 J. W. Hickman
1 8171 J. R. Hogan
1 8174 J. E. Marion
1 8174 C. M. Furnberg
1 8174 L. E. Dighton
1 25 R. N. Brodie
1 2361 R. F. Ellison, Jr.
1 2364 N. F. Siska
1 2530 P. Dressendorfer
1 2541 S. B. Martin
1 2543 K. G. McCaughey
1 2545 J. H. Barnette
1 2551 D. E. Carnicom
1 2551 L. A. Andrews
1 2551 R. D. Holt
1 2850 T. C. Cannon, Jr.

1	5100	G. N. Beeler, Actg.
1	5110	C. C. Burks
1	5111	R. E. Kreutzfeld
1	5113	R. W. Jorgensen
1	5114	W. D. Ulrich
1	5114	J. S. Clabaugh
1	5130	J. P. Abbin, Jr.
1	5131	J. O. Harrison
1	5131	H. T. Lehman
1	5147	G. L. Maxam
1	5150	K. D. Hardin
1	5153	K. Oishi
1	5160	G. R. Otey
1	5167	D. F. McVey
1	5220	J. W. Kane
1	7200	C. H. Mauney
1	7213	H. D. Bickleman
1	7230	J. F. Ney
1	7231	S. D. Spray
1	7231	R. E. Church
1	7232	G. A. Sanders
1	7232	P. E. Rexroth
1	7232	P. E. D'Antonio
1	7260	T. S. Edrington
1	7500	R. A. David, Actg.
1	7550	D. N. Bray
1	7553	M. E. Morris
1	7553	K. C. Chen
2	7553	R. D. Jones
1	7553	L. K. Warne
1	7554	L. D. Scott
50	7554	R. J. Fisher
1	7554	G. H. Schnetzer
1	7555	B. Boverie
1	9000	R. L. Hagengruber
1	9110	C. W. Childers
1	9220	G. H. Mauth
1	9350	J. H. Renken
1	9352	G. J. Scrivner
1	9352	C. D. Turner
1	9352	C. N. Vittitoe
1	8524	J. A. Wackerly
5	3141	S. A. Landenberger
3	3151	G. L. Esch, Actg.
8	3145	Document Processing (for DOE/OSTI)

☆ U.S. GOVERNMENT PRINTING OFFICE 1991 - 573-122/40097